THE INFLUENCE OF FINITE DEFORMATION UPON THE CREEP BEHAVIOR OF CIRCULAR PLATES

Peter Thorvald Tarpgaard

THE INFLUENCE OF FINITE DEFORMATION UPON THE CREEP BEHAVIOR OF CIRCULAR PLATES

by

PETER THORVALD TARPGAARD, JR.

Lieutenant Commander, United States Navy

B.S., United States Naval Academy
(1959)

S.M., Massachusetts Institute of Technology
(1968)

Nav.E., Massachusetts Institute of Technology
(1968)

Submitted in Partial Fulfillment
of the Requirements for the
Degree of Doctor of
Philosophy
at the

Massachusetts Institute of Technology
June, 1970

The Influence of Finite Deformation Upon the Creep Behavior of Circular Plates

by

Peter Thorvald Tarpgaard, Jr.

Submitted to the Department of Naval Architecture and Marine Engineering on May 14, 1970, in partial fulfillment of the requirement for the degree of Doctor of Philosophy"

Abstract

A theoretical and experimental investigation of the creep behavior of initially flat circular plates is described in which particular attention is paid to the effect on this behavior of geometry changes induced during deformation. A method of modeling the constitutive behavior of a material undergoing creep deformation in a multiaxial state of stress is proposed. An energy technique for solving creep problems using this constitutive model is described and solutions are obtained for the cases of clamped and simply supported circular plates under a uniform, time independent, lateral load. The technique retains the effects of both bending moments and in-plane forces in the deformation of the plate. A series of experiments with lead plates is described and compared with the theoretical predictions obtained in this study and with those of previous investigators. Both the theoretical and experimental results show that the effect of finite deformation is of primary importance in the creep behavior of plates and must be taken into consideration even when the maximum deflection is well below the plate thickness.

Thesis Supervisor: Norman Jones
Assistant Professor of Naval Architecture

TABLE OF CONTENTS

TABLE OF CONTENTS
(con't)

LIST OF FIGURES

LIST OF FIGURES
(con't)

SYMBOLS

a = plate radius

c_n = constant in radial deformation profile equation

e = extensional strain

h = plate thickness

K = material constant in Norton's law

M_r, M_θ = radial and circumferential bending forces per unit length

N_r, N_θ = radial and circumferential membrane forces per unit length

n = exponent in Norton's law

q = uniform pressure per unit area

r = radial coordinate of plate

t = time

u = displacement in direction r of undeformed plate

V = internal energy dissipated during deformation

w = transverse deflection perpendicular to undeformed plate

x = r/a

z = thickness coordinate in plate

ε_r, ε_θ = radial and circumferential strains

θ = circumferential coordinate lying in plate

κ_r, κ_θ = radial and circumferential curvatures

ν = Poisson's ratio

σ = stress

$$\Phi = \left[\frac{\left(\frac{\dot{w}_o}{Kaq^n}\right)}{3/4\left(\frac{a}{h}\right)^{2n+1}} \right]^{1/n}$$, non-dimensional parameter used to correlate results

$$(\dot{}) = \frac{\partial}{\partial t}(\ )$$

$$(\ )' = \frac{\partial}{\partial r}(\ )$$

INTRODUCTION

Creep is a term commonly applied to a material deformation process in which the strains are a function of time as well as stress. The phenonmenon occurs in metals when they are stressed at high temperatures, and can result in appreciable plastic deformation even for stresses well below the yield stress. As machinery operating temperatures have risen steadily over the past years in search of higher efficiencies the phenomenon of creep has been of increasing interest to engineers. When designing components which will operate in an environment where creep may occur it is obviously necessary for the engineer to be able to predict creep deformations in order to produce an efficient and workable design. The mechanisms of creep are complex and as yet imperfectly understood, but enough is known to permit a reasonable analysis of some cases of practical importance. It is the purpose of this investigation to examine one such case, that of a thin circular plate exposed to a uniform lateral pressure, and to devise a means of predicting its creep behavior including, in particular, the influence upon this behavior of the geometry changes resulting from the deformation. It is believed that the general procedure developed in the solution of this particular problem can be applied to other structural shapes.

Trouton and Rankine observed and described the phenomenon of creep in lead wire in 1904 (1). In 1910, Andrade (2) made the first systematic investigation of creep using wires of

approximately pure lead and of lead-tin alloy. In 1929, Norton (3) published the results of his investigation of creep in steel at elevated temperatures and suggested that creep rate, for uniaxial stress, could be represented as a function of stress raised to a power n. This relation, which has become known as Norton's law, has been the basis for much of the phenomenological creep analysis in recent years. Other functional relations for uniaxial test data have been suggested, such as a hyperbolic sine function proposed by Prandtl and endorsed by Nadai (4) and an exponential relation suggested by Soderberg (5). The greater mathematical tractability of Norton's law has made its use far more common. A generalization of Norton's law to the multidimensional stress state was proposed by Odqvist in 1933 (6). Odqvist used the concept of octahedral stress to relate the strain rate components to the deviatoric stresses. At about the same time, Bailey (7) proposed a somewhat more complex set of relations for generalizing Norton's law to the multiaxial case in a form appropriate to the principal directions of stress and strain. Soderberg (5) showed how his exponential creep rule could be generalized to multidimensional cases through the stress and strain invariants. Another approach, based on the work of Drucker (8) and Hopkins and Prager (9) in the rigid plastic behavior of circular plates, uses the Tresca yield surface and the condition of normality of strain rate vectors to that surface to extend a uniaxial creep law to a multiaxial problem. This method was used by Wahl (10) for the analysis of rotating discs and by Venkatraman and Hodge

(11) for the bending of circular plates subject to creep deformation. At the present time there seems to be no firm basis, experimental or otherwise, for endorsing or rejecting any of the above theories as a generally applicable constitutive relation in creep. In this paper another model for the generalization of Norton's law to multidimensional cases is proposed in which principal strain rates are assumed to be a function of the nth powers of the principal stresses.

The analysis of the creep behavior of plates has thus far been confined to a bending or infinitesimal deflection analysis, in which in-plane forces are ignored, or a membrane analysis, in which moments are ignored. Odqvist (12) analyzed the bending of thin circular plates with clamped and simply supported edges using his multiaxial relations based on stress invariants. Venkatraman and Hodge (11) solved the same bending problems for circular plates using the Tresca criterion technique mentioned above. Venkatraman and Patel (13)(14) used this same method for the bending of annular plates. The Tresca technique was extended to the case of orthotropic bending of circular plates by Sandaranarayanan (15). A membrane analysis for circular plates undergoing creep deformation has been done by Odqvist (12)(15), again using his stress invariant generalization of Norton's law. Onat and Yuksel (17) have suggested a very simple and ingenious technique for the membrane analysis of a thin circular plate in which it is assumed that the plate deforms through creep behavior into a spherical shape. The

stresses may then be assumed to be everywhere equal and the uniaxial stress-strain rate rule is applied directly. There has apparently been, as yet, no mathematical analysis of the creep behavior of plates which retains both bending moments and in-plate forces and which considers the influence of the geometry changes induced by the deformation. None of the plate analyses cited above were accompanied by any experimental verification nor have any creep tests on plates been noted by the author in the literature. Jones (18)(19) has shown the very important influence of finite deformations in the static and dynamic behavior of rigid-plastic plates and it would seem likely that creep behavior would exhibit a similar dependence.

In this investigation a series of initially flat lead plates of three different thicknesses is subjected to various lateral hydrostatic pressures in a test apparatus which permits measurement of plate deflection at the center and at regular intervals along the radius. By observing deflections at various time intervals one is able to determine the deflection rate of the plate and the plate's deformation profile. Tensile creep tests are also conducted on specimens made from the same lead sheets as the circular plates in order to determine basic material creep parameters. Experimental procedures, apparatus, and results are described in Chapter I. A method for mathematically analyzing the creep behavior of circular plates including the effect of finite deformations is described in Chapter II. The method is based upon computing the rate of

internal energy dissipation in the plate and equating it to the external work rate. It is essentially an adaptation of a technique suggested by Timoshenko (20) for computing the large deflection behavior of circular elastic plates. The problem under study has several inherent nonlinear aspects: nonlinear material constitutive relations, nonlinear geometry with finite deflection, and nonlinear change in creep parameters with time. Despite these multiple nonlinearities, by using the technique herein described, the results for a circular plate may be presented in the simple form of an algebraic equation and a set of graphs. All necessary computer work is incorporated in the graphs from which the deformation rates may be computed directly, with the aid of a slide rule, for plates made from any material whose creep characteristics are adequately described by Norton's law. In Chapter III the theory is compared with the experimental results and with the bending and membrane analyses of other investigators.

Both the theoretical and experimental results demonstrate the strong influence of finite deflections on the creep behavior of circular plates. This influence is significant even for a deflection at the center less than the plate thickness. The proposed method of analysis yields results which are in quite reasonable agreement with the experimental data.

CHAPTER I

A. PLATE DEFORMATION EXPERIMENTS

1. DESCRIPTION OF APPARATUS

The creep behavior of a series of circular plates of very nearly pure lead was examined in the apparatus shown in Figures 1 and 2. The plates were cut from commercially rolled sheets of three different thicknesses commonly known as 4 lb., 6 lb., and 8 lb. plate. These thicknesses were:

Plate Size	Thickness
4 lb	.068"
6 lb	.105"
8 lb	.136"

Local variations within the plates from the above thicknesses were no greater than ±.001". All circular plate specimens and tensile specimens of any one thickness were cut from the same lead sheet. A chemical analysis of each sheet is given in Appendix G. Lead was chosen for these experiments because of the fact that it creeps at room temperature. This fortunate property means that costly furnaces, temperature control devices, and elaborate instrumentation which would be necessary for elevated temperature testing are not required. Although lead is not a commonly used structural material we may expect that its behavior at room temperature will correspond to the behavior of more common structural materials, such as steel, at higher temperatures. Moreover, the theoretical analysis which is to be presented is valid for any material whose creep behavior is governed by the constitutive equation postualted. Thus, if agreement between theoretical predictions

and experiments is achieved for lead plates, then the analysis should remain valid for plates which are made from other materials whose behavior is adequately represented by the constitutive equation.

The test apparatus consisted of a short section of steel pipe with a blank base welded to one end, and a flange and ring on the other end which was used to clamp the test specimen. The flange and ring were machined to have an inner diameter of exactly five inches and square edges at the inner lip. Centering pegs were placed in the flange so that the ring could always be positioned precisely above it by fitting the pegs into holes drilled into the ring. This was necessary as the inner edge of the ring must be exactly above the edge of the pressure vessel to insure proper end conditions. The flange and ring had serrations machined on the gripping surfaces. These serrations were relieved in both surfaces so as not to damage or distort the edge of the plate sample. The sample plate was clamped between the flange and the ring by eight high strength steel bolts tightened to a uniform tension with a torque wrench. Six dial indicators were positioned above the plate with indicator holders attached to the ring. These dial indicators were placed so as to record the deformations at various places on the plate. Positioning of the indicators was facilitated by the use of extension rods of various lengths for the indicator contact points. All dial indicators were graduated to .0001" and were checked for accuracy with gage blocks before commencing the experiments.

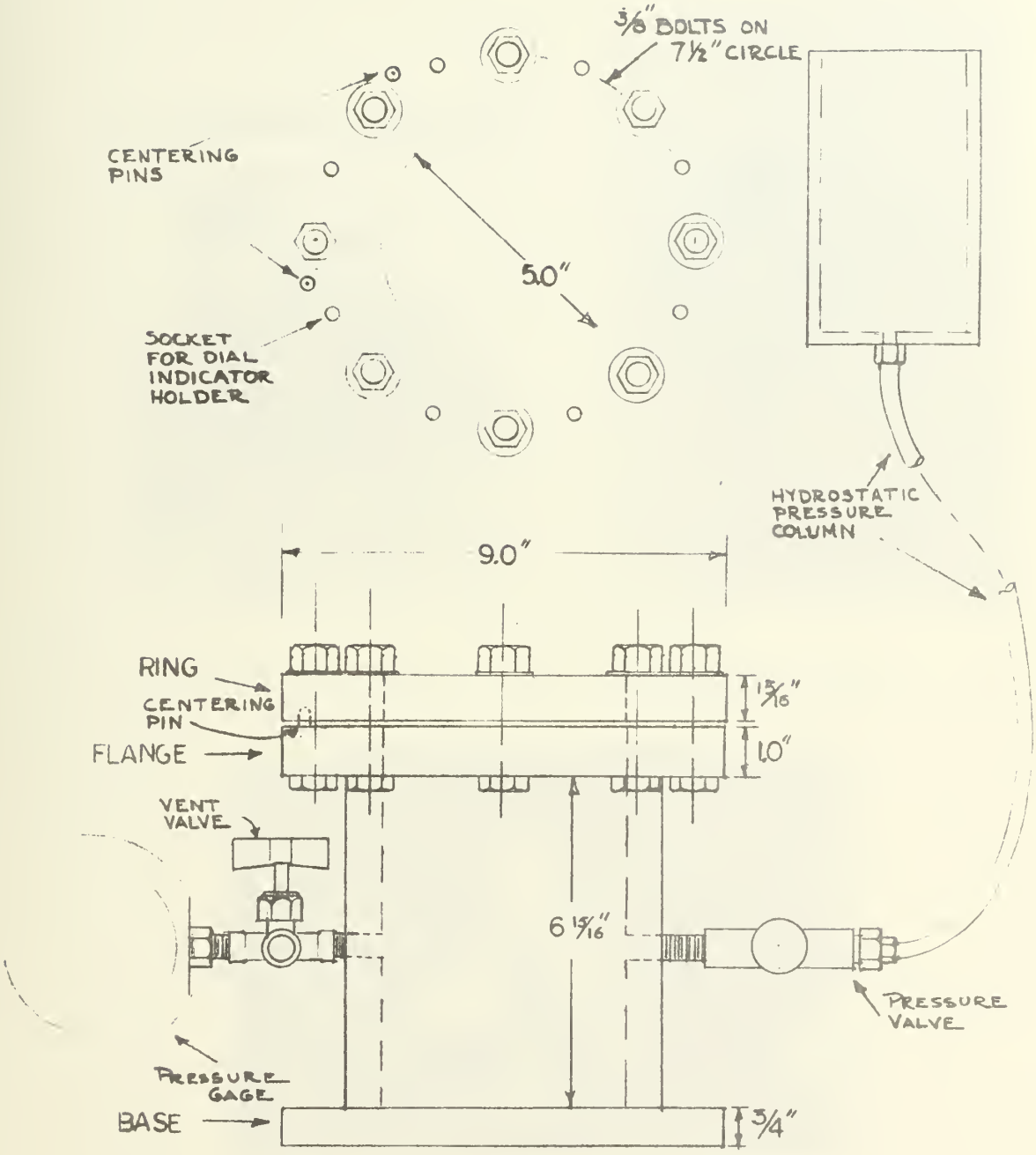

PLATE TEST APPARATUS

FIG. 1.1

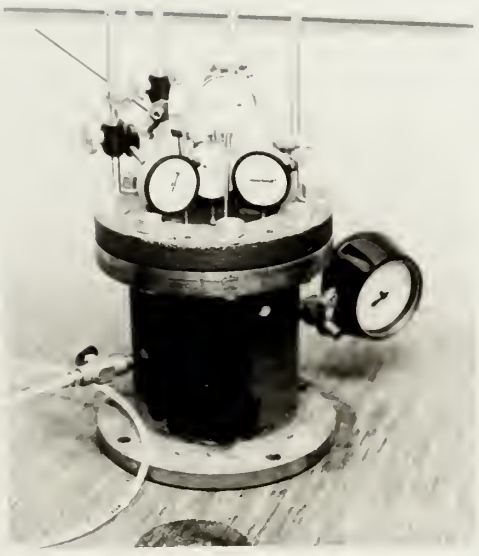

A. Plate Test Apparatus

B. Plate Test Sample
(after deformation)

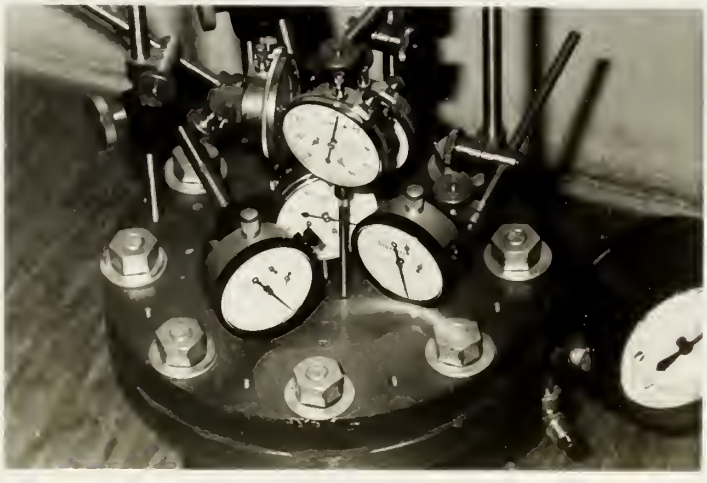

C. Arrangement of Dial Indicators

FIG. 1.2

The apparatus was pressurized by a water column. The water column consisted of a length of plastic tubing connected to a 3" diameter plastic cylinder at one end and, through a valve, to the pressure vessel at the other end. The use of a water column insured that the hydrostatic pressure in the vessel could be both accurately measured and accurately maintained over the long period of time required for a creep test. The cylinder on the upper end of the tube was for the purpose of expanding the volume of the upper part of the column so that small changes in the volume of the pressure vessel from plate deformation could not make an appreciable change in the column height. The pressure vessel was also equipped with a vent valve and a pressure gage. The pressure gage was used as a check to insure the pressure in the vessel was at the level it should be and not blocked in some way. Test pressure data was obtained by measuring the water column height not by reading the gage.

2. EXPERIMENTAL PROCEDURE

The circular plate specimens, having been cut from a single sheet of commercially rolled lead, were flattened with a hydraulic press and then annealed at 200°C for two hours. After cooling to room temperature a sample plate would be mounted in the test apparatus as shown in Figure 1.3. The chamber of the test apparatus and the pressurizing column were filled with water before putting the sample in place. The sample plate was marked by pencil with concentric circles

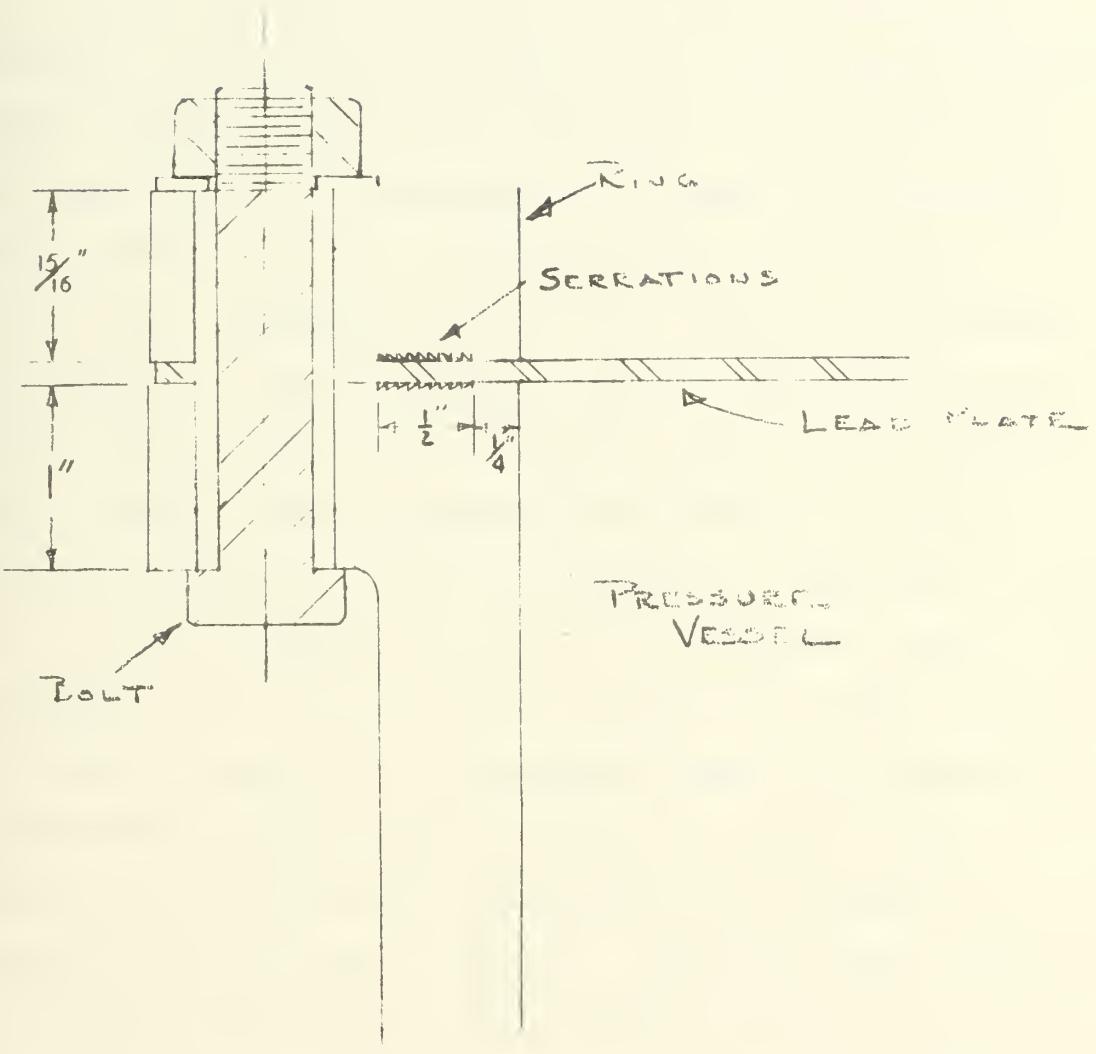

DETAIL OF CLAMPING ARRANGEMENT

FIG. 1.3

from the center at 1/2 inch intervals, and then placed carefully on the upper flange of the test apparatus. The securing ring was then put into position above the specimen and secured with eight bolts tightened to a uniform tension with a torque wrench. The dial indicators, having been previously attached to the securing ring, were then positioned to their desired locations at the center and at intervals along the radius. The assumption was made that deformation was axisymmetric so that readings would be a function of radius only. Observation of the tests revealed no evidence that this was invalid. With the water column adjusted to a height giving the desired hydrostatic pressure the test is ready to begin. Before releasing the pressure, initial readings are taken on all dial indicators. These are the flat plate, or t=0, readings to which all subsequent readings are referred. The test is started by opening the valve between the pressure column and the pressure vessel, thus admitting a hydrostatic pressure to the back of the plate. Dial indicator readings and room temperature are subsequently recorded at various time intervals. Plotting these readings at any given time gives the deformation profile at that time, and plotting the readings at any given radius over all times gives the deformation history. The slope of the deformation history at any particular time is the deformation rate at that time. Of particular interest is the largest deformation which occurs at the center. Two tests were made at each pressure using a different plate of the same thickness in order to check the reproducibility of the results.

3. RESULTS

The results of the plate deformation experiments are summarized in Figures 1.4 through 1.16. Raw data is listed in Appendix F.

Figures 1.4 through 1.6 are plots of the deflection of the center of the plate as a function of time. Two ordinate scales are shown, one for the deflection in inches and another for deflection as a ratio of the corresponding plate thickness.

Figures 1.7 through 1.9 also show center deflection as a function of time, but here all deflections are plotted relative to that at t=1 hour in order to show more clearly the relative deflection rates for different pressures. The time t=1 hour was chosen arbitrarily as a reference point. Some other point could have served equally well.

Figures 1.10 through 1.16 show representative deflection profiles for increasing values of $\frac{w_o}{h}$. The plots are of transverse deflection as a function of radius. Those shown are at time t=1 hour. Similar plots for other times such as t=5 hours show no significant differences. It can be seen from these plots that the deflection profile is approximately bounded by curves of the forms

$$w = w_o\left(1-\frac{r^2}{a^2}\right)^2 \qquad 1.1$$

and

$$w = w_o\left(1-\frac{r^2}{a^2}\right) \qquad 1.2$$

where w_o is deflection at the plate center. For tests at the lower $\frac{w_o}{h}$ ratios, the measured profiles correspond quite closely

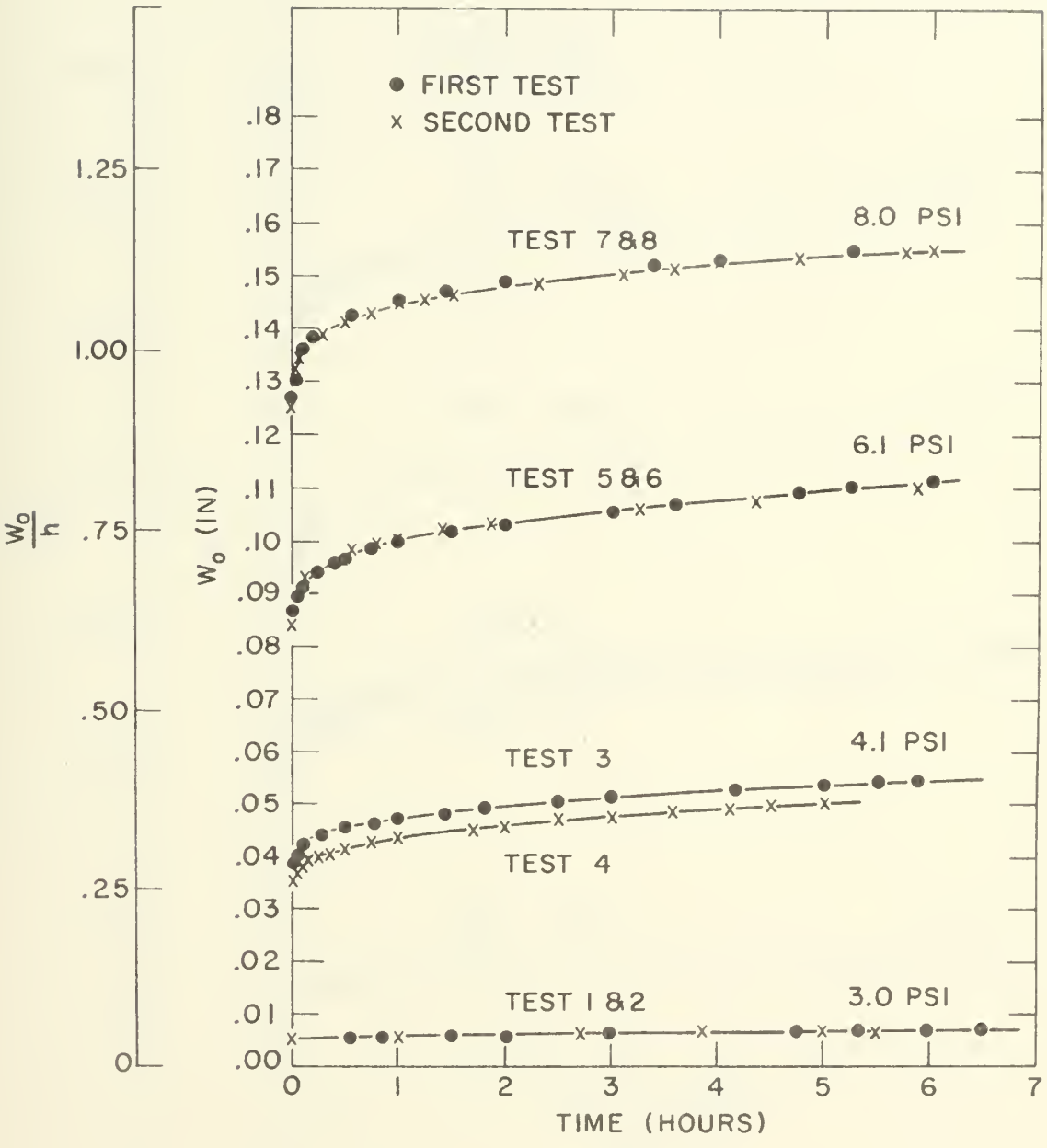

FIG. 1.4

Test Results, 8 lb. plate

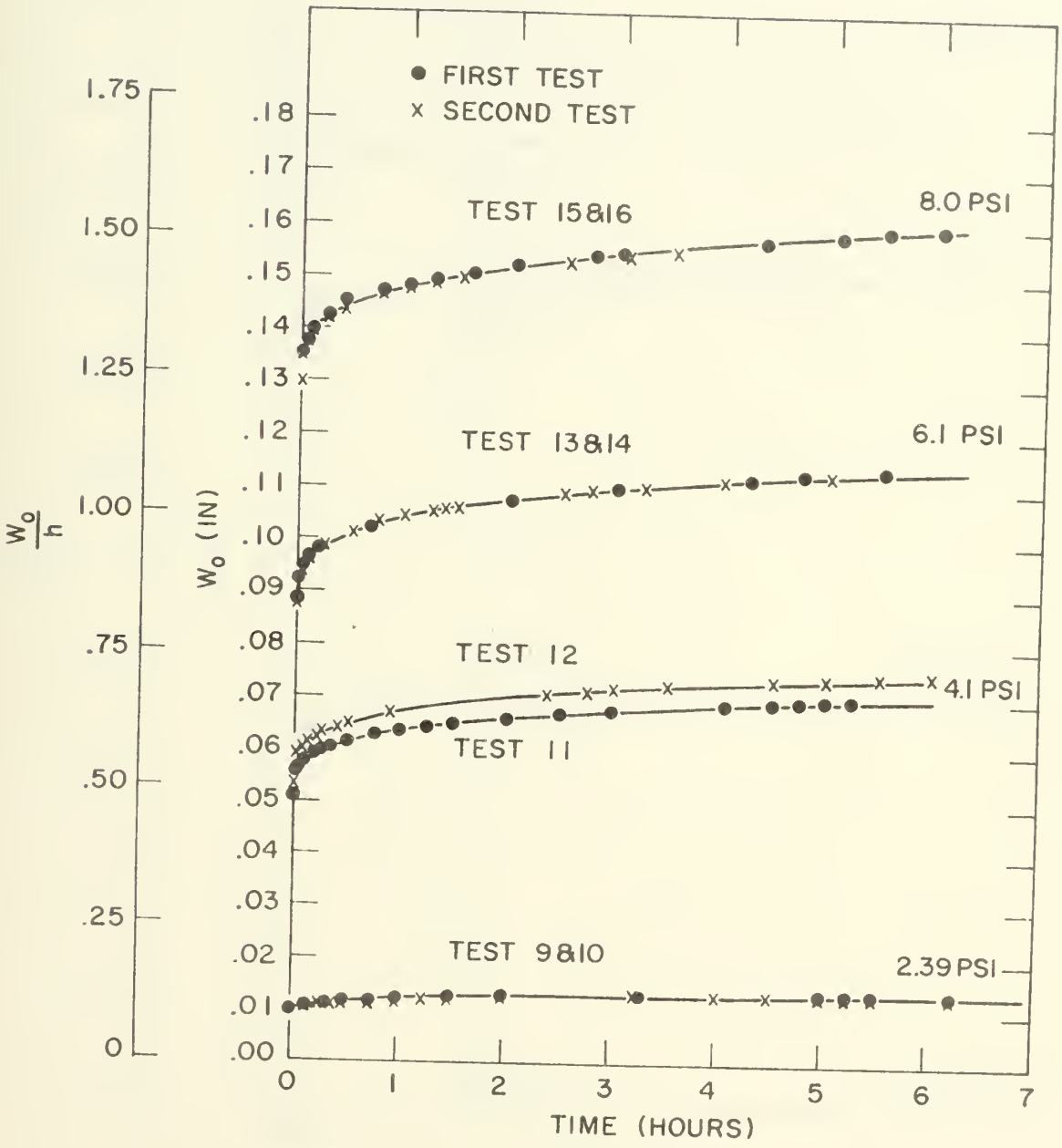

FIG. 1.5

Test Results 6 lb. plate

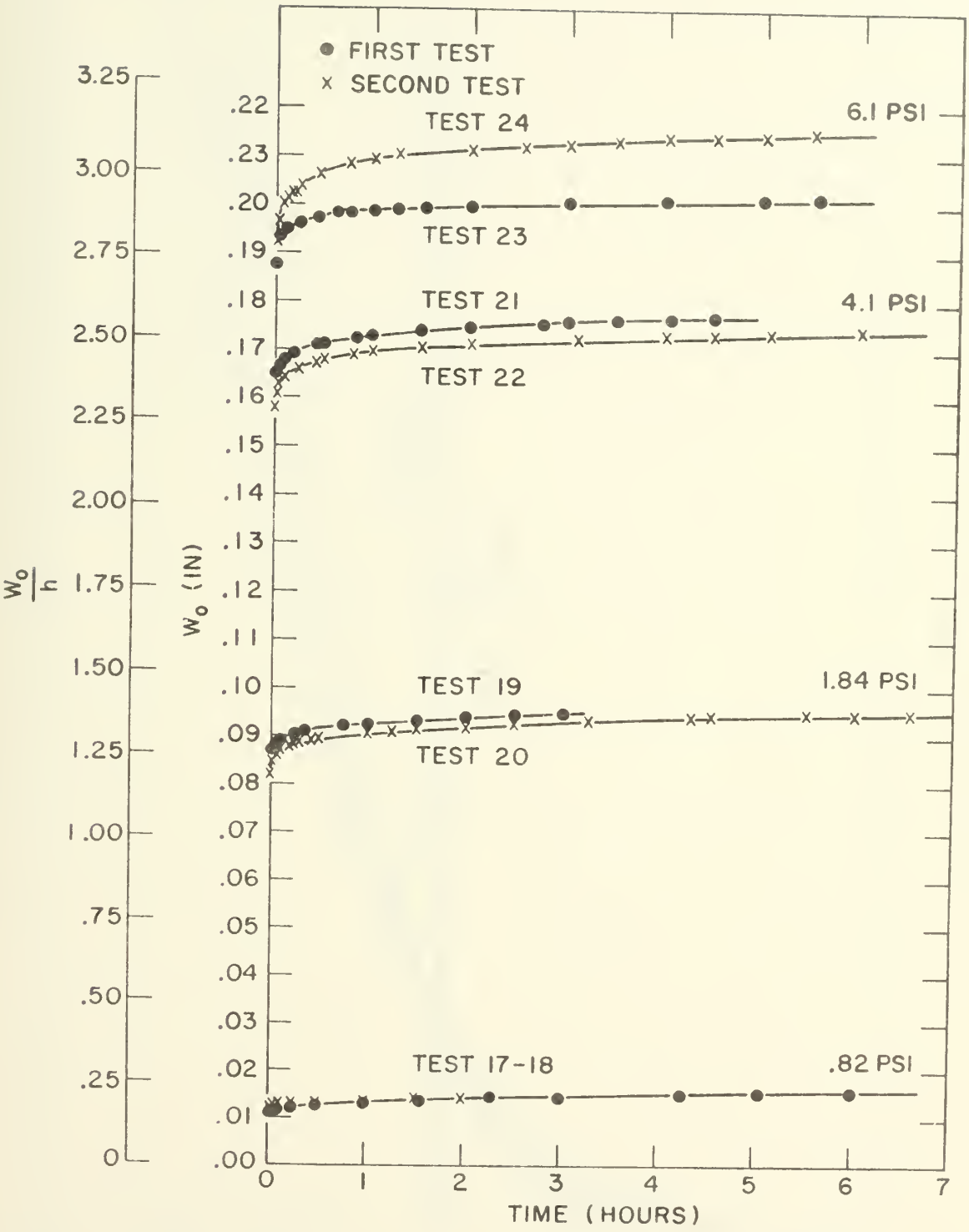

FIG. 1.6

Test Results, 4 lb. plate

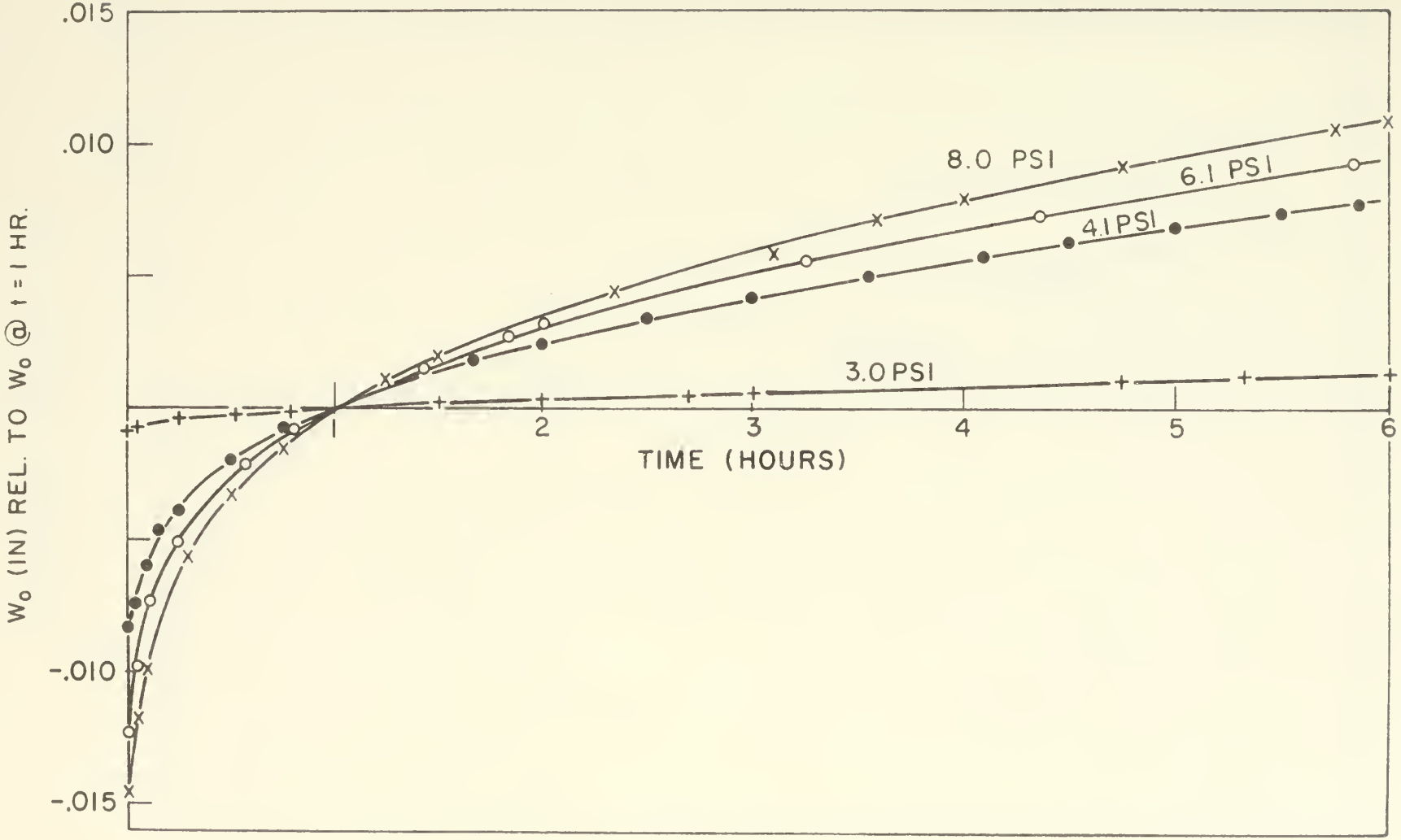

FIG. 1.7

Relative plot of 8 lb. plate results

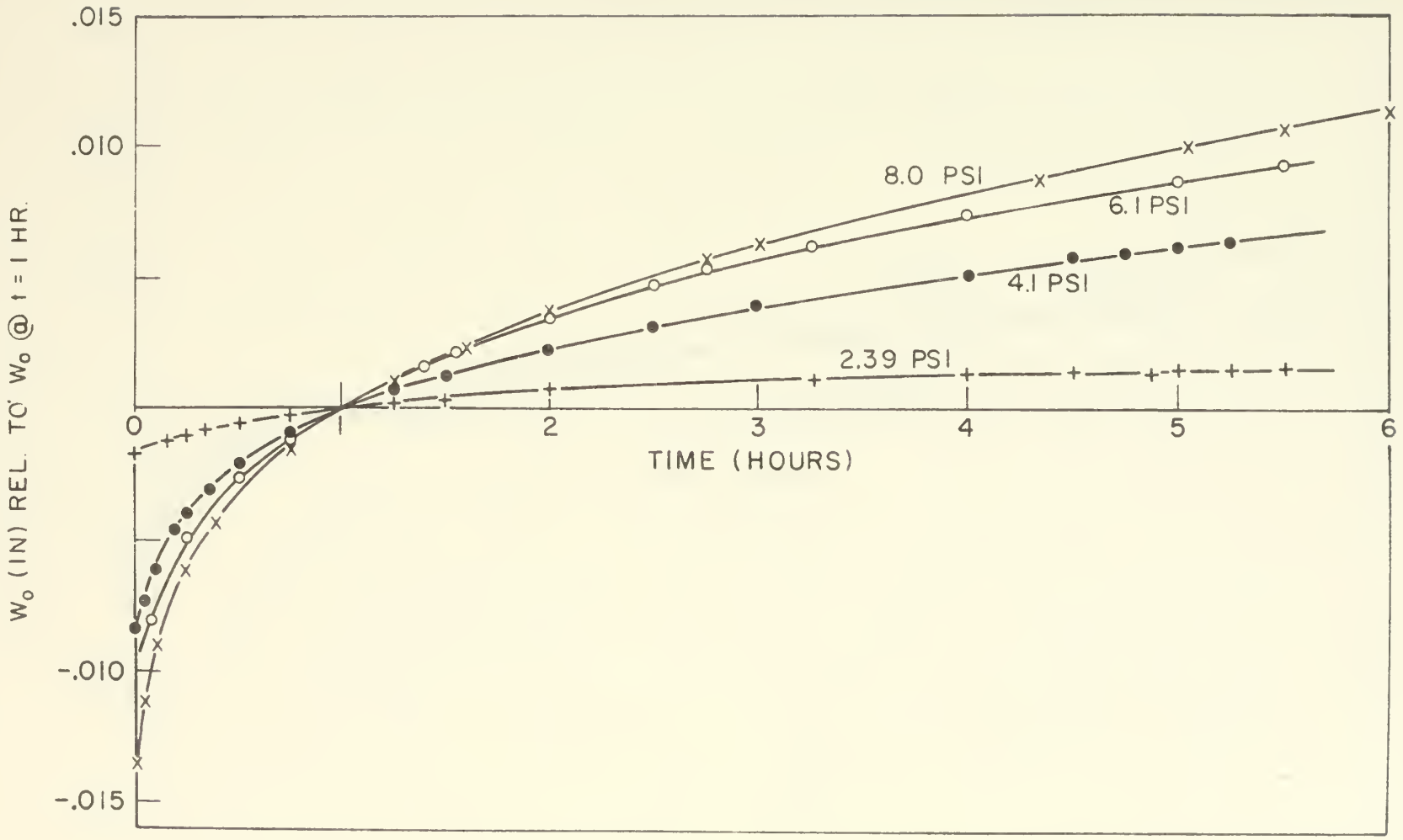

FIG. 1.8

Relative plot of 6 lb. plate results

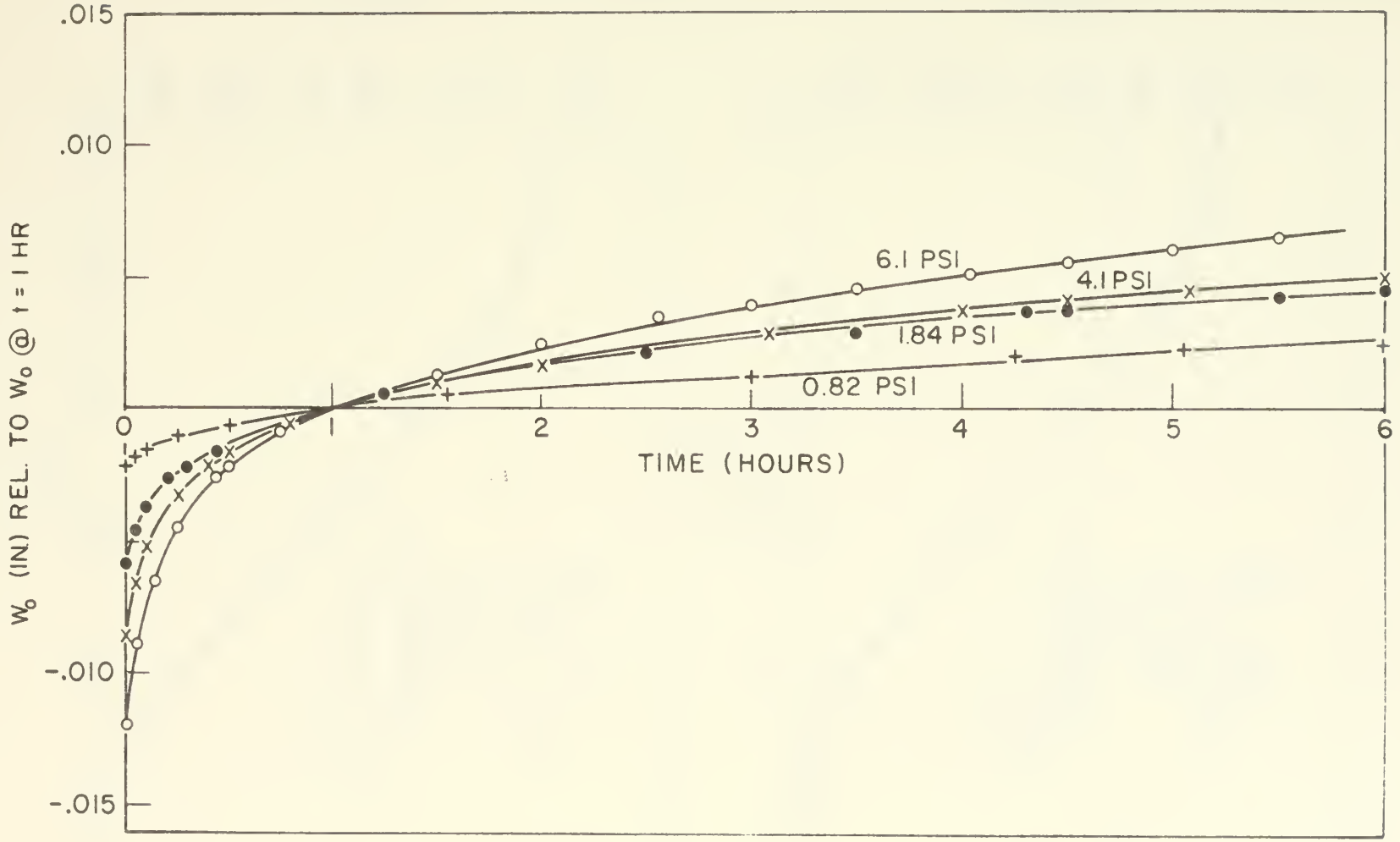

FIG. 1.9

Relative plot of 4 lb. plate results

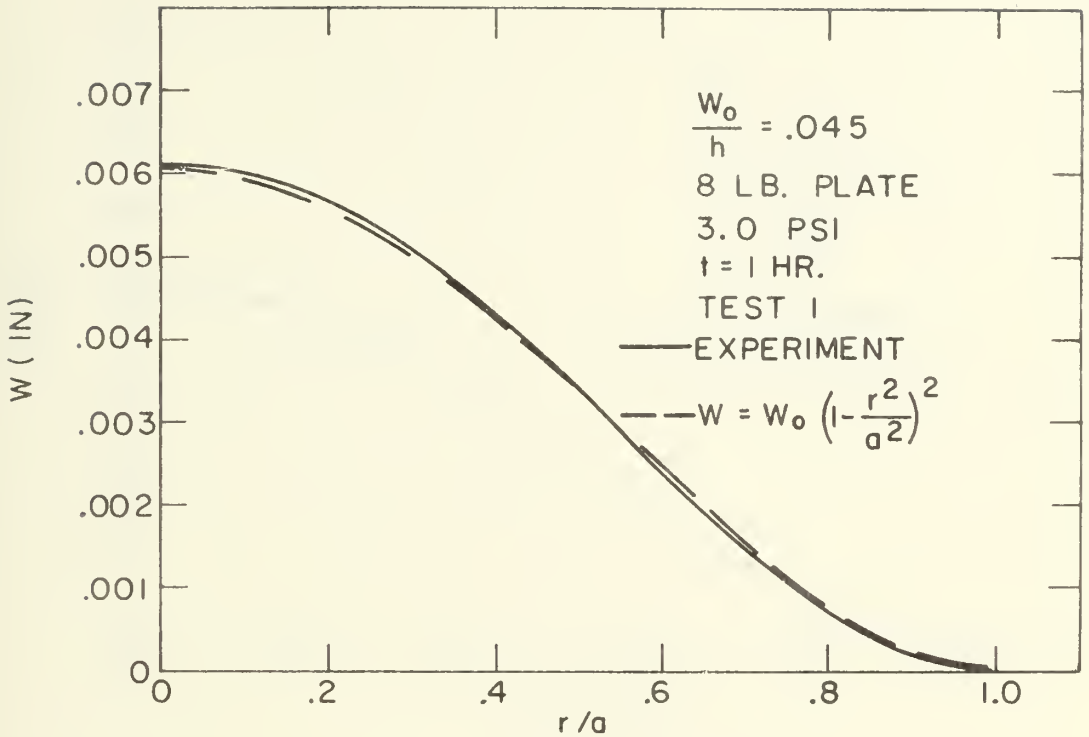

FIG. 1.10

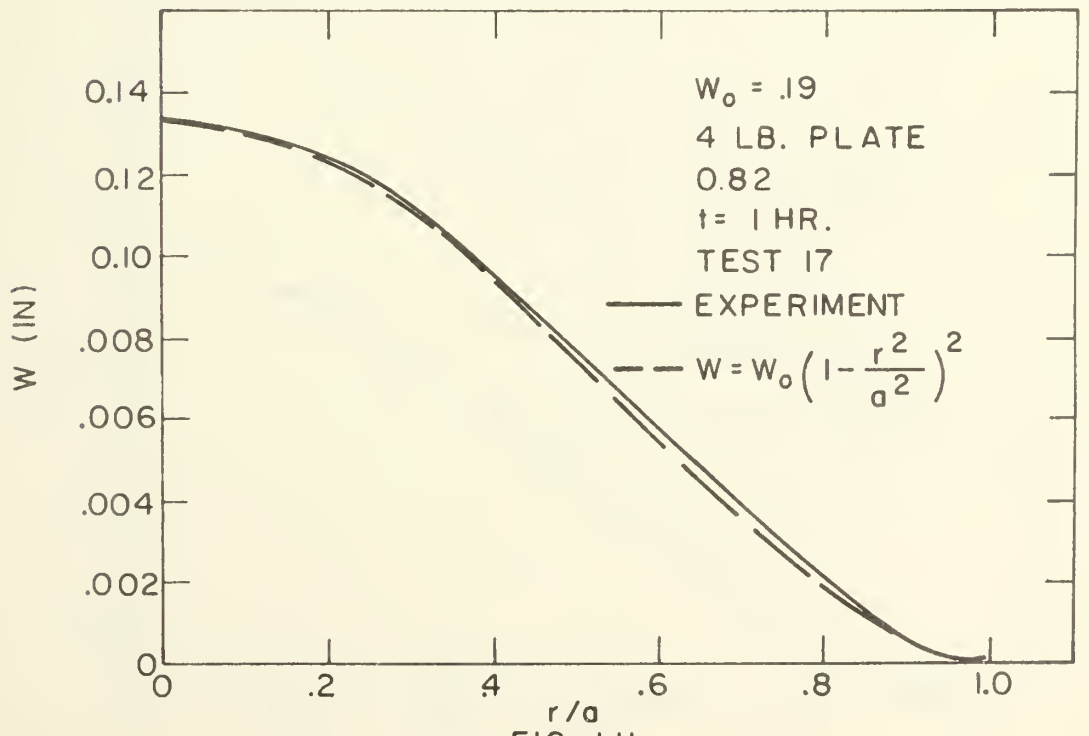

FIG. 1.11

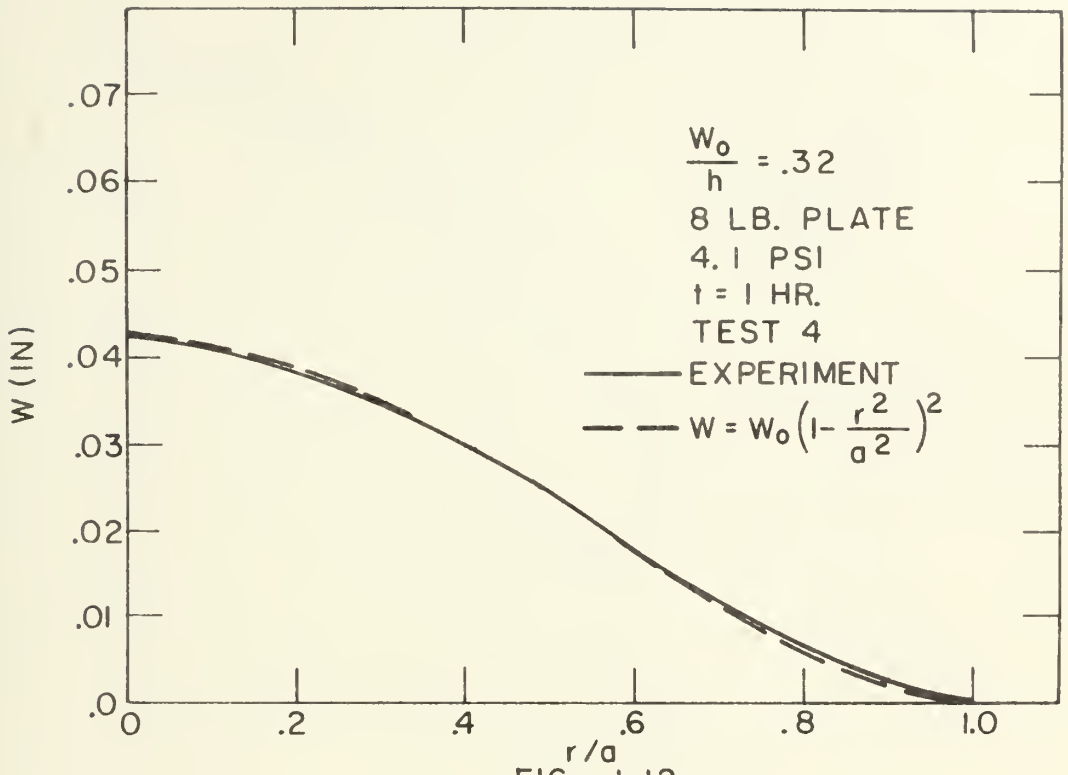

FIG. 1.12

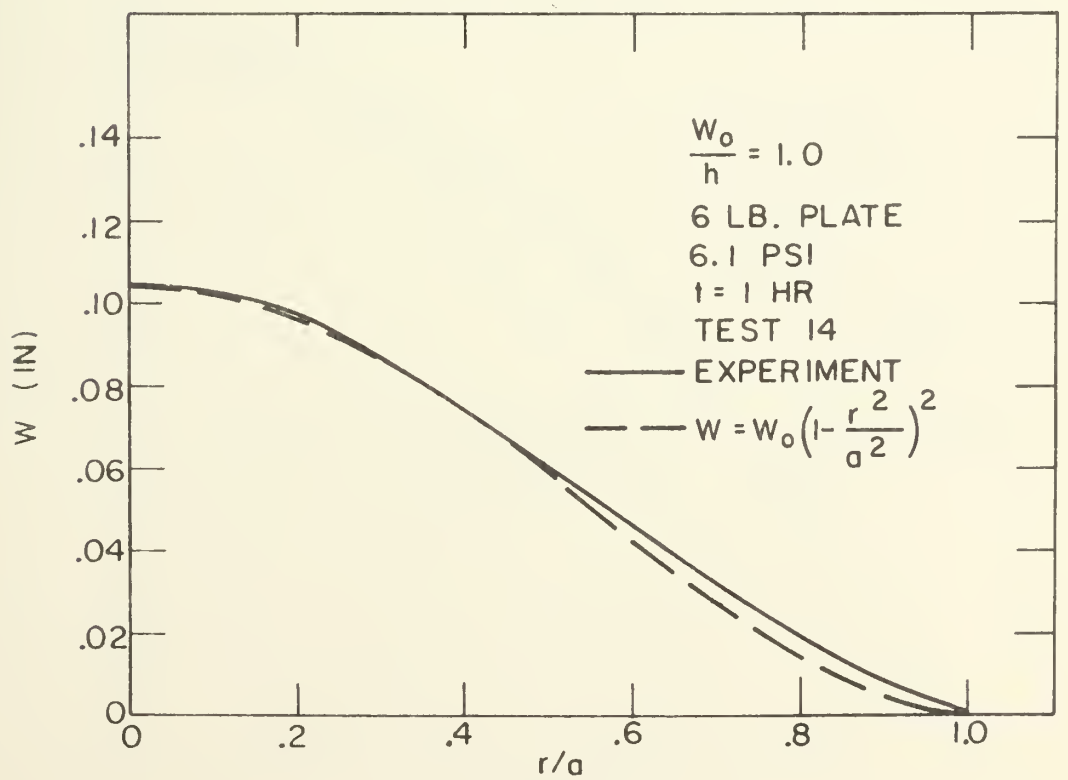

FIG. 1.13

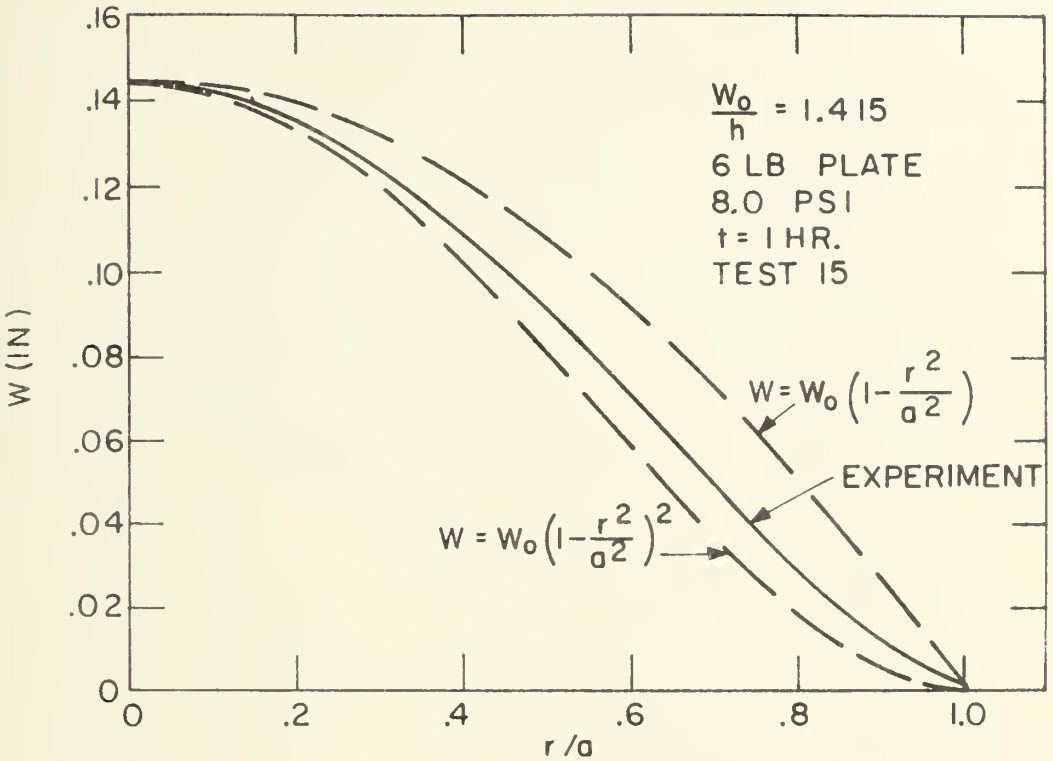

FIG. 1.14

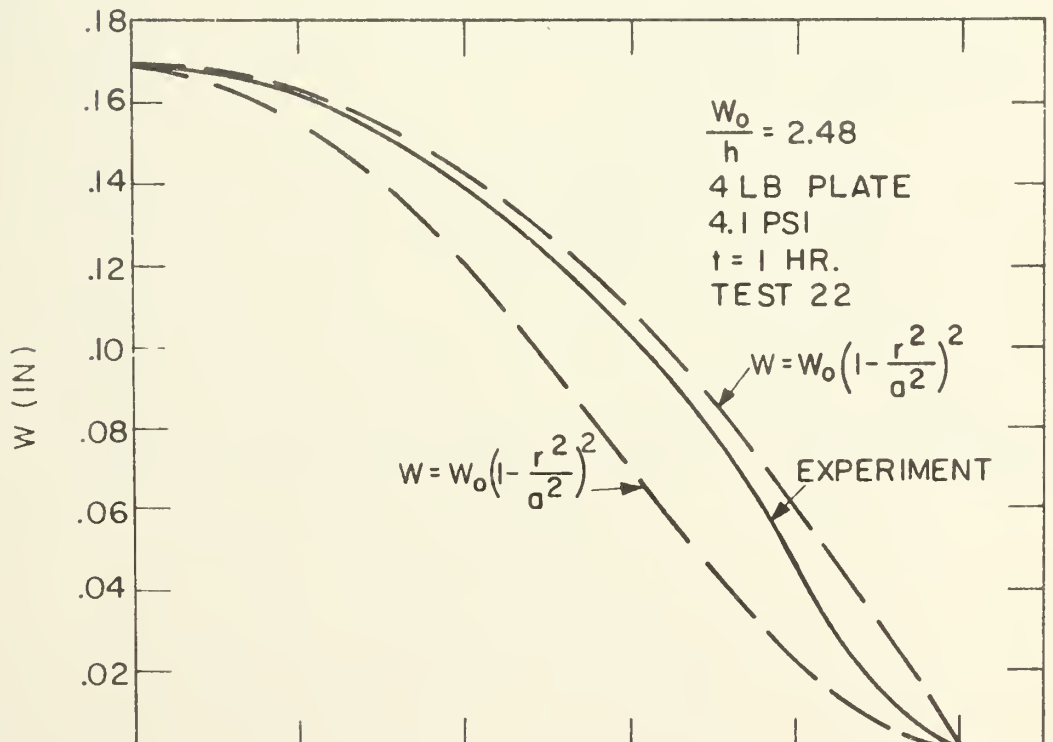

FIG. 1.15

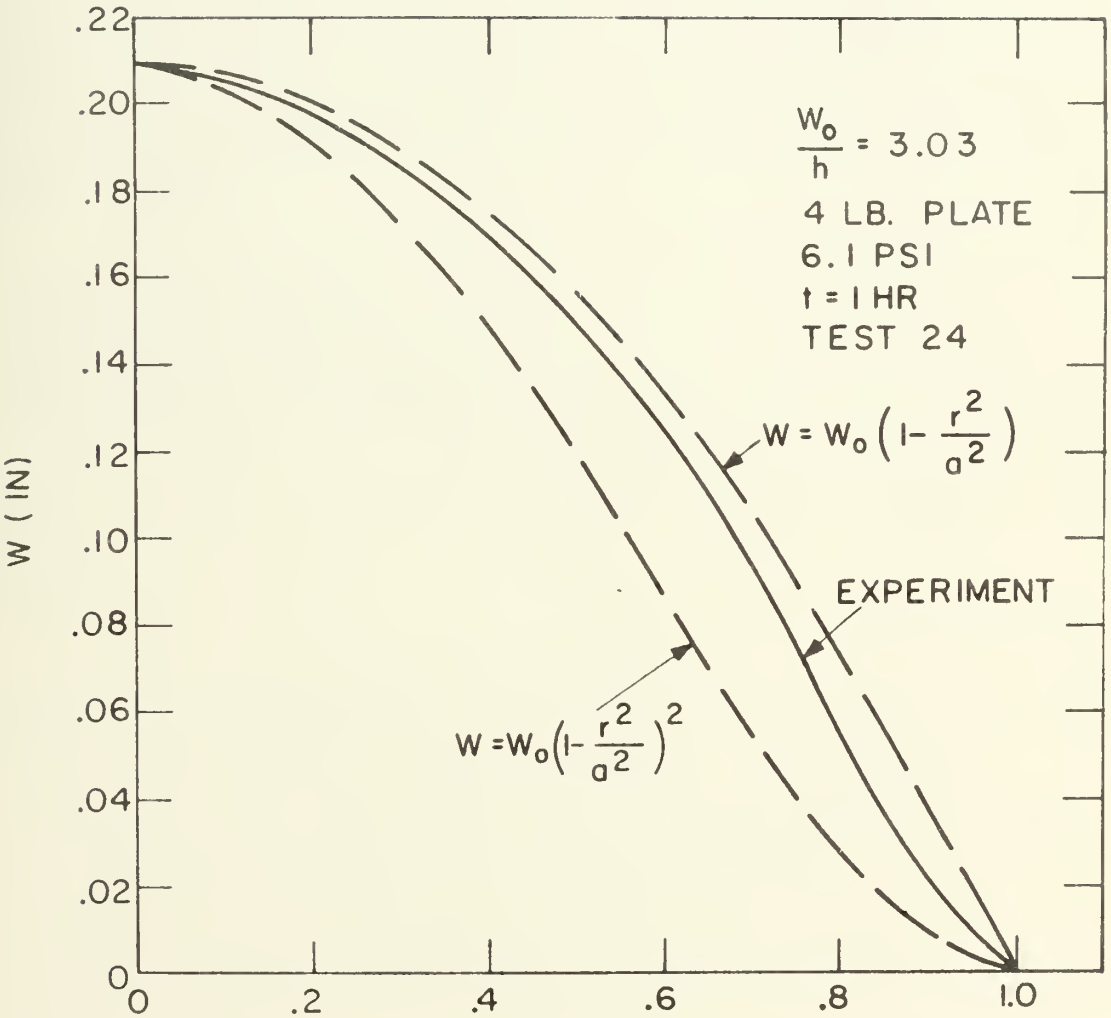
.22
.20
.18
.16
.14
.12
.10
.08
.06
.04
.02
0
W (IN)
0
.2
.4
.6
.8
1.0
r/a
$\frac{W_o}{h}$ = 3.03
4 LB. PLATE
6.1 PSI
t = 1 HR
TEST 24
$W = W_o\left(1-\frac{r^2}{a^2}\right)$
EXPERIMENT
$W = W_o\left(1-\frac{r^2}{a^2}\right)^2$
FIG. 1.16

to the former expression, and at higher $\frac{w_o}{h}$ ratios the observed profile seems to migrate toward the latter parabolic form. This seems rather reasonable as the former expression corresponds to the profile given by Timoshenko (21) for the elastic deformation of a clamped, hydrostatically loaded, circular plate and the latter is the corresponding membrane profile. The fact that the plate behaves in this way was of particular significance in suggesting the method of analysis described in the next chapter.

B. TENSILE CREEP TESTS

1. DESCRIPTION OF APPARATUS

Tensile creep tests were necessary for obtaining the appropriate creep constants, that is, K and n in Norton's law which may be written as:

$$\dot{\varepsilon} = K\sigma^n \qquad 1.3$$

Tensile test specimens were prepared from the same lead sheets from which the plate specimens were made. The tensile specimens were also flattened with the same hydraulic press and annealed for two hours at 200°C in a manner similar to the circular plates. The type of specimen used is illustrated in Figure 1.17D.

The tensile testing apparatus is shown in Figures 1.17 A, B, C, and E. It consists essentially of a frame in which the weighted tensile specimen is suspended and a cathetometer, an optical measuring device, for measuring the distance between two marks inscribed on the specimen. There is also

A. Tensile Test Apparatus

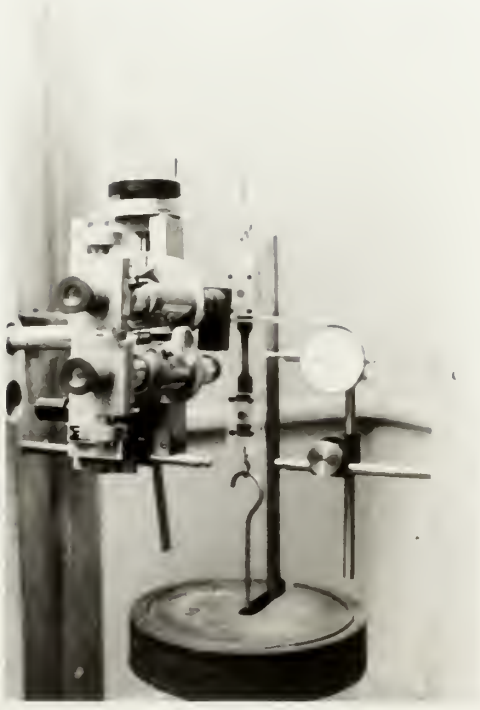

B. Cathetometer and Weight Suspension Arrangement

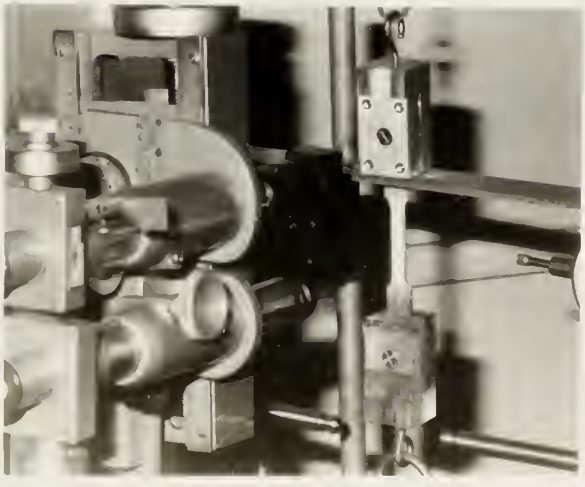

C. Detail of Specimen and Grips

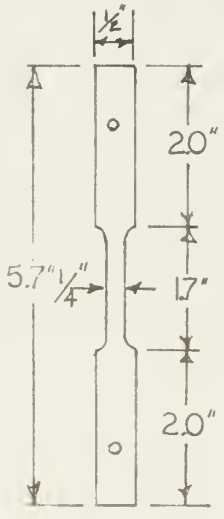

D. Tensile Test Specimen

FIG. 1.17

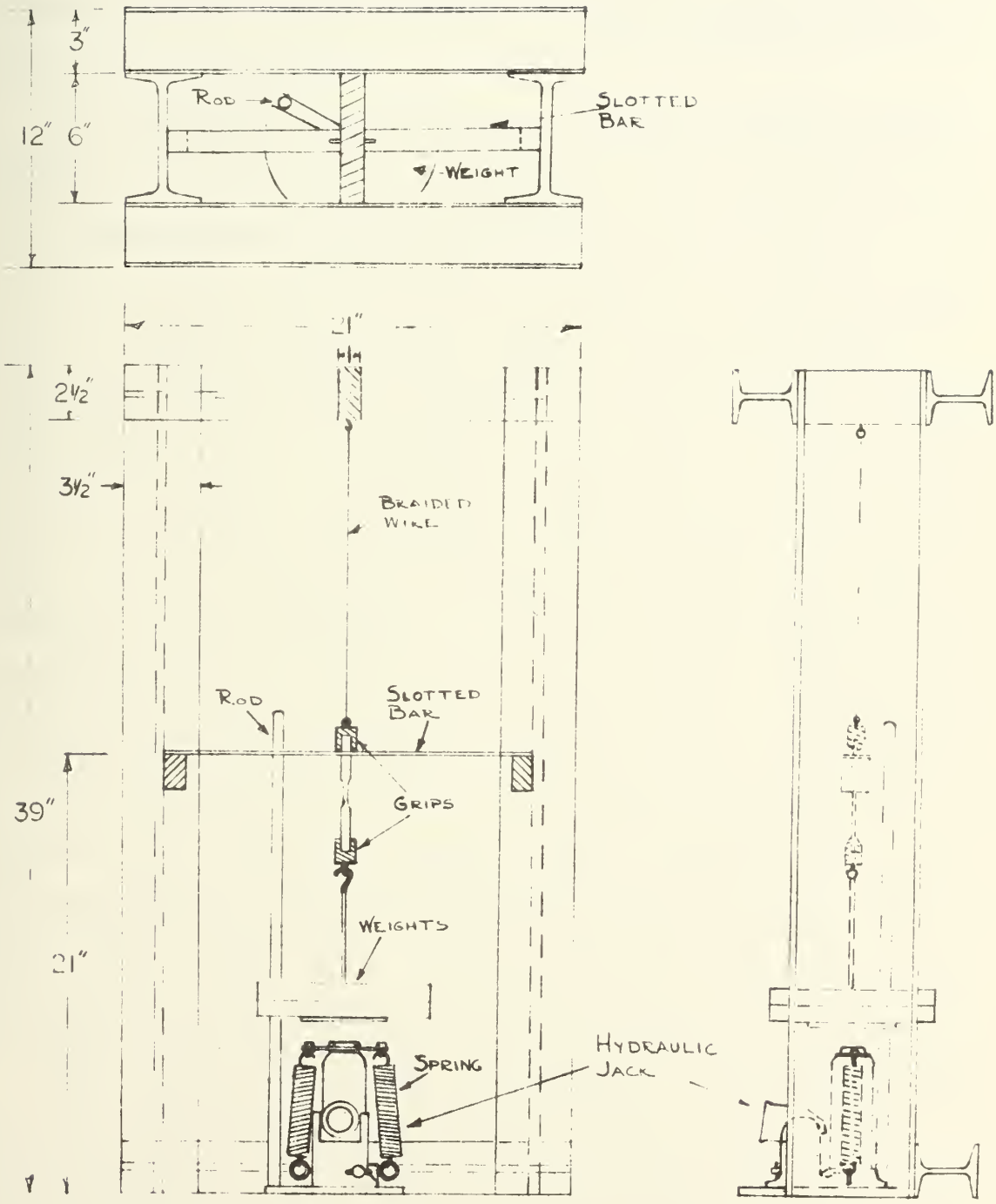

Figure 1.17 E

Tensile Test Apparatus

a modified hydraulic jack used to facilitate the rather important task of smoothly loading the specimen at the commencement of a test. The specimens were loaded with calibrated iron weights mounted on a pan suspended from the lower specimen's grip.

The frame was constructed of aluminum I beams bolted together. The specimen was suspended from an eye mounted in a transverse bar centered in the top of the frame. A flexible braided wire with an eye soldered to each end was used to suspend the specimen. Each of these eyes had its inner edge machined to a knife edge to insure that a specimen would hang freely. A slotted bar, as shown in Figure 1.17C, was used to prevent any rotation of the specimen during the test. This was necessary to insure the marks were always visible by the cathetometer. The bar was placed loosely on its supports and provided only a very gentle, yet sufficient, restraint against any tendency for the specimen to rotate.

The specimen was held between two grips as shown in Figure 1.17C. The upper grip was made of aluminum and the lower of plastic. The use of plastic was to minimize the weight of the lower grip. This assisted in preventing any bending of the specimens while mounting them in the frame.

The initial loading of the specimens was accomplished with the aid of a modified hydraulic jack. Prior to the commencement of a test the weights and weight pan were supported by a small hydraulic jack as shown in Figure 1.17E. The jack is adjusted so that the hook on the weight pan is

barely out of contact with the ring on the lower grip. When the jack's bypass valve is released, two springs draw the piston quickly and smoothly down from the weight pan, thus loading the specimen. As seen in Figure 1.17B the radial slots in the weights ride on a verticle rod. This rod prevents the weights from rotating and twisting the specimen but does not inhibit vertical movement of the weights.

Measurement of tensile strain was accomplished with the aid of the optical device shown in Figure 1.17 A, B, and C, known as a cathetometer. It consists of two telescopes mounted so that they can be moved vertically as a unit or moved apart in the vertical direction. The unit had a vernier for measuring a change in the vertical position of the two telescopes as a unit. Each telescope was equipped with a movable hairline whose deflection from its centered position was measured by a vernier graduated to .0001". By following the separation of two scribed marks initially a known distance apart on the specimen, one can use this instrument to measure creep elongation and have no physical contact with the specimen which could possibly affect the normal deformation process.

2. EXPERIMENTAL PROCEDURE

The tensile specimens, having been prepared from the lead sheet as described in the previous section, were scribed with two thin marks one inch apart on the narrow section of the sample. The scribe marks were made by clamping a one inch gage block over the specimen and drawing a razor blade down

either side of the gage block. Great care was necessary in attaching the grips to the specimen in order to avoid bending the soft lead. A specially prepared block, machined to the proper dimensions, was found useful in this regard for supporting the specimen and grips while they were being attached. The slotted bar, used to prevent rotation of the sample, was placed around the specimen when attaching the grips. This assemblage is then suspended in the frame by placing the hook on the upper grip into the eye at the lower end of the braided wire. The slotted bar rests on ledges placed on either side of the frame. The weight pan is attached to the lower grip and the jack is raised to support the pan. The required weights are then put in place on the pan. The telescopes are adjusted so that, with the crosshairs centered, the crosshair in the upper telescope is aligned with the upper scribe mark and that of the lower telescope with the lower scribe mark. The test is begun by releasing the jack and allowing the weight to be applied to the lower grip. As the specimen strains the scribe marks move away from the crosshairs. The amount of elongation can be measured by keeping the centered crosshair in the upper telescope aligned with the upper scribe mark and moving the lower telescope crosshair to realign it with the lower scribe mark. The amount the lower crosshair is moved can be read from the vernier. The scribe marks, although quite thin to the naked eye, are much wider than the hairline when viewed through the telescope. The accuracy of measurement must therefore be considered as

about ±.0002" rather than within .0001" which is the graduation of the vernier.

By measuring the movement of the scribe marks over a period of time the deformation history of the sample under the given load can be determined. Performing a series of these tests at different loadings yields a family of curves showing the deformation history at different stress levels. By measuring the slope of each curve at some given time one can obtain a strain rate, for that time, at each stress level tested. Plotting strain rate versus stress on a log-log plot will, in the case of a material whose creep properties conform to Norton's law, yeild a straight line from which the creep constants K and n can be determined.

3. RESULTS

Strain versus time for the 8 lb., 6 lb. and 4 lb. plates is plotted in Figures 1.18 and 1.19, Figure 1.20, and in Figures 1.21 and 1.22 respectively. The slopes of these plots are measured at times t=1 hour and t=5 hours. These two times were selected as t=1 hour is a point apparently well within the primary creep region where deformation rate is changing rapidly; and, by constrast, time t=5 hours has an appreciably smaller and nearly constant creep rate more characteristic of secondary creep. Creep rate versus stress is plotted on a log-log scale in Figures 1.23 through 1.25. These data indicate appropriate creep constants as follows:

8 lb. plate	n=3.7	$K = 5.56 \times 10^{-14}$ @ t=1 hr.
		$K = 2.30 \times 10^{-14}$ @ t=5 hrs.
6 lb. plate	n=5.0	$K = 4.10 \times 10^{-18}$ @ t=1 hr.
		$K = 1.70 \times 10^{-18}$ @ t=5 hrs.
4 lb. plate	n=4.0	$K = 8.30 \times 10^{-15}$ @ t=1 hr.
		$K = 3.50 \times 10^{-15}$ @ t=5 hrs.

It is interesting to note the marked differences in the creep characteristics of the samples cut from the three different sheets. All three sheets were made from lead of the same commercial grade and one might have expected them to have exhibited nearly identical creep characteristics. Such was not the case, however, and the differences are too great to be accounted for by experimental error or data scatter. Gifkins (22) made a careful study of the effect of alloying on the creep of lead using lead-thallium alloy. He found that, in very dilute alloys, a change of composition of as little as .01% thallium would result in a significant change in grain size and creep performance. Creep characteristics, therefore, certainly in the case of lead alloys and probably also for other materials, seem to be quite sensitive to small changes in the composition of the material. This means that calculations based on assumed creep constants may be greatly in error unless the constants have been derived from tests on exactly the same material as that being considered.

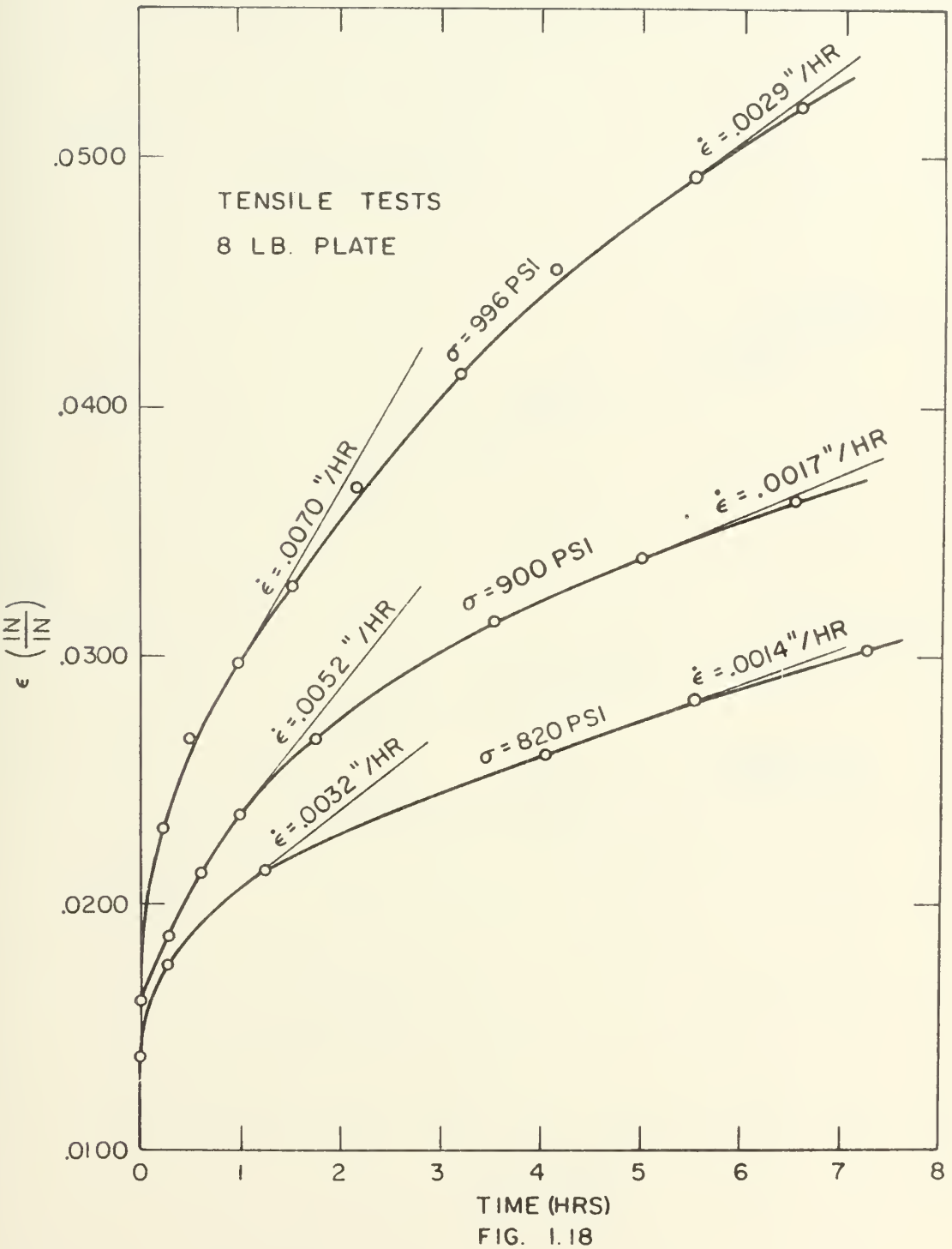
TENSILE TESTS
8 LB. PLATE
$\dot{\epsilon}$ = .0029"/HR
σ = 996 PSI
$\dot{\epsilon}$ = .0070 "/HR
$\dot{\epsilon}$ = .0017"/HR
σ = 900 PSI
$\dot{\epsilon}$ = .0052 "/HR
$\dot{\epsilon}$ = .0014"/HR
σ = 820 PSI
$\dot{\epsilon}$ = .0032"/HR
.0500
.0400
.0300
.0200
.0100
ε (IN/IN)
0
1
2
3
4
5
6
7
8
TIME (HRS)

FIG. 1.18

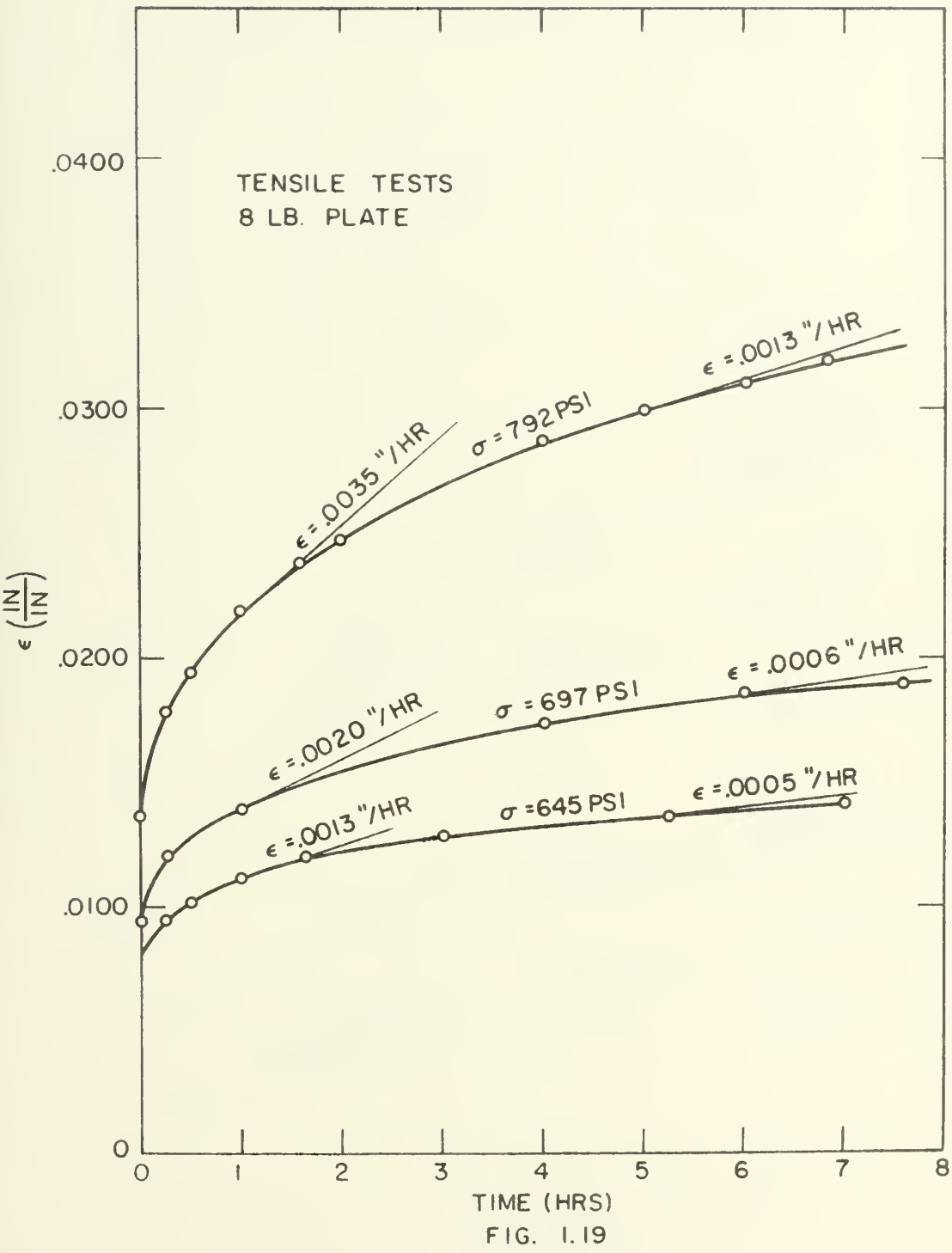
TENSILE TESTS
8 LB. PLATE
.0400
.0300
.0200
.0100
0
ε (IN/IN)
ε = .0035 "/HR
σ = 792 PSI
ε = .0013 "/HR
ε = .0020 "/HR
σ = 697 PSI
ε = .0006 "/HR
ε = .0013 "/HR
σ = 645 PSI
ε = .0005 "/HR
0
1
2
3
4
5
6
7
8
TIME (HRS)

FIG. 1.19

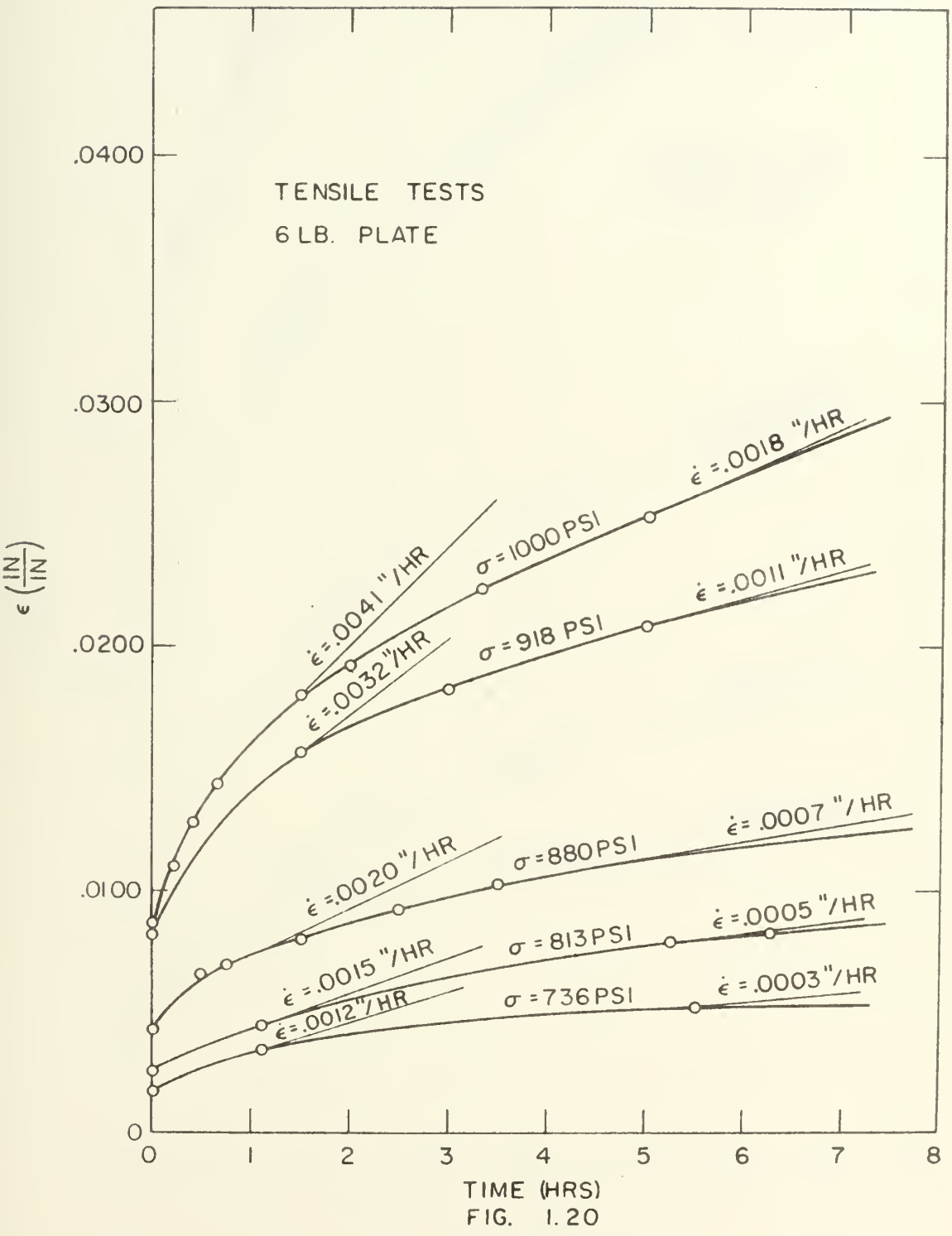
TENSILE TESTS
6 LB. PLATE
.0400
.0300
.0200
.0100
0
ε (IN/IN)
0
1
2
3
4
5
6
7
8
TIME (HRS)
σ = 1000 PSI
σ = 918 PSI
σ = 880 PSI
σ = 813 PSI
σ = 736 PSI
ε̇ = .0041 "/HR
ε̇ = .0032 "/HR
ε̇ = .0018 "/HR
ε̇ = .0011 "/HR
ε̇ = .0020 "/HR
ε̇ = .0015 "/HR
ε̇ = .0012 "/HR
ε̇ = .0007 "/HR
ε̇ = .0005 "/HR
ε̇ = .0003 "/HR

FIG. 1.20

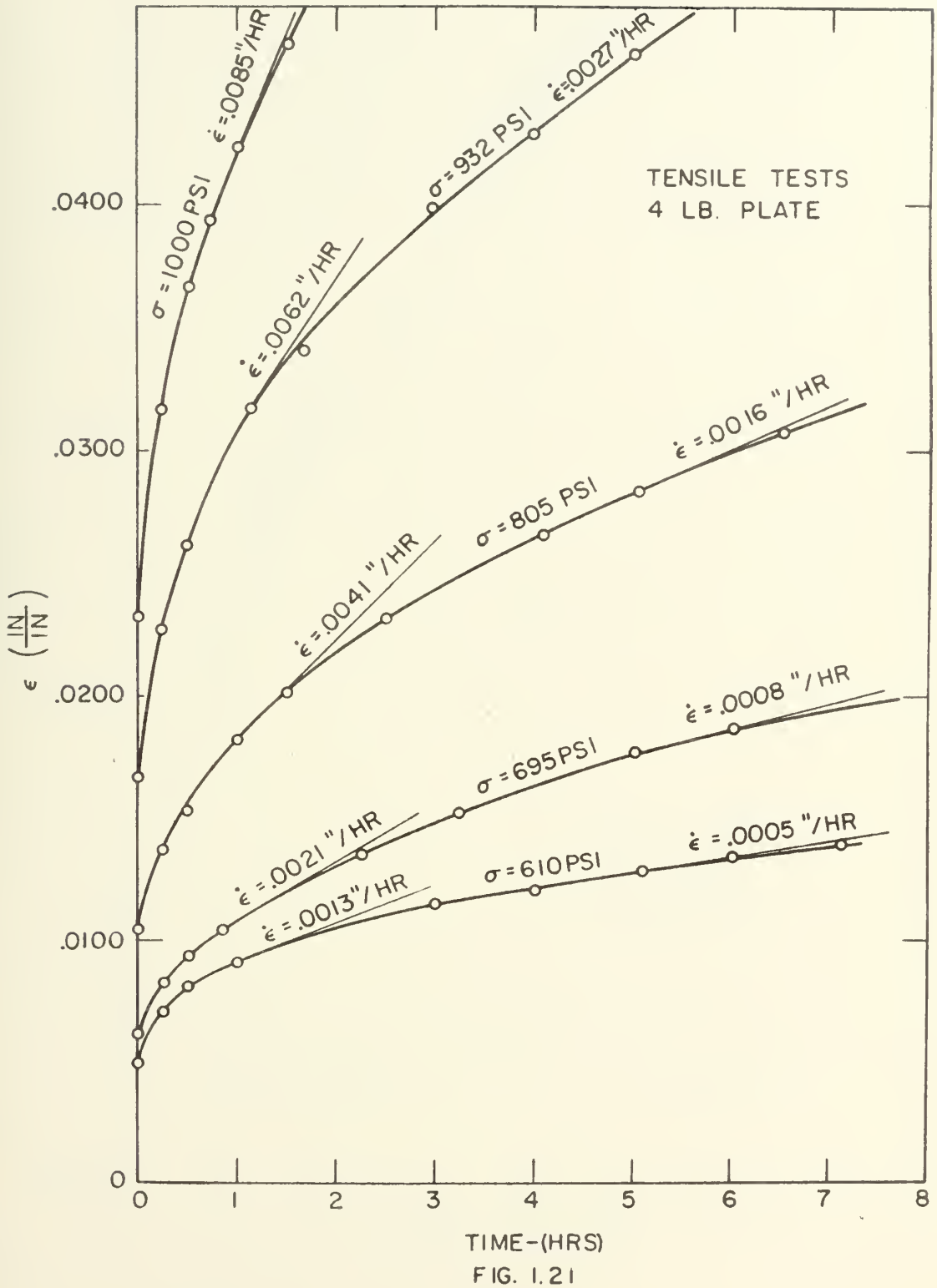
TENSILE TESTS
4 LB. PLATE
σ = 1000 PSI
ε̇ = .0085"/HR
ε̇ = .0062 "/HR
σ = 932 PSI
ε̇ = .0027"/HR
ε̇ = .0041 "/HR
σ = 805 PSI
ε̇ = .0016 "/HR
ε̇ = .0021 "/HR
σ = 695 PSI
ε̇ = .0008 "/HR
ε̇ = .0013"/HR
σ = 610 PSI
ε̇ = .0005 "/HR
ε (IN/IN)
.0400
.0300
.0200
.0100
0
0
1
2
3
4
5
6
7
8
TIME-(HRS)
FIG. 1.21

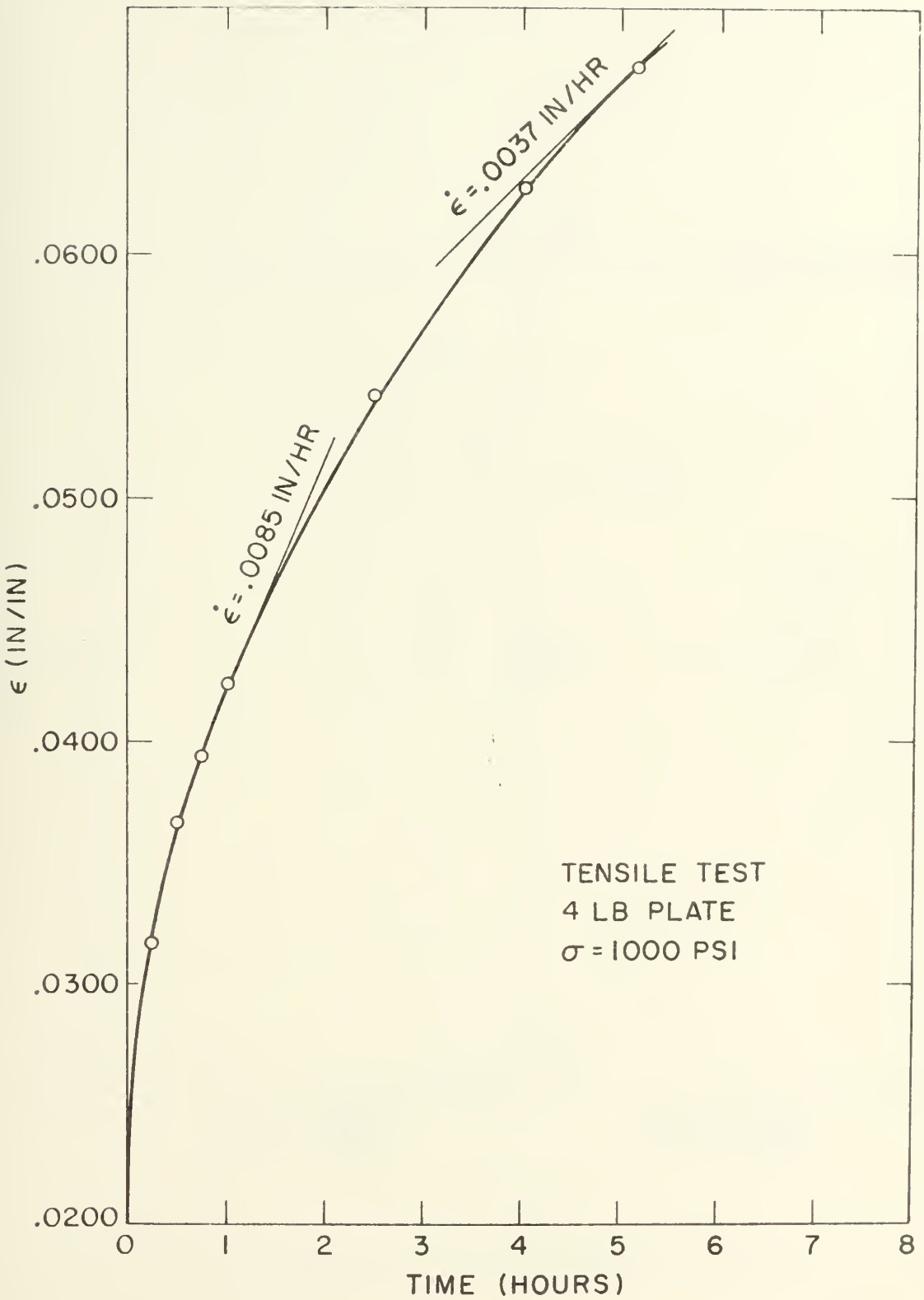
.0600
.0500
.0400
.0300
.0200
ε (IN/IN)
$\dot{\epsilon}$=.0037 IN/HR
$\dot{\epsilon}$=.0085 IN/HR
TENSILE TEST
4 LB PLATE
σ = 1000 PSI
0
1
2
3
4
5
6
7
8
TIME (HOURS)

FIG. 1.22

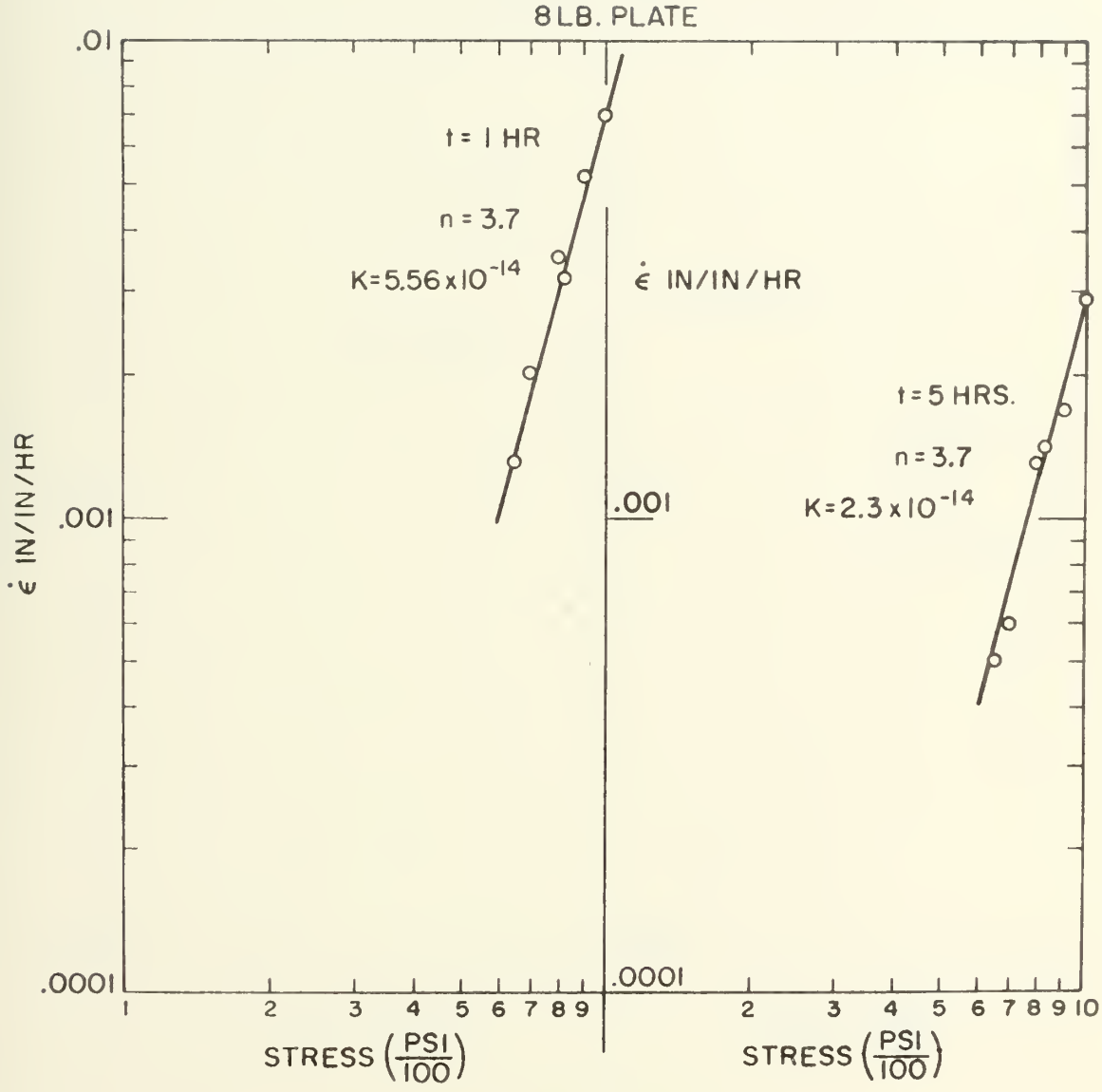

FIG. 1.23

Log-Log plot of Tensile Test Results, 8 lb. plate

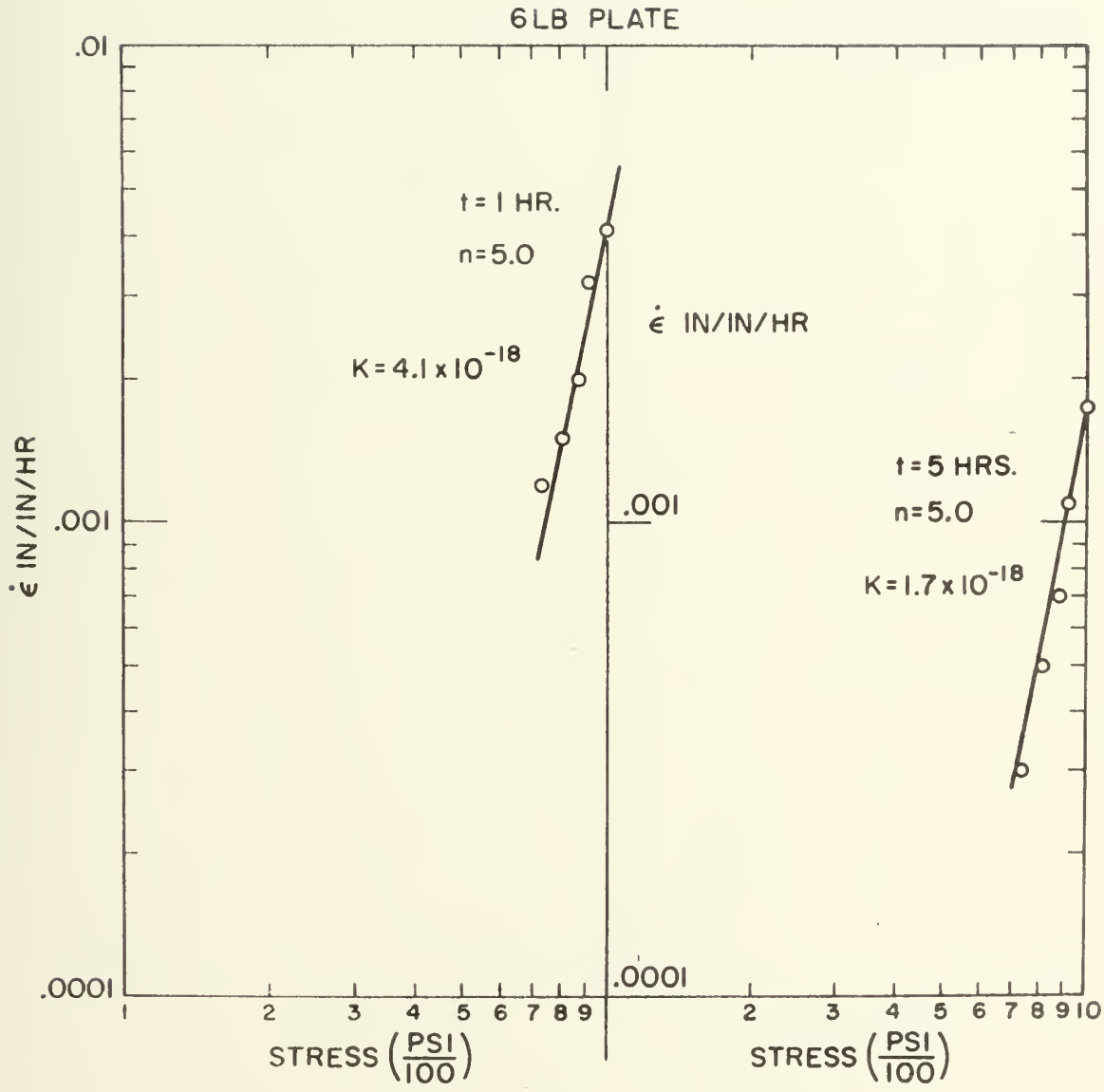

FIG. 1.24

Log-Log plot of Tensile Test Results,
6 lb. plate

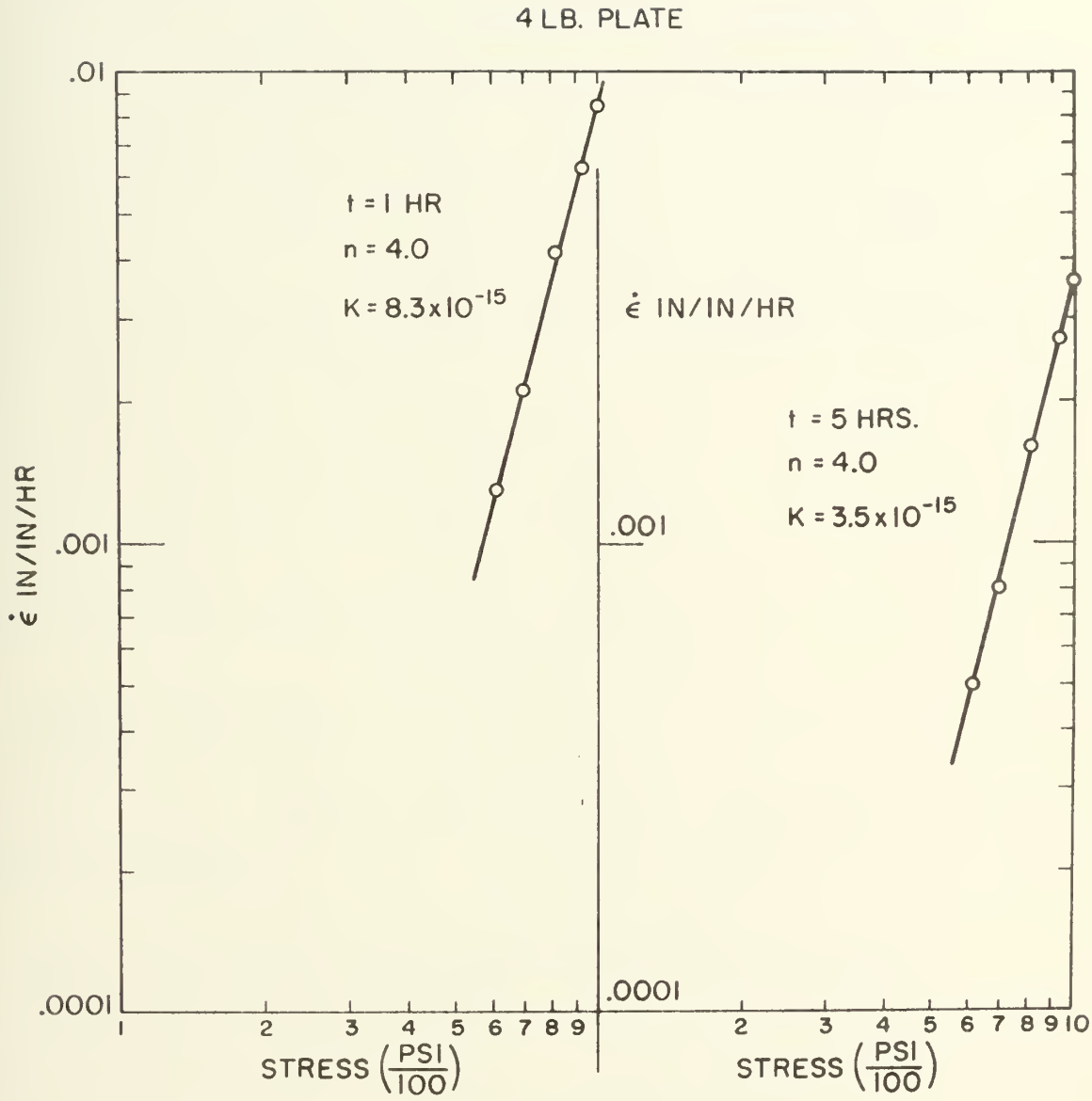

FIG. 1.25

Log-Log plot of Tensile Test Results,
4 lb. plate

CHAPTER II

Theoretical Analysis

A. ASSUMPTIONS

Consider the case of a homogeneous, incompressible, isotropic, circular plate subjected to a time-independent, lateral, hydrostatic pressure. The plate is assumed to be sufficiently thin for the problem to be treated as plane stress with $\sigma_z = 0$. We assume the creep behavior of the material may be modeled in the manner discussed in Appendix A, which for this case gives:

$$\dot{\varepsilon}_1 = K[|\sigma_r|^n \operatorname{sgn} \sigma_r - \tfrac{1}{2}|\sigma_\theta|^n \operatorname{sgn} \sigma_\theta] \qquad 2.1$$

$$\dot{\varepsilon}_2 = K[|\sigma_\theta|^n \operatorname{sgn} \sigma_\theta - \tfrac{1}{2}|\sigma_r|^n \operatorname{sgn} \sigma_r] \qquad 2.2$$

where sgn is the signum function defined as

$$\operatorname{sgn} x = \begin{cases} +1 & x>0 \\ -1 & x<0 \end{cases}$$

In this form 2.1 and 2.2 can be used for negative as well as positive stresses.

B. BASIC EXPRESSIONS FOR MOMENTS AND IN-PLANE FORCES

Solving 2.1 and 2.2 for σ_r and σ_θ in terms of the strain rates we find:

$$\sigma_r = (\tfrac{4}{3K})^{1/n} |\dot{\varepsilon}_r + \tfrac{1}{2}\dot{\varepsilon}_\theta|^{1/n} \operatorname{sgn} (\dot{\varepsilon}_r + \tfrac{1}{2}\dot{\varepsilon}_\theta) \qquad 2.3$$

$$\sigma_\theta = (\tfrac{4}{3K})^{1/n} |\dot{\varepsilon}_\theta + \tfrac{1}{2}\dot{\varepsilon}_r|^{1/n} \operatorname{sgn} (\dot{\varepsilon}_\theta + \tfrac{1}{2}\dot{\varepsilon}_r) \qquad 2.4$$

The extensional strains along the middle surface of the

plate will be denoted as e_r and e_θ and the curvature of the neutral surface as κ_r and κ_θ. Adopting the Kirchoff assumption that sections which are plane before deformation remain plane during deformation, the total strains, ε_r and ε_θ, at any point along the thickness of the plate may be written as:

$$\varepsilon_r = e_r + z\kappa_r \qquad 2.5$$

$$\varepsilon_\theta = e_\theta + z\kappa_\theta \qquad 2.6$$

where z is the distance from the middle surface. Notation and sign conventions are as shown in Figure 2.1. Taking derivatives of 2.5 and 2.6 with respect to time gives the strain rates:

$$\dot{\varepsilon}_r = \dot{e}_r + z\dot{\kappa}_r \qquad 2.7a$$

$$\dot{\varepsilon}_\theta = \dot{e}_\theta + z\dot{\kappa}_\theta \qquad 2.7b$$

Substituting into 2.3 and 2.4:

$$\sigma_r = \left(\frac{4}{3K}\right)^{1/n} \left|\dot{e}_r + \tfrac{1}{2}\dot{e}_\theta + z(\dot{\kappa}_r + \tfrac{1}{2}\dot{\kappa}_\theta)\right|^{1/n} \qquad 2.8$$

$$\operatorname{sgn}[\dot{e}_r + \tfrac{1}{2}\dot{e}_\theta + z(\dot{\kappa}_r + \tfrac{1}{2}\dot{\kappa}_\theta)]$$

$$\sigma_\theta = \left(\frac{4}{3K}\right)^{1/n} \left|\dot{e}_\theta + \tfrac{1}{2}\dot{e}_r + z(\dot{\kappa}_\theta + \tfrac{1}{2}\dot{\kappa}_r)\right|^{1/n} \qquad 2.9$$

$$\operatorname{sgn}[\dot{e}_\theta + \tfrac{1}{2}\dot{e}_r + z(\dot{\kappa}_\theta + \tfrac{1}{2}\dot{\kappa}_r)]$$

From this point conventional notation for the signum function will become rather onerous and we shall define the symbol

$$\left|f(x_1, x_2, \text{----}x_n)\right|_s^p$$

as meaning the absolute value of the function f is raised to the power p, the result is then assigned the sign which function $f(x_1, x_2, \text{----}x_n)$ assumes when evaluated with the

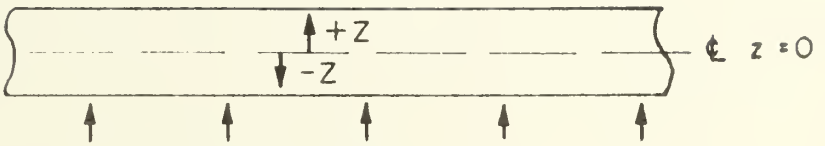

SECTION OF PLATE

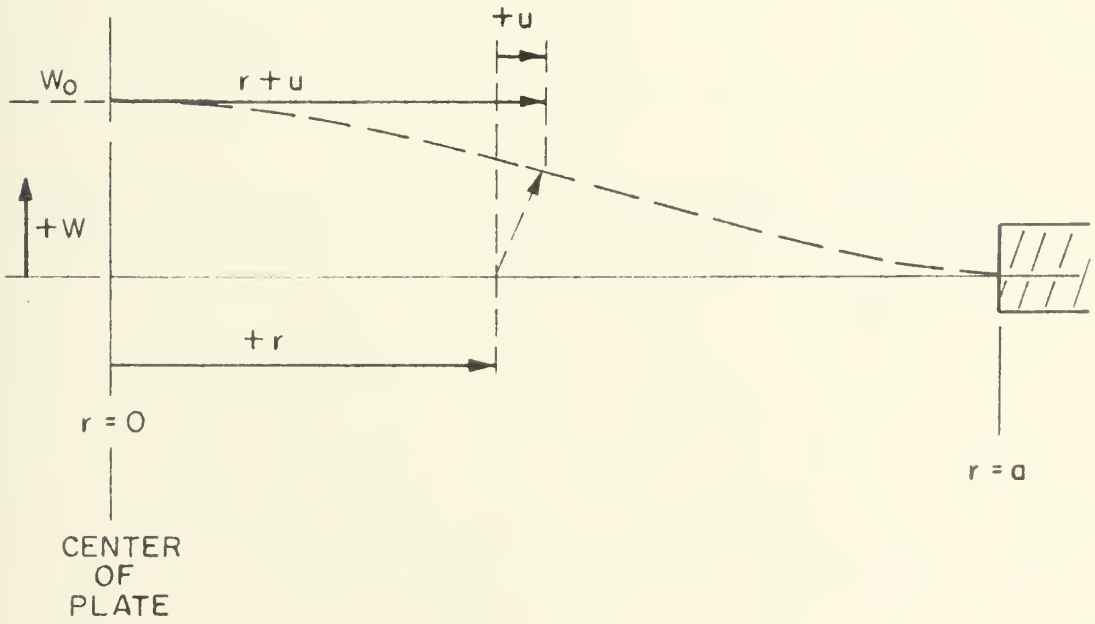

CIRCULAR PLATE PROFILE
AND NOTATION

FIG. 2.1

appropriate arguments (x_1, x_2, ----x_n) for the case in question.

Considering a homogeneous thin plate we may compute in-plane equivalent forces per unit length, N_r and N_θ, as:

$$N_r = \int_{-\frac{h}{2}}^{\frac{h}{2}} \sigma_r dz \qquad 2.10$$

$$N_\theta = \int_{-\frac{h}{2}}^{\frac{h}{2}} \sigma_\theta dz \qquad 2.11$$

Equivalent moments per unit length are:

$$M_r = \int_{-\frac{h}{2}}^{\frac{h}{2}} \sigma_r z dz \qquad 2.12$$

$$M_\theta = \int_{-\frac{h}{2}}^{\frac{h}{2}} \sigma_\theta z dz \qquad 2.13$$

By substituting (2.8) and (2.9) into the above equations, (2.10) through (2.13), and integrating over z, we may obtain expressions for the plate force and moment resultants, N_r, N_θ, M_r, and M_θ. Some care, however, must be exercised in performing this integration. The signs of various terms in the result depend upon the relative magnitude and directional sense of the extensional strain rate and the curvature rates in the plate. It can be shown, however, that upon integration all cases may be represented by expressions of the form:

$$N_r = \left(\frac{4}{3K}\right)^{1/n} \frac{n}{n+1} \frac{1}{\dot{\kappa}_r + \frac{1}{2}\dot{\kappa}_\theta} \left[\left|\dot{e}_r+\tfrac{1}{2}\dot{e}_\theta + \frac{h}{2}(\dot{\kappa}_r+\tfrac{1}{2}\dot{\kappa}_\theta)\right|^{1+1/n}\right.$$

$$\left. -\left|\dot{e}_r+\tfrac{1}{2}\dot{e}_\theta-\frac{h}{2}(\dot{\kappa}_r+\tfrac{1}{2}\dot{\kappa}_\theta)\right|^{1+1/n}\right] \qquad 2.14$$

$$N_\theta = \left(\frac{4}{3K}\right)^{1/n} \frac{n}{n+1} \frac{1}{\dot{\kappa}_\theta + \frac{1}{2}\dot{\kappa}_r} \left[\left|\dot{e}_\theta +\tfrac{1}{2}\dot{e}_r + \frac{h}{2}(\dot{\kappa}_\theta+\tfrac{1}{2}\dot{\kappa}_r)\right|^{1+1/n}\right.$$

$$\left. -\left|\dot{e}_\theta+\tfrac{1}{2}\dot{e}_r - \frac{h}{2}(\dot{\kappa}_\theta+\tfrac{1}{2}\dot{\kappa}_r)\right|^{1+1/n}\right] \qquad 2.15$$

$$M_r = \left(\frac{4}{3K}\right)^{1/n} \frac{n}{n+1} \frac{1}{\dot{\kappa}_r + \frac{1}{2}\dot{\kappa}_\theta} \left[\frac{h}{2}\left|\dot{e}_r+\tfrac{1}{2}\dot{e}_\theta+\frac{h}{2}(\dot{\kappa}_r+\tfrac{1}{2}\dot{\kappa}_\theta)\right|^{1+1/n}\right.$$

$$- \frac{n}{(2n+1)(\dot{\kappa}_r+\frac{1}{2}\dot{\kappa}_\theta)} \left|\dot{e}_r+\tfrac{1}{2}\dot{e}_\theta +\frac{h}{2}(\dot{\kappa}_r+\tfrac{1}{2}\dot{\kappa}_\theta)\right|_s^{2+1/n}$$

$$+ \frac{h}{2}\left|\dot{e}_r+\tfrac{1}{2}\dot{e}_\theta-\frac{h}{2}(\dot{\kappa}_r+\tfrac{1}{2}\dot{\kappa}_\theta)\right|^{1+1/n} + \frac{n}{(2n+1)(\dot{\kappa}_r+\frac{1}{2}\dot{\kappa}_\theta)}$$

$$\left.\left|\dot{e}_r + \tfrac{1}{2}\dot{e}_\theta - \frac{h}{2}(\dot{\kappa}_r+\tfrac{1}{2}\dot{\kappa}_\theta)\right|_s^{2+1/n}\right] \qquad 2.16$$

$$M_\theta = \left(\frac{4}{3K}\right)^{1/n} \frac{n}{n+1} \frac{1}{\dot{\kappa}_\theta + \frac{1}{2}\dot{\kappa}_r} \left[\frac{h}{2}\left|\dot{e}_\theta +\tfrac{1}{2}\dot{e}_r+\frac{h}{2}(\dot{\kappa}_\theta+\tfrac{1}{2}\dot{\kappa}_r)\right|^{1+1/n}\right.$$

$$- \frac{n}{(2n+1)(\dot{\kappa}_\theta+\frac{1}{2}\dot{\kappa}_r)} \left|\dot{e}_\theta +\tfrac{1}{2}\dot{e}_r + \frac{h}{2}(\dot{\kappa}_\theta+\tfrac{1}{2}\dot{\kappa}_r)\right|_s^{2+1/n}$$

$$+ \frac{h}{2}\left|\dot{e}_\theta+\tfrac{1}{2}\dot{e}_r - \frac{h}{2}(\dot{\kappa}_\theta+\tfrac{1}{2}\dot{\kappa}_r)\right|^{1+1/n} + \frac{n}{(2n+1)(\dot{\kappa}_\theta+\frac{1}{2}\dot{\kappa}_r)}$$

$$\left.\left|\dot{e}_\theta+\tfrac{1}{2}\dot{e}_r - \frac{h}{2}(\dot{\kappa}_\theta+\tfrac{1}{2}\dot{\kappa}_r)\right|_s^{2+1/n}\right] \qquad 2.17$$

C. DEFORMATION PROFILE AND STRAIN RATES

For a circular plate undergoing finite deformation the curvatures and extensional strains can be written:

$$\kappa_r = -w'' \qquad \kappa_\theta = -\frac{w'}{r} \tag{2.18}$$

$$e_r = u' + \frac{(w')^2}{2} \qquad e_\theta = \frac{u}{r} \tag{2.19}$$

where w and u are the transverse and radial deflections respectively with directional sense as shown in Figure 2.1. Taking derivatives with respect to time we obtain the rates:

$$\dot{\kappa}_r = -\dot{w}'' \qquad \dot{\kappa}_\theta = -\frac{\dot{w}'}{r} \tag{2.20}$$

$$\dot{e}_r = \dot{u}' + \dot{w}'w' \qquad \dot{e}_\theta = \frac{\dot{u}}{r} \tag{2.21}$$

To proceed further, the transverse and radial deformation rate profiles for a plate with a given set of edge conditions must be determined. For the finite linear elastic deflections of a clamped circular plate Timoshenko and Woinowsky-Kreiger (23) employed the elastic bending analysis profile:

$$w = w_o\left(1-\frac{r^2}{a^2}\right)^2 \tag{2.22}$$

where w_o is the deflection at the center and a is the outer radius. In the experiments described in Chapter I it was noted, for the $\frac{a}{h}$ ratios examined, that the measured deformation profile could be represented by equation (2.22), especially at lower values of $\frac{w_o}{h}$. Assuming, therefore, that the vertical deformation profile may be represented by (2.22)the curvatures and curvature rates may be written:

$$\kappa_r = \frac{4w_o}{a^2}\left(1-\frac{3r^2}{a^2}\right) \qquad \kappa_\theta = \frac{4w_o}{a^2}\left(1-\frac{r^2}{a^2}\right) \tag{2.23}$$

$$\dot{\kappa}_r = \frac{4\dot{w}_o}{a^2}\left(1-\frac{3r^2}{a^2}\right) \qquad \dot{\kappa}_\theta = \frac{4\dot{w}_o}{a^2}\left(1-\frac{r^2}{a^2}\right). \tag{2.24}$$

For the deflection rate in the radial direction, $\dot{u}$, we adopt an expression suggested by Timoshenko and Woinowsky-Kreiger (24) for large deflections of clamped circular elastic plates which, adapted for time dependent problems, is:

$$\dot{u} = r(a-r)(c_1 + c_2 r + c_3 r^2 + \text{----} c_{n-1} r^n). \tag{2.25}$$

This expression satisfies the end conditions $\dot{u}=0$ at $r=0$ and $r=a$ and provides for a wide variety of possible profiles through variation of the c_i values. The constants, c_i, will be determined by requiring minimum internal energy dissipation in the plate. Taking the first two terms of the series we have:

$$\dot{u} = c_1 ar - c_1 r^2 + c_2 ar^2 - c_2 r^3 \tag{2.26}$$

from which:

$$\dot{u}' = (a-2r)c_1 + (2ar-3r^2)c_2 \tag{2.27}$$

$$\frac{\dot{u}}{r} = (a-r)c_1 + (ar-r^2)c_2 \tag{2.28}$$

With these expressions the extensional strain rates, (2.21), become:

$$\dot{e}_r = (a-2r)c_1 + (2ar-3r^2)c_2 + \frac{16\dot{w}_o w_o r^2}{a^4}\left(1-\frac{r^2}{a^2}\right)^2 \tag{2.29}$$

$$\dot{e}_\theta = (a-r)c_1 + (ar-r^2)c_2 \tag{2.30}$$

Examining the expressions for $\dot{e}_r$ and $\dot{e}_\theta$ we are led by dimensional considerations to suspect that c_1 and c_2 are of the form:

$$c_1 = c_1' \frac{\dot{w}_o w_o}{a^3} \qquad c_2 = c_2' \frac{\dot{w}_o w_o}{a^4} \qquad 2.31$$

where c_1' and c_2' are pure numbers. In order for each term in the sum to have the time dimension each must contain $\dot{w}_o$. If $\dot{e}_r$ and $\dot{e}_\theta$ are to be zero at any point on the plate when $w_o = 0$, then each term should contain w_o. To be consistent with the last term in (2.29) the diameter, a, is selected as a length factor. If one considers extensional energy dissipation only and solves analytically the n=1 case for c_1 and c_2, it is seen that they are indeed of the above form.

Defining $x \equiv \frac{r}{a}$, we may now write the curvature rates and extensional strain rates as:

$$\dot{\kappa}_r = \frac{4\dot{w}_o}{a^2} (1-3x^2) \qquad 2.32$$

$$\dot{\kappa}_\theta = \frac{4\dot{w}_o}{a^2} (1-x^2) \qquad 2.33$$

$$\dot{e}_r = \frac{\dot{w}_o w_o}{a^2} [(1-2x)c_1' + (2x-3x^2)c_2' + 16x^2(1-x^2)^2] \qquad 2.34$$

$$\dot{e}_\theta = \frac{\dot{w}_o w_o}{a^2} [(1-x)c_1' + (x-x^2)c_2'] \qquad 2.35$$

We now have expressions for the curvature rates and extensional strain rates in terms of geometrical parameters for a clamped circular plate. These expressions can now be substituted into 2.14 through 2.17, the force and moment resultants. For the higher values of $\frac{w_o}{h}$ the experiments showed that the deformation profile tends to the parabolic membrane form:

$$w = w_o (1-\frac{r^2}{a^2}) \qquad 2.36$$

The problem may be solved using this profile also and, as will be seen, the solution for the center deflection rate, $\dot{w}_o$, tends to converge to the same value for the two profiles as $\frac{w_o}{h}$ increases. The same procedure can be done with other assumed profiles as seen in Appendix D for the simply supported case.

D. ENERGY EXPRESSIONS

The total internal energy dissipation in the plate during creep deformation may be expressed as:

$$\dot{V} = \int_0^{2\pi} \int_0^a (M_r\dot{\kappa}_r + M_\theta\dot{\kappa}_\theta + N_r\dot{e}_r + N_\theta\dot{e}_\theta) r dr d\theta \qquad 2.37$$

where transverse shear energy dissipation is neglected. The integration, strictly speaking, extends over the deformed surface area of a plate. However, if attention is confined to moderate transverse deflections and small strains then the deformed surface can be taken to equal the original surface area. This procedure is usually adopted for deriving a consistent set of equilibrium equations and strain relations when using the principle of virtual work. (25) Using the previously derived relations, equations 2.14 through 2.17 and 2.32 through 2.35, we may now write for the clamped case:

$$M_r\dot{\kappa}_r = \left(\frac{4}{3K}\right)^{1/n} \frac{n}{n+1} h^{2+1/n} \left(\frac{\dot{w}_o}{a^2}\right)^{1+1/n} \left[\frac{1}{A} |B+A|^{1+1/n}\right.$$

$$- \frac{n}{(2n+1)\ A^2} |B+A|_s^{2+1/n} + \frac{1}{A} |B-A|^{1+1/n}$$

$$\left. + \frac{n}{(2n+1)\ A^2} |B-A|_s^{2+1/n}\right] \cdot [1-3x^2] \qquad 2.38$$

$$M_\theta\dot{\kappa}_\theta = \left(\frac{4}{3K}\right)^{1/n} \frac{n}{n+1} h^{2+1/n} \left(\frac{\dot{w}_o}{a^2}\right)^{1+1/n} \left[\frac{1}{D}|E+D|^{1+1/n}\right.$$

$$- \frac{n}{(2n+1)D^2} |E+D|_s^{2+1/n} + \frac{1}{D}|E-D|^{2+1/n}$$

$$\left. + \frac{n}{(2n+1)D^2} |E-D|_s^{2+1/n}\right] \cdot [1-x^2] \qquad 2.39$$

$$N_r\dot{e}_r = \left(\frac{4}{3K}\right)^{1/n} \frac{n}{n+1} h^{2+1/n} \left(\frac{\dot{w}_o}{a^2}\right)^{1+1/n} \frac{1}{2A} \left[|B+A|^{1+1/n}\right.$$

$$\left. -|B-A|^{1+1/n}\right] \cdot \left[(1-2x)c_1' \frac{w_o}{h} + (2x-3x^2)c_2' \frac{w_o}{h}\right.$$

$$\left. + 16x^2(1-x^2)^2 \frac{w_o}{h}\right] \qquad 2.40$$

$$N_\theta\dot{e}_\theta = \left(\frac{4}{3K}\right)^{1/n} \frac{n}{n+1} h^{2+1/n} \left(\frac{\dot{w}_o}{a^2}\right)^{1+1/n} \frac{1}{2D} \left[|E+D|^{1+1/n}\right.$$

$$\left. -|E-D|^{1+1/n}\right] \cdot \left[(1-x)c_1' \frac{w_o}{h} + (x-x^2)c_2' \frac{w_o}{h}\right] \qquad 2.41$$

where:

$$A \equiv (3-7x^2)$$

$$B \equiv \left(\tfrac{3}{2} - \tfrac{5}{2}x\right)c_1' \frac{w_o}{h} + \left(\tfrac{5}{2}x - \tfrac{7}{2}x^2\right)c_2' \frac{w_o}{h} + 16x^2(1-x^2)^2 \frac{w_o}{h}$$

$$D \equiv (3-5x^2)$$

$$E \equiv \left(\tfrac{3}{2} - 2x\right)c_1' \frac{w_o}{h} + \left(2x - \tfrac{5}{2}x^2\right)c_2' \frac{w_o}{h} + 8x^2(1-x^2)^2 \frac{w_o}{h}$$

With these expressions 2.37 can be written as:

$$\dot{V} = 2\pi a^2 \left(\frac{4}{3K}\right)^{1/n} \frac{n}{n+1} h^{2+1/n} \left(\frac{\dot{w}_o}{a^2}\right)^{1+1/n}$$

$$\int_0^1 \left(f_{M_r} + f_{M_\theta} + f_{N_r} + f_{N_\theta}\right) x\,dx \qquad 2.42$$

where the quantities f_{a_b} are all functions of x, c_1', c_2', $\frac{w_o}{h}$, and n. These symbols, f_{a_b}, represent the terms containing x in 2.38 through 2.41 which must be integrated over the radius. The result of this integration over x will be a function of c_1', c_2', $\frac{w_o}{h}$, and n which will be denoted I. The equation for $\dot{V}$ may now be written as:

$$\dot{V} = 2\pi a^2 \left(\frac{4}{3K}\right)^{1/n} \frac{n}{n+1} h^{2+1/n} \left(\frac{\dot{w}_o}{a^2}\right)^{1+1/n} I\left(c_1', c_2', \frac{w_o}{h}, n\right) \qquad 2.43$$

The quantities c_1' and c_2' as previously discussed determine the radial deformation rate profile. They must be chosen such that the rate of energy dissipation in the plate is minimized. Clearly, minimizing $\dot{V}$ with respect to c_1' and c_2' is equivalent to minimizing I with respect to c_1' and c_2'. The minimization of I must be done for the current value of $\frac{w_o}{h}$ and n. The correct values of c_1' and c_2' for one set of values for the parameters $\frac{w_o}{h}$ and n may, in general, be different from those for some other set. One way of determining the appropriate values of c_1' and c_2' might be to substitute values for $\frac{w_o}{h}$ and n into an expression for I and take derivatives with respect to c_1' and c_2', set them equal to zero, and solve for the values

resulting in a minimum I. Unfortunately, the expression

$$\int_0^1 (f_{M_r} + f_{M_\theta} + f_{N_r} + f_{N_\theta})xdx$$

is such that the integral cannot be evaluated analytically so there is no analytical expression for I which can be differentiated with respect to c_1' and c_2'. We must, therefore, evaluate I numerically and search for those values of c_1' and c_2' which result in the miminum value of I for a given case (w_o/h, n). This was done, for the cases considered, with the computer programs whose listings are given in Appendix H. These programs were used with an IBM 1130 Computing System at Massachusetts Institute of Technology. The computer output yielded a series of smooth curves for regular variations of c_1' and c_2'. These curves showed clearly identifiable minima with respect to c_1' and c_2' for the function I. The procedure is illustrated for a typical case in Appendix E.

E. SOLUTION FOR DEFORMATION RATE

If a structure is assumed to deform in a manner prescribed by a kinematically admissible virtual velocity field, (i.e., continuous and satisfies the velocity boundary conditions), then the principle of virtual velocities states that the total virtual internal energy dissipation is equal to the total virtual external energy dissipation.

Having minimized the integral I for some case ($\frac{w_o}{h}$, n) we find the deformation rate, $\dot{w}_o$, by using the principle of virtual velocities and considering a small variation of the deformation rate about its equlibrium value. This gives:

$$\frac{d\dot{V}}{d\dot{w}_o}\,\delta\dot{w}_o = 2\pi \int_0^a q\delta\dot{w}\, r\,dr \qquad 2.44$$

where q is a time-independent, transverse pressure. For the case of the clamped plate we have:

$$2\pi \int_0^a q\delta\dot{w}\, r\,dr = 2\pi q\delta\dot{w}_o \int_0^a (1-\frac{r^2}{a^2})^2 r\,dr = \frac{\pi q a^2}{3}\,\delta\dot{w}_o \qquad 2.45$$

and:

$$\frac{d\dot{V}}{d\dot{w}_o}\,\delta\dot{w}_o = \dot{w}_o^{1/n}\,[2\pi a^2 (\frac{4}{3K})^{1/n} (\frac{1}{a^2})^{1+1/n} h^{2+1/n} I]\,\delta\dot{w}_o \qquad 2.46$$

The expression 2.46 is the derivative of $\dot{V}$ for some specific value of $\frac{w_o}{h}$ and the derivative is properly taken considering $\frac{w_o}{h}$ as a constant. We are seeking the value of $\dot{w}_o$ for a given instant when $\frac{w_o}{h}$ has some fixed value. An instant later w_o will, of course, have some other value and at that time $\dot{w}_o$ will also have some other value, but at a given instant w_o/h may be considered fixed. Equating 2.45 and 2.46 we obtain the result:

$$\dot{w}_o = [\frac{q a^{2+2/n}}{(\frac{4}{3K})^{1/n} h^{2+1/n} 6I}]^n \qquad 2.47$$

or

$$\dot{w}_o = [(\frac{a}{h})^{2+1/n} (\frac{3Ka}{4})^{1/n} q(\frac{1}{6I})]^n \,. \qquad 2.48$$

If we define the quantity Φ as:

$$\Phi = \left[\frac{\left(\frac{\dot{w}_o}{Kaq^n}\right)}{3/4\left(\frac{a}{h}\right)^{2n+1}}\right]^{1/n} \qquad 2.49$$

This can be written in the non-dimensional form:

$$\left(\frac{\dot{w}_o}{Kaq^n}\right) = 3/4\left(\frac{a}{h}\right)^{2n+1} \Phi^n. \qquad 2.50$$

The parameter Φ is a direct function of I, the form of this function depending upon the assumed velocity profile. For the clamped case:

$$\Phi = \left(\frac{1}{6I}\right) \qquad 2.51$$

It is convenient to define Φ as it permits a direct correlation of results among the different velocity profiles considered. When the quantity I has been minimized with respect to c_1' and c_2', Φ is a function of n and $\frac{w_o}{h}$. Values of Φ, for the clamped case, are plotted versus $\frac{w_o}{h}$ for various values of n in Figure 2.2. Use of these values with any of the equations 2.47 through 2.50 will give the center deflection rate $\dot{w}_o$ as a function of the applied pressure and the plate's material and geometrical properties. Once $\dot{w}_o$ has been determined, the deflection rate at any other point on the plate can be found from the assumed velocity profile, which in this case is given by equation 2.22.

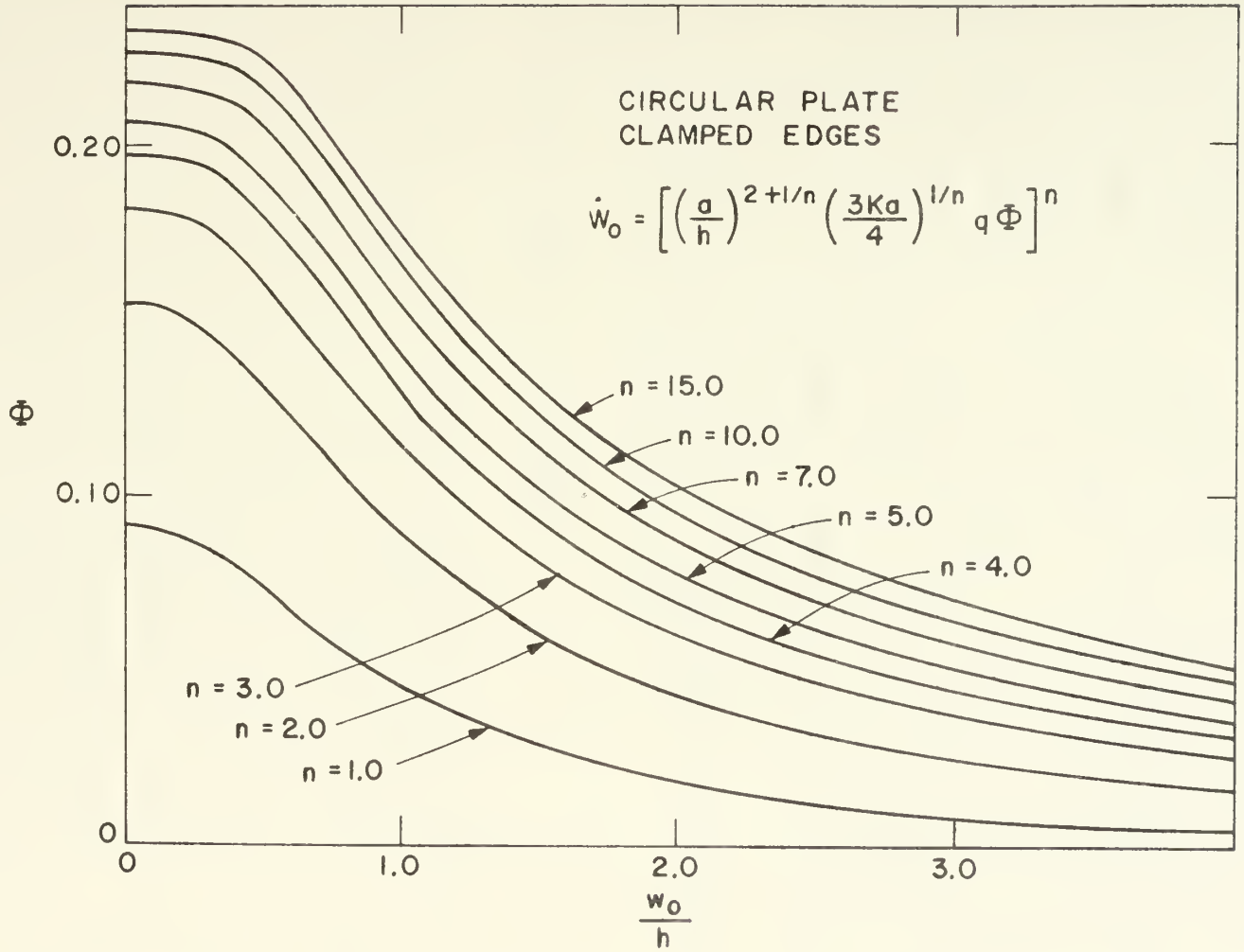
CIRCULAR PLATE
CLAMPED EDGES
$\dot{W}_o = \left[\left(\frac{a}{h}\right)^{2+1/n}\left(\frac{3Ka}{4}\right)^{1/n} q\Phi\right]^n$
n = 15.0
n = 10.0
n = 7.0
n = 5.0
n = 4.0
n = 3.0
n = 2.0
n = 1.0
0.20
0.10
0
Φ
0
1.0
2.0
3.0
$\frac{w_o}{h}$

FIG. 2.2

It was noted in the plate experiments that for the higher values of $\frac{w_o}{h}$ the profile began to tend toward a parabolic form (or membrane profile) described by the equation 2.36. The entire analysis just described can be repeated using the profile 2.36 vice 2.22 to obtain values of Φ for the parabolic configuration. When this is done it is found, as shown in Figure 2.3, that the difference between the two solutions is small for $\frac{w_o}{h} = 1.5$ and has virtually disappeared when $\frac{w_o}{h} = 3.0$. It seems, therefore, that when the plate deforms to a value of $\frac{w_o}{h}$ large enough for there to be a significant deviation from the profile of equation 2.22 it will have deformed enough so that the solution for $\dot{w}_o$ is relatively insensitive to the assumed profile.

The computer program listed in Appendix H is written for an assumed velocity profile of the form:

$$\dot{w} = \dot{w}_o[\alpha_1(1-\frac{r^2}{a^2})^2 + \alpha_2(1-\frac{r^2}{a^2})] \qquad 2.52$$

where $\alpha_1 + \alpha_2 = 1$. The analysis utilizing this profile is outlined in Appendix C. If we assign the values $\alpha_1 = 1$ and $\alpha_2 = 0$, the analysis with 2.52 is the same as for the clamped profile, 2.22. If we assign values $\alpha_1 = 0$ and $\alpha_2 = 1$ the analysis is for the parabolic membrane profile, 2.36. Some experimentation with fractional values for α_1 and α_2 was attempted, but these produced no more useful results. The best agreement with experimental data came with α_1 and α_2 at their extreme values as above. The final result using this profile is:

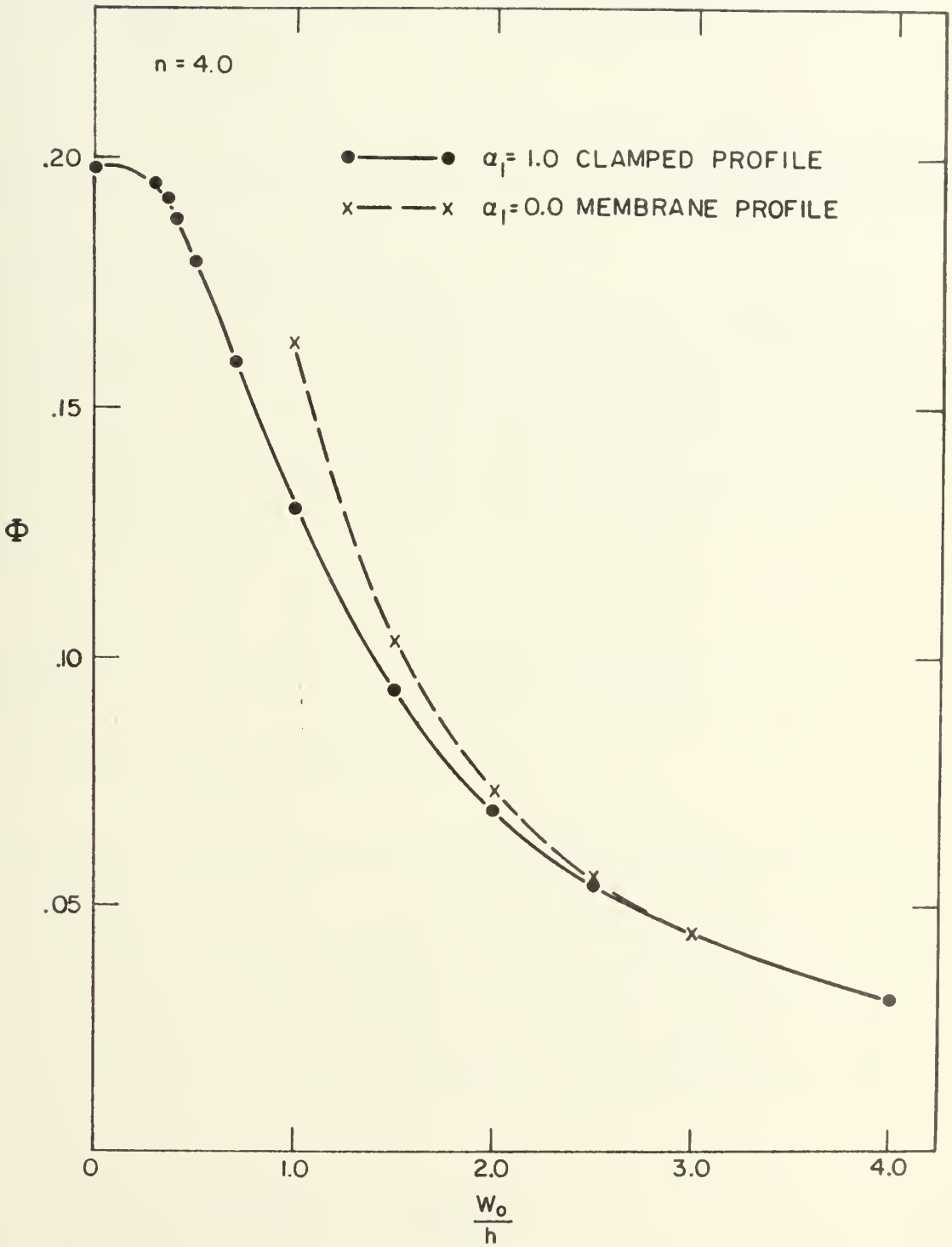

FIG. 2.3

Comparison of clamped and membrane solutions for n = 4.0

$$\left(\frac{\dot{w}_o}{Kaq^n}\right) = 3/4\left(\frac{a}{h}\right)^{2n+1}\left(\frac{3-\alpha_1}{12\ I_c}\right)^n \qquad 2.53$$

so in this case

$$\Phi = \left(\frac{3-\alpha_1}{12\ I_c}\right) \qquad 2.54$$

where I_c is the appropriate integral for the combined profile.

F. SIMPLY SUPPORTED CASE

The simply supported circular plate may be treated in the same manner as above if the velocity profile appropriate to it is known. In the elastic bending analysis of this case Timoshenko and Woinowsky-Krieger [26] determined a deflection profile of the form:

$$w = w_o\left(1-\frac{r^2}{a^2}\right)\left(1-\frac{1+\nu}{5+\nu}\ \frac{r^2}{a^2}\right) \qquad 2.55$$

which for $\nu = 1/2$ gives the velocity profile:

$$\dot{w} = \dot{w}_o\left(1-\frac{r^2}{a^2}\right)\left(1-\frac{3}{11}\ \frac{r^2}{a^2}\right) . \qquad 2.56$$

There is no experimental data available in order to verify this profile as in the clamped case, but at least a reasonable estimate of the creep behavior of the simply supported case can be expected from an analysis with the profile of 2.56. This analysis is outlined in Appendix D and yields a final result of:

$$\left(\frac{\dot{w}_o}{Kaq^n}\right) = 3/4\left(\frac{a}{h}\right)^{2n+1}\left(\frac{5}{22\ I_s}\right)^n \qquad 2.57$$

so that in this case:

$$\Phi = \left(\frac{5}{22\ I_s}\right) \qquad 2.58$$

where I_s is the integral appropriate to the simple support profile. Curves of Φ versus $\frac{w_o}{h}$ for various values of n are given in Figure 2.4. In Figure 2.5 the results of the clamped and simply supported cases are compared for the case n = 4.

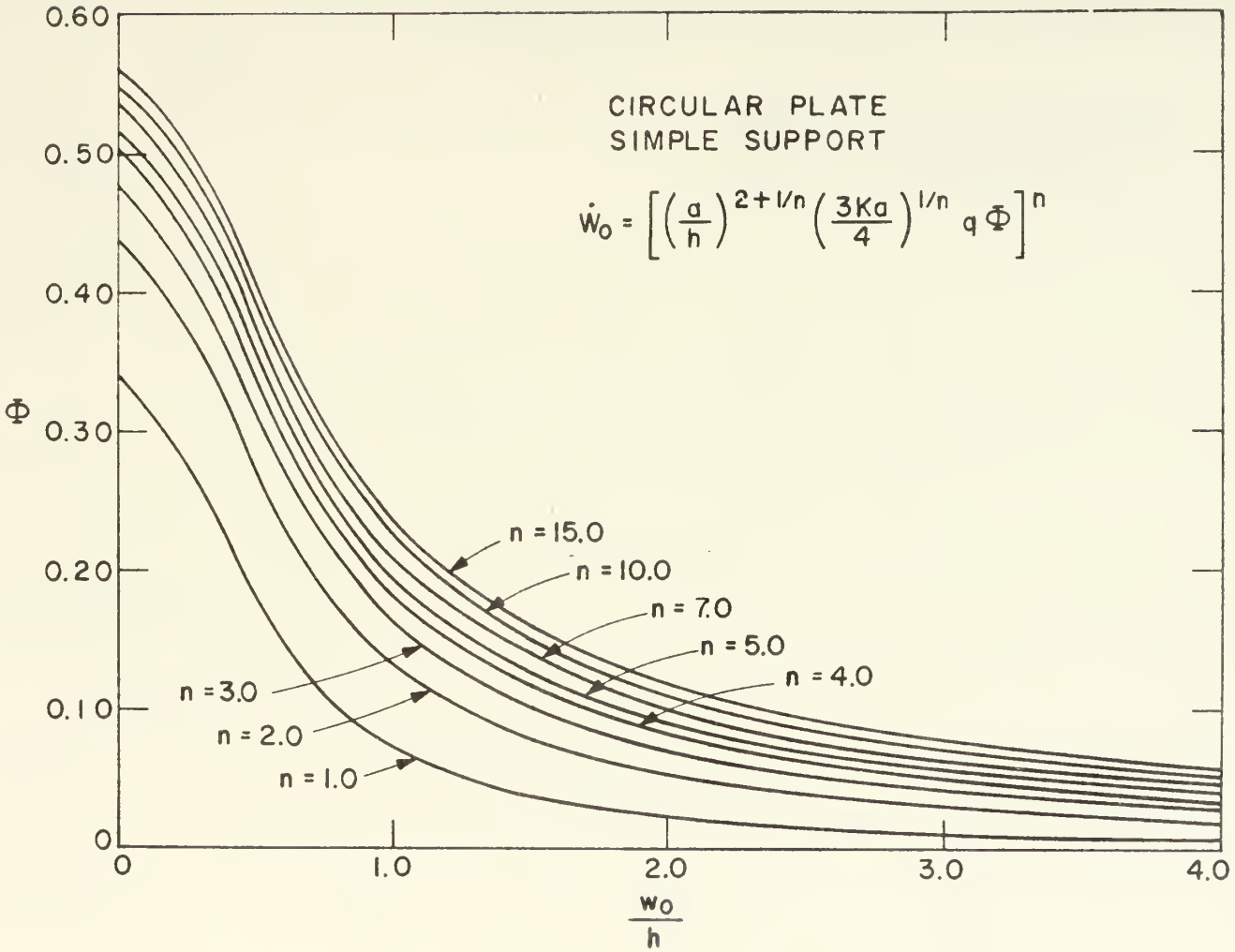
CIRCULAR PLATE
SIMPLE SUPPORT
$\dot{W}_0 = \left[\left(\frac{a}{h}\right)^{2+1/n}\left(\frac{3Ka}{4}\right)^{1/n} q\Phi\right]^n$
0.60
0.50
0.40
0.30
0.20
0.10
0
Φ
n = 15.0
n = 10.0
n = 7.0
n = 5.0
n = 4.0
n = 3.0
n = 2.0
n = 1.0
0
1.0
2.0
3.0
4.0
$\frac{w_0}{h}$

FIG. 2.4

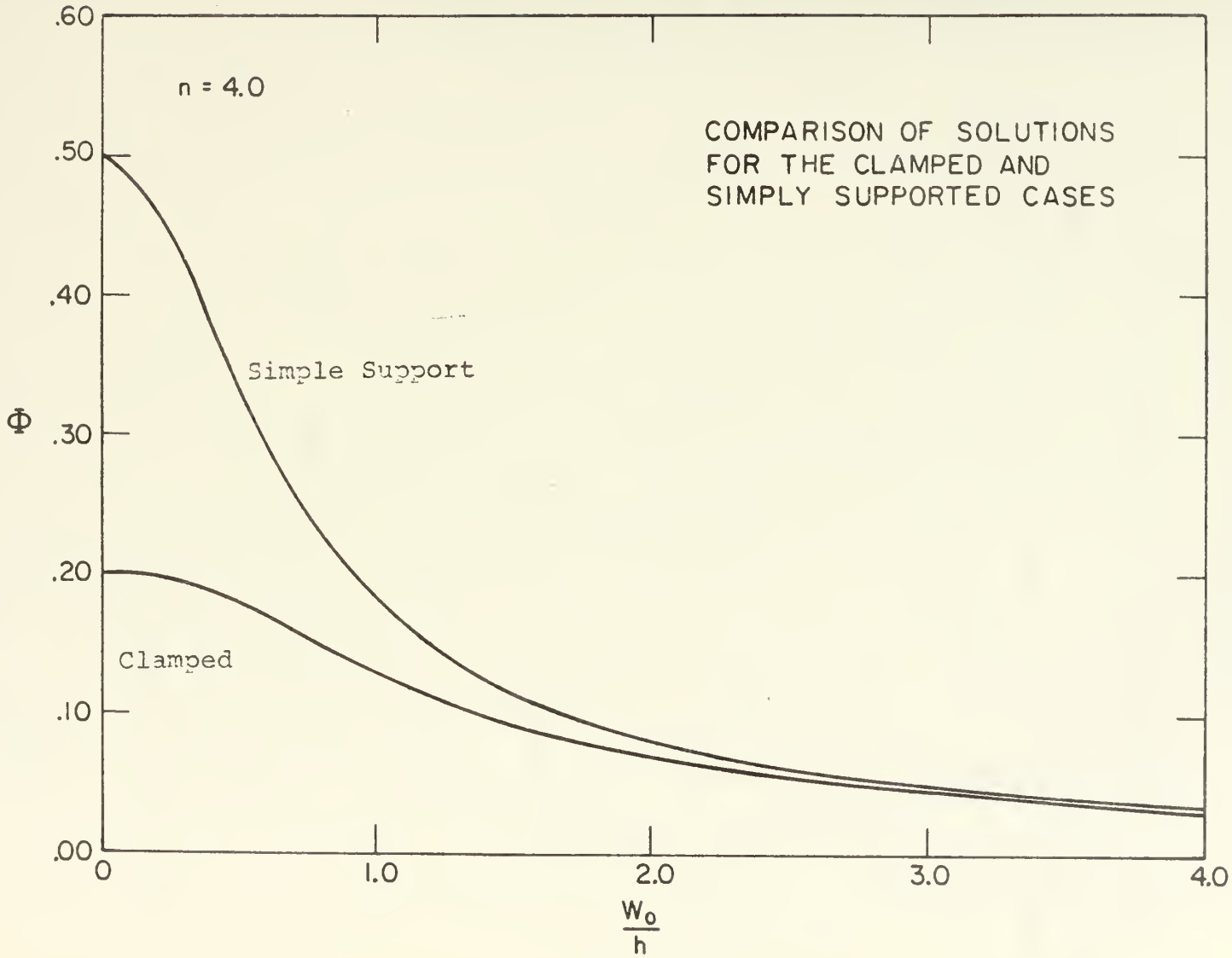
.60
.50
.40
.30
.20
.10
.00
Φ
n = 4.0
COMPARISON OF SOLUTIONS
FOR THE CLAMPED AND
SIMPLY SUPPORTED CASES
Simple Support
Clamped
0
1.0
2.0
3.0
4.0
W0/h

FIG. 2.5

CHAPTER III

Comparison of Theoretical and Experimental Results and Results of Previous Investigations

A comparison of the experimental and theoretical results is shown in Figures 3.1, 3.2, and 3.3. Here the non-dimensional quantity $(\frac{\dot{w}_o}{Kaq^n})/(\frac{a}{h})^{2n+1}$ is plotted versus the non-dimensionalized center deflection, $\frac{w_o}{h}$, for the creep parameter n appropriate to each of the three types of plate tested. In these plots the appropriate analytical results for comparison with the experiments are, of course, those for the clamped case. Also shown are plots of the bending analysis results of Venkatraman and Hodge [11], and of Odqvist [12]; and the membrane analyses of Odqvist [12][16], and of Onat and Yü ksel [17]. The mathematical details of reducing these various analyses to a form appropriate to this plot are given in Appendix B. The bending analysis solutions are horizontal lines since that type of analysis does not consider geometry changes. The membrane analyses consider geometry changes but not bending moments within the plate. Experimental points are given at each pressure tested for times of 1 hour and 5 hours. These points are found by obtaining the deflection rate at the indicated times from the plate test experimental data and substituting this value along with the appropriate creep constants found in the tensile tests and the pressure and geometrical constants into the form $(\frac{\dot{w}_o}{Kaq^n})/(\frac{a}{h})^{2n+1}$. The

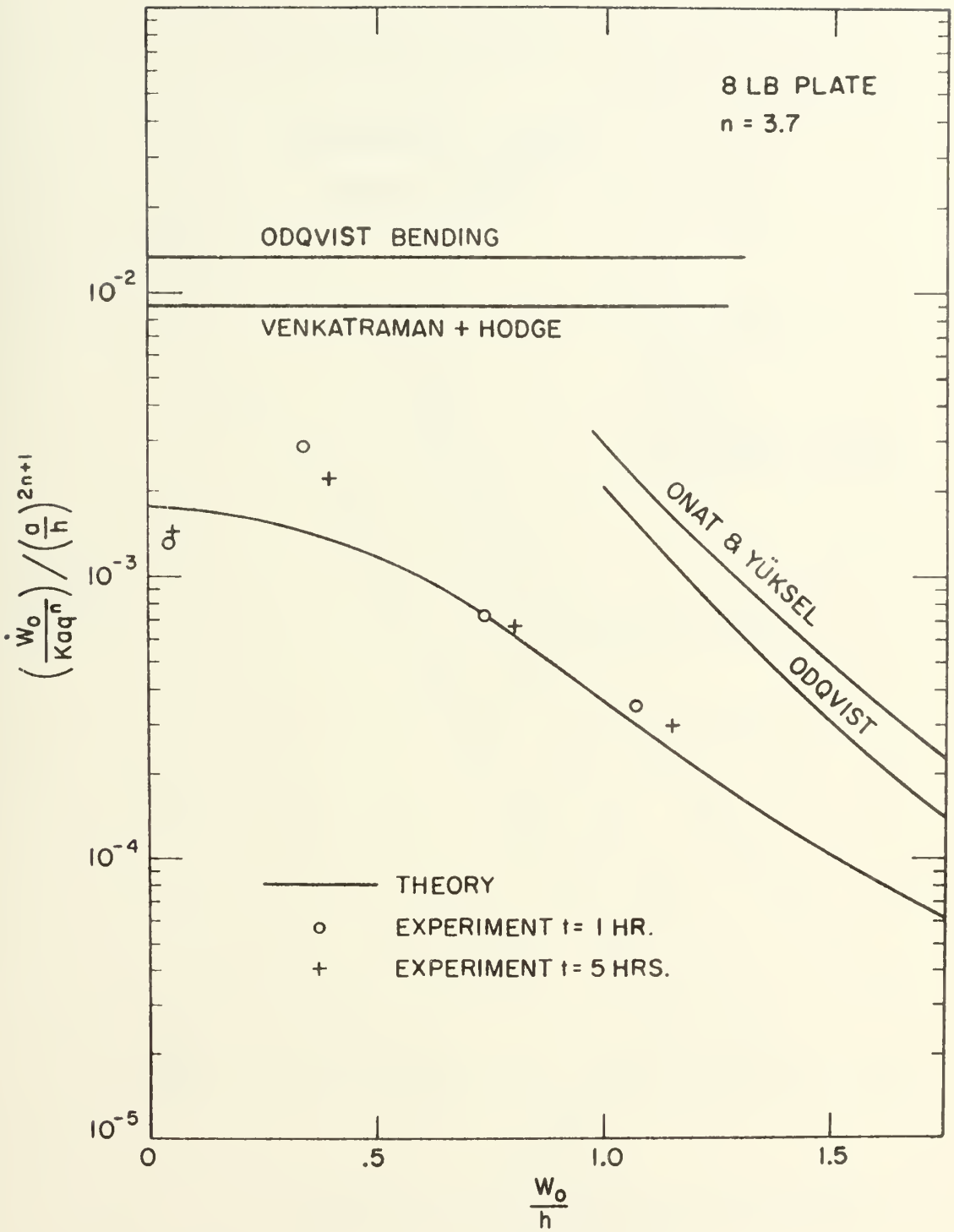

FIG. 3.1

Comparison of experiment and theory, 8 lb. plate

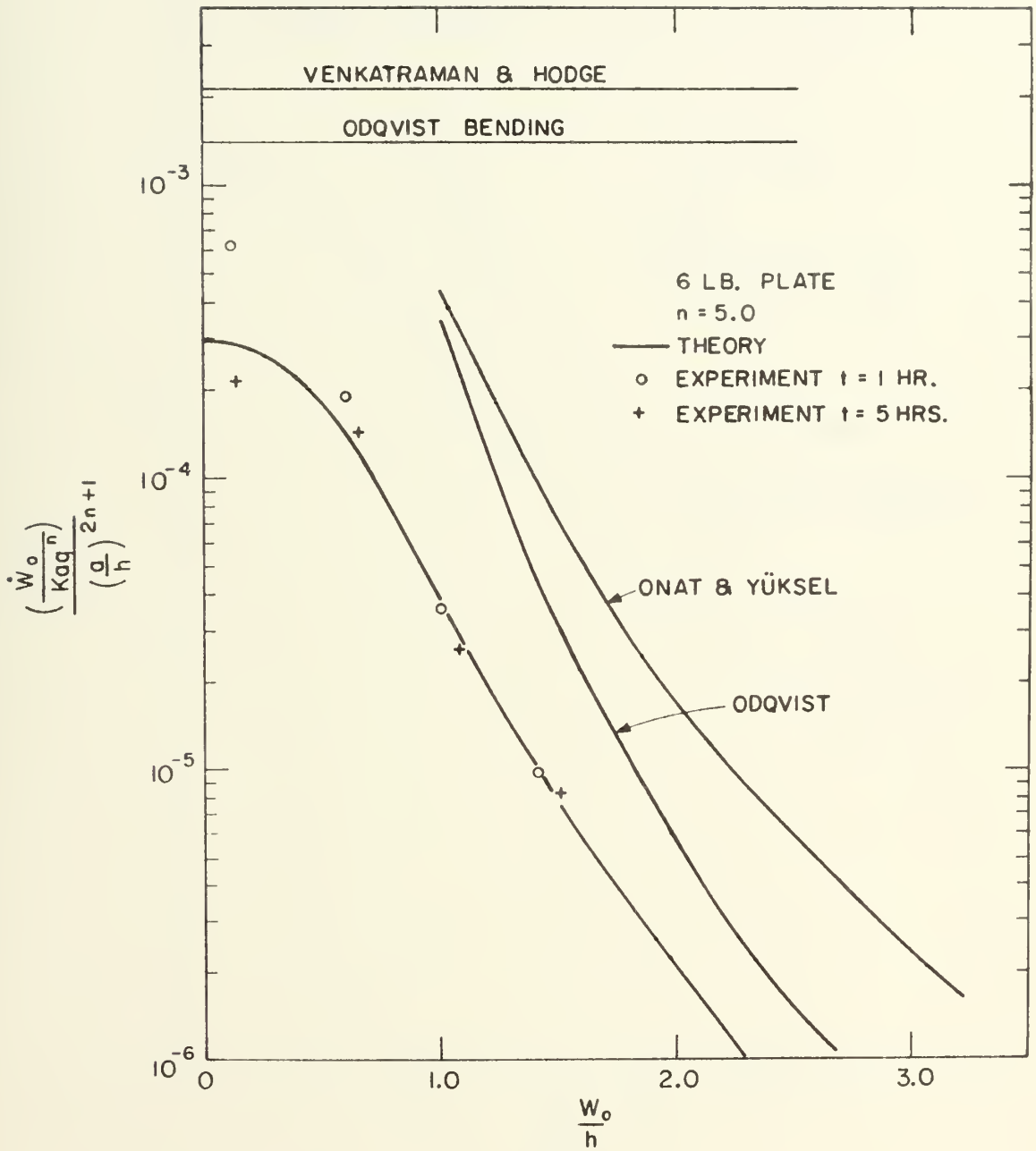

FIG. 3.2

Comparison of experiment and theory, 6 lb. plate

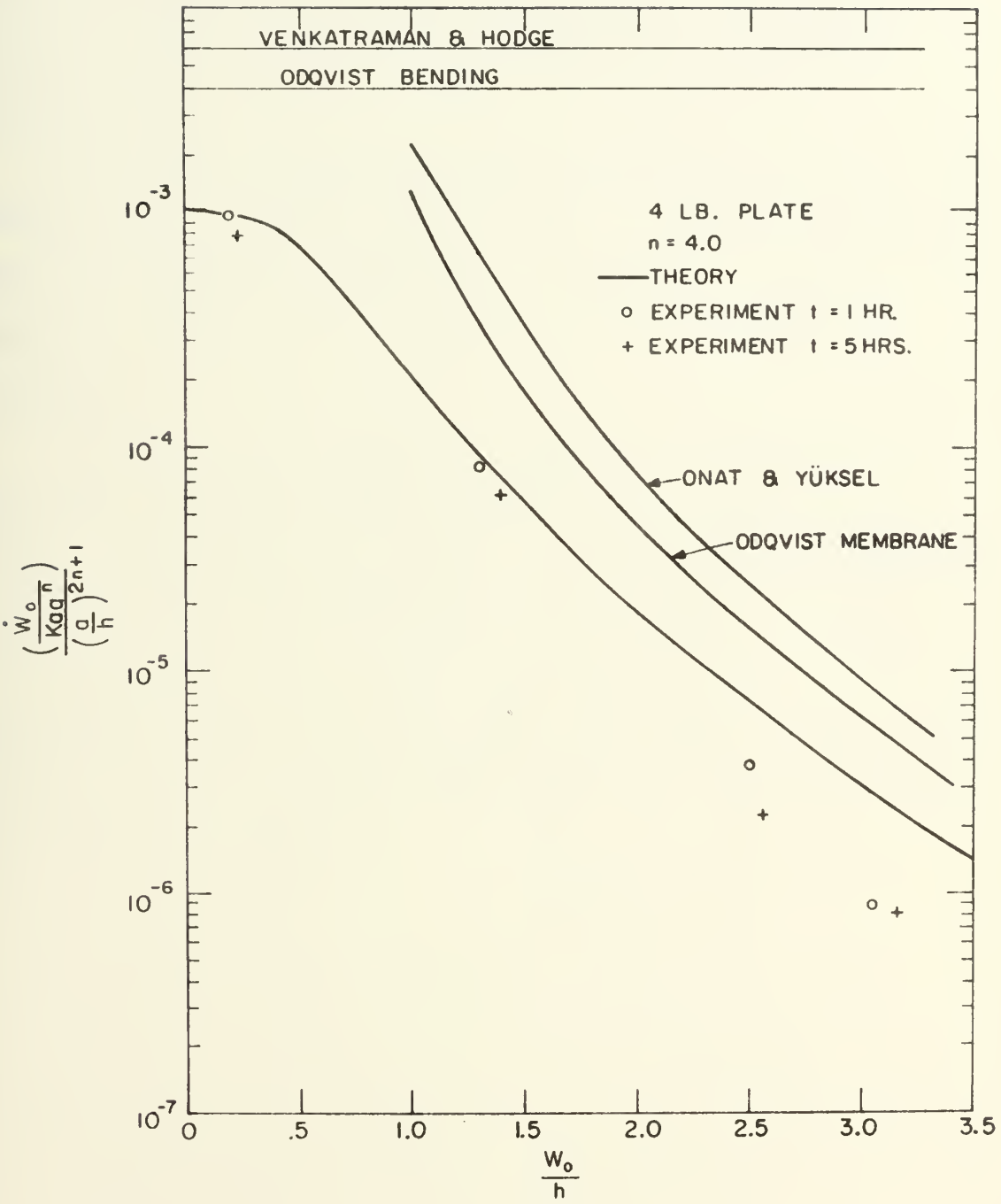

FIG. 3.3

Comparison of experiment and theory, 4 lb. plate

value thus obtained is then plotted versus the appropriate value of $\frac{w_o}{h}$ as determined from the plate test data. The times t=1 hour and t=5 hours were chosen as representing cases of rather rapid and relatively slower deformation respectively.

The marked influence of finite deformation on the creep behavior of a clamped circular plate is clearly indicated by both the theoretical prediction of equation 2.50 and the experimental results, which are seen to be in substantial agreement.

A similar plot, Figure 3.4, shows the relationship of the simply supported case analysis to the results of the simple support bending analysis of Venkatraman and Hodge [11] and of Odqvist [12] and the membrane solutions of Odqvist [12] [16] and of Onat and Yüksel [17], for the case n = 4. No experimental data is available for this type of end condition, but the analytical results also indicate a marked influence from finite deformation.

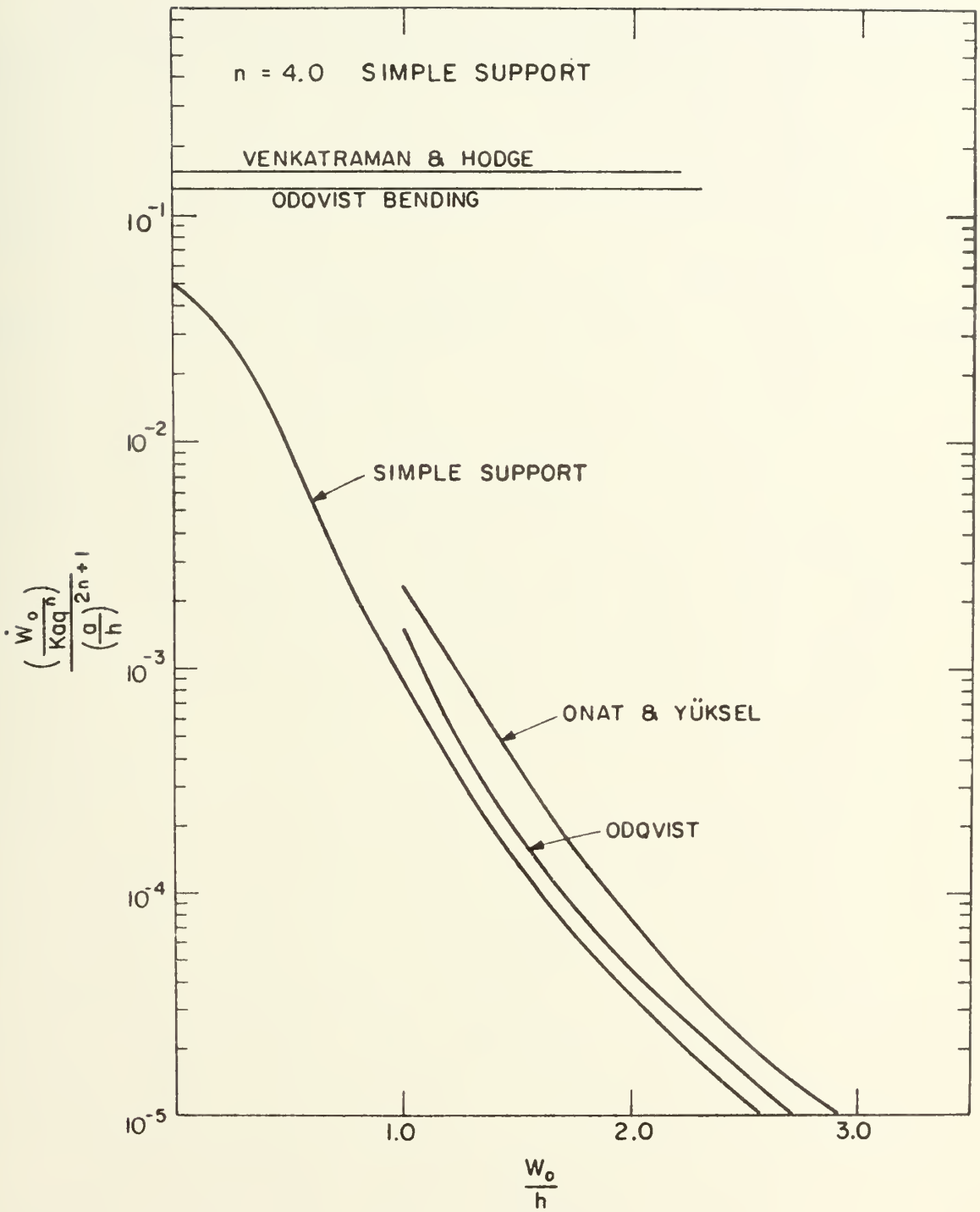

FIG. 3.4

Comparison of simply supported plate theories

Summary and Conclusions

Experimental and theoretical results have been presented which show that the effect of finite deformation upon the creep behavior of circular plates is of primary importance. It is necessary to consider this effect even when the maximum deflection of the plate might be well below the plate thickness.

A method of modeling the constitutive behavior of a material undergoing creep deformation under a multiaxial state of stress has been proposed. A technique for solving multiaxial creep problems by using an energy method and the suggested constitutive equations yields a result in the form of an equation and graphs which can be quite easily applied. Solutions were obtained for a circular plate under a time independent uniform lateral load with clamped and simply supported edge conditions. A comparison of theoretical and experimental results for the clamped case showed substantial agreement; indicating that the analytical technique described may be expected to provide quite reasonable estimates of plate deformation rate when the creep behavior of the material may be adequately represented by Norton's law, and the appropriate values of the material creep parameters are known. A comparison of these results with those of several previous investigators has also been presented. Lead was selected for the experimental material in these tests but the analytical results should remain valid for any material whose behavior is adequately represented by the constitutive equations.

Specific consideration was given only to circular plates; it can be expected, however, that the conclusion as to the importance of finite deformation will apply as well to plates of other shapes, initially straight beams, and to initially straight cylindrical shells.

APPENDIX A

Constitutive Equations for Multiaxial Creep

Creep data is not plentiful, and that which is available is almost always the result of uniaxial tests. It has been found that much of this experimental creep data can be represented by an expression of the form:

$$\dot{\varepsilon} = K \sigma^n \tag{A.1}$$

where K and n are material parameters which are, in general, functions of time and temperature. This expression is commonly known as Norton's law. [3]

In generalizing Norton's law to a form suitable for multidimensional problems the most common approach has been to use the concept of equivalent stress and equivalent strain rate for determining the proportionality between strain rate and deviatoric stress. Mendelson [27] uses a relation of the type:

$$\dot{\varepsilon}_{ij} = \frac{3}{2} \frac{\dot{\varepsilon}_e}{\sigma_e} s_{ij} \tag{A.2}$$

where creep equivalent strain rate, $\dot{\varepsilon}_e$, may be related to the equivalent stress, σ_e, by Norton's law.

Here:

$$\sigma_e = \sqrt{3J_2} \tag{A.3}$$

and $\dot{\varepsilon}_e$ is the strain rate resulting from a stress of this magnitude. Odqvist [6] uses the expression:

$$\dot{\varepsilon}_{ij} = \frac{3}{2} \dot{\varepsilon}_c \left(\frac{\sigma_e}{\sigma_c}\right)^{n-1} \frac{s_{ij}}{\sigma_c} \tag{A.4}$$

where $\dot{\varepsilon}_c$ is some standard value of creep rate for which $\sigma=\sigma_c$.

These expressions seem reasonable and satisfy the mathematical requirements for multiaxial creep constitutive relations, but are often rather intractible for analytical work since one must always compute σ_e in order to know the proportionality between the local stress and creep rate.

In this analysis the constitutive behavior of a material undergoing creep deformation in a multiaxial state of stress will be modeled in the following way:

$$\dot{\varepsilon}_i = K[\sigma_i^n - \nu\,\sigma_j^n - \nu\,\sigma_k^n] \qquad (A.5)$$

where the subscripts i, j, and k represent principal directions of stress and strain rate. It can be shown that for conservation of volume we must have $\nu = 1/2$. In real materials such things as voids and inclusions may give rise to situations in which volume is not conserved. If this effect is important then in such cases some other value for ν must be assigned as appropriate to the specific material under consideration.

It is also desirable that the constitutive relation (A.5) hold for both positive and negative σ for all values of n. The significance of positive and negative signs here is merely one of direction, tensile or compressive, and this directional sense must be retained for all values of n. This may be accomplished through the use of the signum function defined as:

$$\operatorname{sgn} x = \begin{cases} +1 & x > 0 \\ -1 & x < 0 \end{cases} \qquad (A.6)$$

An expression of the form $|x|^n \operatorname{sgn} x$ is used to denote that the absolute value of x is raised to the n power and the result is assigned the sign of x.

For homogeneous isotropic materials, therefore, the proposed constitutive relation takes the form:

$$\dot{\varepsilon}_i = K[|\sigma_i|^n \operatorname{sgn} \sigma_i - \tfrac{1}{2}|\sigma_j|^n \operatorname{sgn} \sigma_j - \tfrac{1}{2}|\sigma_k|^n \operatorname{sgn} \sigma_k] \qquad (A.7)$$

These equations are valid for a material which has the following properties:

(1) Homogeneous, incompressible, isotropic material.

(2) Coaxial stress and strain rate tensors.

(3) Zero deformation rate under hydrostatic pressure.

(4) Coordinates correspond to principal directions of stress and strain.

(5) Creep behavior corresponds to Norton's law in uniaxial stress.

It should be noted that this model predicts an effect from a hydrostatic pressure superimposed on a deviatoric stress. The validity of this may be questionable and was not really tested in the cases studied in this investigation. For applications where larger hydrostatic pressures are involved it may be better to use only the deviatoric components of the stresses.

For the case of a thin circular plate, choosing cylindrical coordinates and assuming $\sigma_3 = \sigma_z = 0$, equations A.7 become:

$$\begin{aligned}
\dot{\varepsilon}_r &= K[|\sigma_r|^n \operatorname{sgn} \sigma_r - \tfrac{1}{2}|\sigma_\theta|^n \operatorname{sgn} \sigma_\theta] \\
\dot{\varepsilon}_\theta &= K[|\sigma_\theta|^n \operatorname{sgn} \sigma_\theta - \tfrac{1}{2}|\sigma_r|^n \operatorname{sgn} \sigma_r] \qquad (A.8) \\
\dot{\varepsilon}_z &= K[-\tfrac{1}{2}|\sigma_r|^n \operatorname{sgn} \sigma_r - \tfrac{1}{2}|\sigma_\theta|^n \operatorname{sgn} \sigma_\theta].
\end{aligned}$$

APPENDIX B

Interpretation of Results of Previous Investigators

Introduction

The following theoretical treatments all apply to circular plates loaded with a time independent pressure uniformly distributed over the entire plate area. The infinitesimal solutions in Sections I and II retain only bending moments while solutions in III and IV consider geometry changes but retain only membrane forces.

I. Venkatraman and Hodge Solution [11]

a. Clamped Edges

The maximum deflection rate, at the plate center, is expressed in the form

$$\dot{w}_o = \dot{w}^* \, Ga^2 \, (\frac{qa^2}{12\mu})^n \tag{B.I.1}$$

where G is an arbitrary function of time and

$$\mu = 2\lambda \, \frac{n}{2n+1} \, (\frac{h}{2})^{2+1/n}. \tag{B.I.2}$$

The term λ is obtained from the assumed form of Norton's law given as

$$\dot{\varepsilon} = (\frac{\sigma}{\lambda})^n. \tag{B.I.3}$$

When compared with the form given by equation A.1 which was:

$$\dot{\varepsilon} = K\sigma^n \tag{B.I.4}$$

we have

$$\lambda = \frac{1}{K} \, 1/n \tag{B.I.5}$$

Substituting B.I.2, B.I.3, and B.I.5 into B.I.1:

$$\dot{w}_o = \dot{w}^* \, G(\frac{a}{h})^{2n+1} \, Kaq^n \, [\frac{2^{2+1/n}(2n+1)}{24n}]^n \tag{B.I.6}$$

or

$$\frac{(\frac{\dot{w}_o}{Kaq^n})}{(\frac{a}{h})^{2n+1}} = \dot{w}^* \, G[\frac{2^{2+1/n}(2n+1)}{24n}]^n \tag{B.I.7}$$

which interprets B.I.1 in terms of parameters introduced in Chapter III.

For comparison with the results in this paper we take G=1. The term $\dot{w}^*$ is plotted as a function of n in reference [11].

b. Simple Support

For simply supported edges the deflection rate at the plate center is of the form:

$$\dot{w}_o = \dot{w}^* \, Ga^2 \left(\frac{qa^2}{6\mu}\right)^n \qquad \text{(B.I.8)}$$

Substituting and rearranging as above this becomes:

$$\frac{\left(\frac{\dot{w}_o}{Kaq^n}\right)}{\left(\frac{a}{h}\right)^{2n+1}} = \dot{w}^* \, G\left[\frac{2^{2+1/n}(2n+1)}{12n}\right]^n \qquad \text{(B.I.9)}$$

where as before $\dot{w}^*$ is plotted in reference [11].

II. Odqvist Bending Solution [12]

This result is of the form

$$\dot{w}_o = a \Pi^n V(o) \qquad \text{(B.II.1)}$$

where

$$\Pi = \frac{2n+1}{n} \left(\frac{3a^2}{h^2}\right)^{\frac{n+1}{2n}} \frac{qa}{h\sigma_c} \qquad \text{(B.II.2)}$$

and V(o) is plotted as a function of n in reference [12] for the clamped and simply supported cases. The term σ_c is from the assumed constitutive relation:

$$\dot{\varepsilon}ij = \frac{3}{2}\left(\frac{\sigma_e}{\sigma_c}\right)^{n-1} \frac{s_{ij}}{\sigma_c} \qquad \text{(B.II.3)}$$

which for uniaxial stress reduces to

$$\dot{\varepsilon} = \frac{1}{\sigma_c{}^n} \sigma^n \qquad \text{(B.II.4)}$$

and when compared with our notation:

$$\dot{\varepsilon} = K\sigma^n \qquad \text{(B.II.5)}$$

gives:

$$\sigma_c = \left(\frac{1}{K}\right)^{1/n} \qquad \text{(B.II.6)}$$

Substituting these expressions into B.II.1 and rearranging we have:

$$\frac{\left(\frac{\dot{w}_o}{Kaq^n}\right)}{\left(\frac{a}{h}\right)^{2n+1}} = \left(\frac{2n+1}{n}\right)^n (3)^{\frac{n+1}{2}} V(o) \qquad \text{(B.II.7)}$$

III. Odqvist Membrane Solution [16]

In this analysis the transverse deflection at the center of the plate is expressed in the form:

$$w_o = \frac{2\sigma_c h\, W(o)}{q} \qquad \text{(B.III.1)}$$

where

$$W(o) = \frac{\rho_1^2}{4s}\left\{1+\tfrac{1}{2}C+\left[\frac{(4n^2+27n+9)}{18(n+3)}\right]C^2\right\}, \qquad \text{(B.III.2)}$$

$$\rho_1 = \frac{aq}{2\sigma_c h}, \qquad \text{(B.III.3)}$$

$$\frac{\dot{s}\,\rho_1^2}{8(n+3)s^{n+3}} = -C, \qquad \text{(B.III.4)}$$

$$s = \left[\frac{1}{s_o^{n+2}} + 8(n+2)(n+3)\frac{Ct}{\rho_1^2}\right]^{-\frac{1}{n+2}}, \qquad \text{(B.III.5)}$$

h is half the plate thickness, and C is tabulated as a function of n in the reference. In this form equation B.III.1 gives the center deflection as a function of time. For the deflection rate we take the derivative with respect to time:

$$\dot{w}_o = \frac{2\sigma_c h}{q}\,\dot{W}(o). \qquad \text{(B.III.6)}$$

Differentiating B.III.2 with respect to time:

$$\dot{W}(o) = -\frac{\rho_1^2}{4}\frac{\dot{s}}{s^2}\left\{1+\tfrac{1}{2}C+\frac{(4n^2+27n+9)C^2}{18(n+3)}\right\} \qquad \text{(B.III.7)}$$

from B.III.4:

$$\dot{s} = -C\,\frac{8(n+3)s^{n+3}}{\rho_1^2} \qquad \text{(B.III.8)}$$

Substituting B.III.5 and B.III.8 into B.III.7:

$$\dot{W}(o) = 2C(n+3)\left[1+\tfrac{1}{2}C+ \frac{(4n^2+27n+9)C^2}{18(n+3)}\right]$$

$$\left[\frac{1}{s_o^{n+2}} + 8(n+2)(n+3)\frac{Ct}{\rho_1^2}\right]^{-\frac{n+1}{n+2}} \qquad \text{(B.III.9)}$$

Substituting B.III.5 into B.III.2:

$$W(o) = \frac{\rho_1^2}{4}\left[\frac{1}{s_o^{n+2}} + 8(n+2)(n+3)\frac{Ct}{\rho_1^2}\right]^{\frac{1}{n+2}}$$

$$\left[1+\tfrac{1}{2}C+ \frac{(4n^2+27n+9)}{18(n+3)}C^2\right] \qquad \text{(B.III.10)}$$

Solving for t:

$$t = \frac{\rho_1^2}{8C(n+2)(n+3)}\left[\left(\frac{4\,W(o)}{\rho_1^2\,B}\right)^{n+2} - \frac{1}{s_o^{n+2}}\right] \qquad \text{(B.III.11)}$$

where $$B = 1 + \tfrac{1}{2}C + \frac{(4n^2+27n+9)}{18(n+3)}C^2 \quad . \qquad \text{(B.III.12)}$$

Substituting for t in B.III.9:

$$\dot{W}(o) = \frac{2C\,B^{n+2}(n+3)}{4^{n+1}} \quad \frac{\rho_1^{2n+2}}{(W(o))^{n+1}} =$$

$$\dot{\Phi} \quad \frac{\rho_1^{2n+2}}{(W(o))^{n+1}} \qquad \text{(B.III.13)}$$

where

$$\dot{\Phi} = \frac{2C\,B^{n+2}(n+3)}{4^{n+1}} \quad . \qquad \text{B.III.14)}$$

Note that $\dot{\Phi}$ here is that of reference [16] and bears no relation to the quantity Φ as used in Chapter II.

Odqvist's constitutive relation was:

$$\dot{\varepsilon}_{ij} = \frac{3}{2} \left(\frac{\sigma_e}{\sigma_c}\right)^{n-1} \frac{s_{ij}}{\sigma_c} \qquad \text{(B.III.15)}$$

which reduces in uniaxial stress to:

$$\varepsilon = \left(\frac{1}{\sigma_c}\right)^n \sigma^n \qquad \text{(B.III.16)}$$

giving:

$$\sigma_c = \left(\frac{1}{K}\right)^{1/n} \qquad \text{(B.III.17)}$$

Substituting B.III.1, B.III.3, B.III.6, B.III.14, and B.III.17 into B.III.13 and rearranging:

$$\frac{\left(\frac{\dot{w}_o}{Kaq^n}\right)}{\left(\frac{a}{2h}\right)^{2n+1}} = \dot{\Phi} \left(\frac{2h}{w_o}\right)^{n+1} \qquad \text{(B.III.18)}$$

Odqvist uses the symbol h to denote half of the plate thickness rather than the full thickness. If we call the full thickness h, we have a form analagous to that of the other results:

$$\frac{\left(\frac{\dot{w}_o}{Kaq^n}\right)}{\left(\frac{a}{h}\right)^{2n+1}} = \dot{\Phi} \frac{1}{\left(\frac{w_o}{h}\right)^{n+1}} \qquad \text{(B.III.19)}$$

where

$$\dot{\Phi} = \frac{2C\left[1+\frac{1}{2}C + \frac{4n^2 + 27n + 9}{18(n+3)} C^2\right]^{n+2} (n+3)}{4^{n+1}}$$

and C is tabulated as a function of n in reference [16].

IV. Membrane Solution for a Circular Plate, Onat and Yüksel [17]

Onat and Yüksel assume that an initially flat circular plate deforms into a spherical surface upon application of a lateral hydrostatic pressure. Consideration of this geometry shows that the middle surface strain rate tensors have principal directions which are directed along the sphere's parallel, meridian, and the normal to the surface. The first two strain rates are positive and the third is given by

$$\dot{\varepsilon}_3 = \frac{\dot{\alpha}}{h} = \frac{dh}{d\alpha} = -\dot{\alpha}\tan\frac{\alpha}{2} \qquad \text{(B.IV.1)}$$

For a spherical membrane:

$$\sigma_1 = \sigma_2 = \sigma = \frac{pR}{2h} = \frac{D_o}{2h_o}\,\frac{p}{\sin\alpha\,(1+\cos\alpha)} \qquad \text{(B.IV.2)}$$

Creep deformations are governed by the relation:

$$\dot{\alpha}\tan\frac{\alpha}{2} = f(\sigma) \qquad \text{(B.IV.3)}$$

where for Norton's law

$$f(\sigma) = \dot{\varepsilon}_o\left(\frac{\sigma}{\sigma_o}\right)^n = \frac{\dot{\varepsilon}_o}{\sigma_o^{\,n}}\,\sigma^n = K\sigma^n \qquad \text{(B.IV.4)}$$

The symbol p in B.IV.2 above represents the uniform pressure per unit area as used in [17], D_o is the diameter of the built-in support, and h_o is the original membrane thickness.

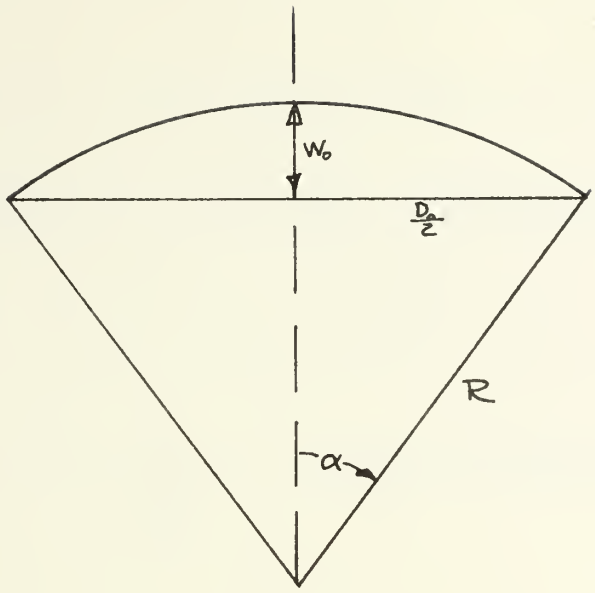

Figure B.IV.1

From the geometry of the above figure we see

$$w_o = R(1 - \cos \alpha) \tag{B.IV.5}$$

$$\frac{D_o}{2} = R \sin \alpha \tag{B.IV.6}$$

Equating R $$\frac{\sin \alpha}{(1-\cos\alpha)} = \frac{D_o}{2\, w_o} \tag{B.IV.7}$$

By trigonometric identity: $\tan \frac{\alpha}{2} = \frac{1-\cos\alpha}{\sin\alpha}$,

therefore, $\tan \frac{\alpha}{2} = \frac{2w_o}{D_o}$. (B.IV.8)

Differentiating with respect to time

$$\frac{d}{dt} (\tan\tfrac{\alpha}{2}) = \dot{\tfrac{\alpha}{2}} \sec^2\tfrac{\alpha}{2} = \frac{2\dot{w}_o}{D_o}$$

or $$\dot{\alpha} = \frac{4\dot{w}_o}{D_o \sec^2\frac{\alpha}{2}} \tag{B.IV.9}$$

Substituting B.IV.2, B.IV.4, B.IV.8, and B.IV.9 into B.IV.3

$$\left(\frac{4\dot{w}_o}{D_o \sec^2\frac{\alpha}{2}}\right)\left(\frac{2w_o}{D_o}\right) = K\left(\frac{D_o p}{2h_o}\right)^n \left(\frac{1}{\sin\alpha\ (1+\cos\alpha)}\right)^n$$

and rearranging

$$\frac{\left(\frac{\dot{w}_o}{Kap^n}\right)}{\left(\frac{a}{h_o}\right)^{n+1}} = \frac{1}{\left(\frac{w_o}{h_o}\right)}\left[\tfrac{1}{2}\left(\frac{1}{\sin\alpha\ (1+\cos\alpha)}\right)^n \sec^2\frac{\alpha}{2}\right] \qquad \text{(B.IV.10)}$$

where $a = \frac{D_o}{2}$.

The non-dimensional parameter resulting from the energy analysis is

$$\frac{\left(\frac{\dot{w}_o}{Kap^n}\right)}{\left(\frac{a}{h_o}\right)^{2n+1}} .$$

Transforming B.IV.10 to this form:

$$\frac{\left(\frac{\dot{w}_o}{Kap^n}\right)}{\left(\frac{a}{h_o}\right)^{2n+1}} = \frac{1}{\left(\frac{a}{h_o}\right)^n \left(\frac{w_o}{h_o}\right)}\left[\tfrac{1}{2}\left(\frac{1}{\sin\alpha\ (1+\cos\alpha)}\right)^n \sec^2\frac{\alpha}{2}\right] \qquad \text{(B.IV.11)}$$

Given $\frac{w_o}{h_o}$ and $\frac{a}{h_o}$, angle α can be found from B.IV.7 and values of

$\frac{\dot{w}_o}{Kap^n}\Big/\left(\frac{a}{h_o}\right)^{2n+1}$ computed as functions of $\frac{w_o}{h_o}$ and $\frac{a}{h_o}$.

APPENDIX C

Mathematical Details for Analysis with Combined Bending and Membrane Profile for the Clamped Circular Plate

Experiments indicate that a clamped circular plate undergoing creep deformation from a transverse hydrostatic pressure assumes a velocity profile described by:

$$\dot{w} = \dot{w}_o \left(1-\frac{r^2}{a^2}\right)^2 \tag{C.1}$$

when $\frac{w_o}{h}$ is relatively small. At larger values of $\frac{w_o}{h}$ the profile tends to the membrane form given by:

$$\dot{w} = \dot{w}_o\left(1-\frac{r^2}{a^2}\right) \tag{C.2}$$

These two forms can be combined by writing the velocity profile as:

$$\dot{w} = \dot{w}_o\left[\alpha_1\left(1-\frac{r^2}{a^2}\right)^2 + \alpha_2\left(1-\frac{r^2}{a^2}\right)\right] \tag{C.3}$$

where:

$$\alpha_1 + \alpha_2 = 1 \tag{C.4}$$

and:

$$0 \leq \alpha_1 \leq 1$$
$$0 \leq \alpha_2 \leq 1 \tag{C.5}$$

Equation C.3 reduces to the small deflection profile, C.1, for $\alpha_1 = 1$, $\alpha_2 = 0$; and to the membrane profile, C.2, for $\alpha_1 = 0$, $\alpha_2 = 1$. Using this profile and proceeding as in Chapter II:

$$\dot{\kappa}_r = -\dot{w}'' = \dot{w}_o[\alpha_1 \frac{4}{a^2}(1-\frac{3r^2}{a^2}) + \alpha_2 \frac{2}{a^2}] \qquad (C.6)$$

$$\dot{\kappa}_\theta = -\frac{\dot{w}'}{r} = \dot{w}_o[\alpha_1 \frac{4}{a^2}(1-\frac{r^2}{a^2}) + \alpha_2 \frac{2}{a^2}] \qquad (C.7)$$

and

$$\dot{\kappa}_r + \tfrac{1}{2}\dot{\kappa}_\theta = \frac{\dot{w}_o}{a^2}[2\alpha_1(3-7\frac{r^2}{a^2}) + 3\alpha_2] \qquad (C.8)$$

$$\dot{\kappa}_\theta + \tfrac{1}{2}\dot{\kappa}_r = \frac{\dot{w}_o}{a^2}[2\alpha_1(3-5\frac{r^2}{a^2}) + 3\alpha_2] \; . \qquad (C.9)$$

In these equations and those to follow we may, of course, eliminate either α_1 or α_2 by using C.4. This was not done here, however, in order to keep the terms from the C.1 profile and those from the C.2 profile directly visible and separated in each equation.

For the radial deflection rate, $\dot{u}$, we use the form:

$$\dot{u} = r(a-r)(c_1+c_2 r) \qquad (C.10)$$

The extensional deflection rates are:

$$\dot{e}_r = \dot{u}' + \dot{w}'w' \qquad \dot{e}_\theta = \frac{\dot{u}}{r} \qquad (C.11)$$

Using as before:

$$x = \frac{r}{a}, \; c_1 = c_1' \frac{\dot{w}_o w_o}{a^3}, \; c_2 = c_2' \frac{\dot{w}_o w_o'}{a^4},$$

$$\dot{e}_r = \frac{\dot{w}_o w_o}{a^2}[(1-2x)c_1' + (2x-3x^2)c_2' + 16x^2\alpha_1^2(1-x^2)^2$$

$$+ 16x^2\alpha_1\alpha_2(1-x^2) + 4x^2\alpha_2^2] \qquad (C.12)$$

$$\dot{e}_\theta = \frac{\dot{w}_o w_o}{a^2}[(1-x)c_1' + (x-x^2)c_2'] \qquad (C.13)$$

These reduce to the appropriate expressions for the small deflection profile when $\alpha_1 = 1$, $\alpha_2 = 0$, and to the appropriate membrane profile expressions for $\alpha_1 = 0$, and $\alpha_2 = 1$.

$$\dot{e}_r + \tfrac{1}{2}\dot{e}_\theta = \frac{\dot{w}_o w_o}{a^2}\left[\left(\tfrac{3}{2} - \tfrac{5}{2}x\right)c_1' + \left(\tfrac{5}{2}x - \tfrac{7}{2}x^2\right)c_2' + 16x^2\alpha_1^2(1-x^2)^2\right.$$

$$\left. + 16x^2\alpha_1\alpha_2(1-x^2) + 4x^2\alpha_2^2\right] \qquad \text{(C.14)}$$

$$\dot{e}_\theta + \tfrac{1}{2}\dot{e}_r = \frac{\dot{w}_o w_o}{a^2}\left[\left(\tfrac{3}{2} - 2x\right)c_1' + \left(2x - \tfrac{5}{2}x^2\right)c_2'\right.$$

$$\left. + 8x^2\alpha_1^2(1-x^2)^2 + 8x^2\alpha_1\alpha_2(1-x^2) + 2x^2\alpha_2^2\right] \qquad \text{(C.15)}$$

The general expression for moment per unit length derived earlier is:

$$M = \left(\frac{4}{3K}\right)^{1/n}\frac{n}{n+1}\frac{1}{b}\left[\frac{h}{2}\left|a+\frac{bh}{2}\right|^{1+1/n} - \frac{n}{(2n+1)b}\left|a+\frac{bh}{2}\right|_s^{2+1/n}\right.$$

$$\left. + \frac{h}{2}\left|a-\frac{bh}{2}\right|^{1+1/n} + \frac{n}{(2n+1)b}\left|a-\frac{bh}{2}\right|_s^{2+1/n}\right] \qquad \text{(C.16)}$$

and for extensional forces is:

$$N = \left(\frac{4}{3K}\right)^{1/n}\frac{n}{n+1}\frac{1}{b}\left[\left|a+\frac{bh}{2}\right|^{1+1/n} - \left|a-\frac{bh}{2}\right|^{1+1/n}\right] \qquad \text{(C.17)}$$

Where for M_r and N_r: $\begin{cases} a = \dot{e}_r + \frac{1}{2}\dot{e}_\theta \\ b = \dot{\kappa}_r + \frac{1}{2}\dot{\kappa}_\theta \end{cases}$

and for M_θ and N_θ : $\begin{cases} a = \dot{e}_\theta + \frac{1}{2}\dot{e}_r \\ b = \dot{\kappa}_\theta + \frac{1}{2}\dot{\kappa}_r \end{cases}$

Defining:

$$A_c \equiv 2\alpha_1(3 - 7x^2) + 3\alpha_2$$

$$B_c \equiv (\tfrac{3}{2} - \tfrac{5}{2}x)c_1' \frac{w_o}{h} + (\tfrac{5}{2}x - \tfrac{7}{2}x^2)c_2' \frac{w_o}{h}$$

$$+ 16x^2\alpha_1^2(1-x^2)^2 \frac{w_o}{h} + 16x^2\alpha_1\alpha_2(1-x^2) \frac{w_o}{h} + 4x^2\alpha_2^2 \frac{w_o}{h}$$

$$D_c \equiv 2\alpha_1(3 - 5x^2) + 3\alpha_2$$

$$E_c \equiv (\tfrac{3}{2} - 2x)c_1' \frac{w_o}{h} + (2x - \tfrac{5}{2}x^2)c_2' \frac{w_o}{h} + 8x^2\alpha_1^2(1-x^2)^2 \frac{w_o}{h}$$

$$+ 8x^2\alpha_1\alpha_2(1-x^2) \frac{w_o}{h} + 2x^2\alpha_2^2 \frac{w_o}{h} ,$$

we may write:

$$M_r\dot{\kappa}_r = (\frac{4}{3K})^{1/n} \frac{n}{n+1} h^{2+1/n} (\frac{\dot{w}_o}{a^2})^{1+1/n} [\frac{1}{2A_c}|B_c + \tfrac{1}{2}A_c|^{1+1/n}$$

$$-\frac{n}{(2n+1)\ A_c^2} |B_c + \tfrac{1}{2}A_c|_s^{2+1/n} + \frac{1}{2A_c}| B_c - \tfrac{1}{2}A_c|^{1+1/n}$$

$$+\frac{n}{(2n+1)\ A_c^2} | B_c - \tfrac{1}{2}A_c|_s^{2+1/n}] \cdot [4\alpha_1(1-3x^2)+2\alpha_2] \quad (C.18)$$

$$N_r\dot{e}_r = (\frac{4}{3K})^{1/n} \frac{n}{n+1} h^{2+1/n} (\frac{\dot{w}_o}{a^2})^{1+1/n} \frac{1}{A_c} [|B_c + \tfrac{1}{2}A_c|^{1+1/n}$$

$$-|B_c - \tfrac{1}{2}A_c|^{1+1/n}] \cdot [(1-2x)c_1' \frac{w_o}{h} + (2x - 3x^2)c_2' \frac{w_o}{h}$$

$$+ 16x^2\alpha_1^2(1-x^2)^2 \frac{w_o}{h} + 16\alpha_1\alpha_2(1-x^2)x^2 \frac{w_o}{h}$$

$$+ 4x^2\alpha_2^2 \frac{w_o}{h}] \quad (C.19)$$

$$M_\theta \dot{\kappa}_\theta = \left(\frac{4}{3K}\right)^{1/n} \frac{n}{n+1} \; h^{2+1/n} \left(\frac{\dot{w}_o}{a^2}\right)^{1+1/n} \left[\frac{1}{2D_c}\left|E_c + \tfrac{1}{2}D_c\right|^{1+1/n}\right.$$

$$- \frac{n}{(2n+1)D_c^2}\left|E_c + \tfrac{1}{2}D_c\right|_s^{2+1/n} + \frac{1}{2D_c}\left|E_c - \tfrac{1}{2}D_c\right|^{1+1/n}$$

$$\left. + \frac{n}{(2n+1)D_c^2}\left|E_c - \tfrac{1}{2}D_c\right|_s^{2+1/n}\right] \cdot [4\alpha_1(1-x^2) + 2\alpha_2] \quad (C.20)$$

$$N_\theta \dot{e}_\theta = \left(\frac{4}{3K}\right)^{1/n} \frac{n}{n+1} \; h^{2+1/n} \left(\frac{\dot{w}_o}{a^2}\right)^{1+1/n} \frac{1}{D_c} \left[\left|E_c + \tfrac{1}{2}D_c\right|^{1+1/n}\right.$$

$$\left. -\left|E_c - \tfrac{1}{2}D_c\right|^{1+1/n}\right] \cdot \left[(1-x)c_1' \frac{w_o}{h} + (x-x^2)c_2' \frac{w_o}{h}\right]. \quad (C.21)$$

The total energy dissipation rate is obtained by integrating these expressions over the deformed surface area of the plate. This gives:

$$\dot{V} = 2\pi a^2 \left(\frac{4}{3K}\right)^{1/n} \frac{n}{n+1} \; h^{2+1/n} \left(\frac{\dot{w}_o}{a^2}\right)^{1+1/n} I_c \quad (C.22)$$

where I_c is the integral of the bracketed expressions above over x for a particular case $\left(\frac{w_o}{h}, n\right)$, and where the integral has been minimized with respect to c_1' and c_2' for the value of α_1 and α_2 under consideration.

Taking a small variation of $\dot{w}_o$ about its equlibrium position for some particular value of $\frac{w_o}{h}$:

$$\frac{d\dot{V}}{d\dot{w}_o} \; \delta\dot{w}_o = 2\pi \int_o^a q \; \delta\dot{w}_r dr \quad (C.23)$$

or

$$\dot{w}_o^{1/n} \left[2\pi a^2 \left(\frac{4}{3K}\right)^{1/n} h^{2+1/n} \left(\frac{1}{a^2}\right)^{1+1/n} I_c\right] \delta\dot{w}_o =$$

$$2\pi q \delta\dot{w}_o \int_o^a \left[\alpha_1\left(1-\frac{r^2}{a^2}\right)^2 + \alpha_2\left(1-\frac{r^2}{a^2}\right)\right] r dr. \quad (C.24)$$

Solving for $\dot{w}_o$:

$$\dot{w}_o = \left[\frac{q\, a^{2+2/n}}{\left(\frac{4}{3K}\right)^{1/n} h^{2+1/n} \frac{12}{3-\alpha_1} I_c}\right]^n , \qquad (C.25)$$

or

$$\dot{w}_o = \left[\left(\frac{a}{h}\right)^{2+1/n} \left(\frac{3Ka}{4}\right)^{1/n} q \left(\frac{3-\alpha_1}{12\, I_c}\right)\right]^n , \qquad (C.26)$$

and in non-dimensional form:

$$\left(\frac{\dot{w}_o}{Kaq^n}\right) = \frac{3}{4} \left(\frac{a}{h}\right)^{2n+1} \left(\frac{3-\alpha_1}{12\, I_c}\right)^n \qquad (C.27)$$

APPENDIX D

Mathematical Details for Analysis of a Simply Supported Circular Plate

In calculating the elastic deflection of a simply supported circular plate subjected to a uniform lateral pressure Timoshenko and Woinowsky-Krieger [26] find that the deformation profile assumes the following form:

$$w = w_o \left(1 - \frac{r^2}{a^2}\right)\left(1 - \frac{1 + \nu}{5 + \nu} \frac{r^2}{a^2}\right) \tag{D.1}$$

where w_o is the center deflection. If we make $\nu = 1/2$ and take derivatives with respect to time, we get the deformation rate profile:

$$\dot{w} = \dot{w}_o \left(1 - \frac{r^2}{a^2}\right)\left(1 - \frac{3}{11} \frac{r^2}{a^2}\right). \tag{D.2}$$

One may now compute:

$$\dot{\kappa}_r = -\dot{w}'' = \frac{\dot{w}_o}{a^2} \left[\frac{28}{11} - \frac{36}{11} \frac{r^2}{a^2}\right] \tag{D.3}$$

$$\dot{\kappa}_\theta = -\frac{\dot{w}'}{r^2} = \frac{\dot{w}_o}{a^2} \left[\frac{28}{11} - \frac{12}{11} \frac{r^2}{a^2}\right], \tag{D.4}$$

and

$$\dot{\kappa}_r + \tfrac{1}{2}\dot{\kappa}_\theta = \frac{\dot{w}_o}{a^2} \left[\frac{42}{11} - \frac{42}{11} \frac{r^2}{a^2}\right] \tag{D.5}$$

$$\dot{\kappa}_\theta + \tfrac{1}{2}\dot{\kappa}_r = \frac{\dot{w}_o}{a^2} \left[\frac{42}{11} - \frac{30}{11} \frac{r^2}{a^2}\right]. \tag{D.6}$$

Using, as in Chapter II, the expression:

$$\dot{u} = r(a-r)(c_1 + c_2 r) \tag{D.7}$$

for radial deflection rate where,

$$c_1 = c_1' \frac{\dot{w}_o w_o}{a^3} \qquad c_2 = c_2' \frac{\dot{w}_o w_o}{a^4} \tag{D.8}$$

and letting $x \equiv r/a$:

$$\dot{e}_r = \dot{u}' + \dot{w}'w' = \frac{\dot{w}_o w_o}{a^2} [(1-2x)c_1' + (2x-3x^2)c_2' + x^2(\frac{28}{11} - \frac{12}{11} x^2)^2] \tag{D.9}$$

$$\dot{e}_\theta = \frac{\dot{u}}{r} = \frac{\dot{w}_o w_o}{a^2} [(1-x)c_1' + (x-x^2)c_2'] \tag{D.10}$$

and

$$\dot{e}_r + \tfrac{1}{2}\dot{e}_\theta = \frac{\dot{w}_o w_o}{a^2} [(\tfrac{3}{2} - \tfrac{5}{2}x)c_1' + (\tfrac{5}{2}x - \tfrac{7}{2}x^2)c_2' + x^2(\frac{28}{11} - \frac{12}{11}x^2)^2] \tag{D.11}$$

$$\dot{e}_\theta + \tfrac{1}{2}\dot{e}_r = \frac{\dot{w}_o w_o}{a^2} [(\tfrac{3}{2} - 2x)c_1' + (2x - \tfrac{5}{2}x)c_2' + \frac{x^2}{2}(\frac{28}{11} - \frac{12}{11} x^2)^2] \tag{D.12}$$

These expressions may now be substituted into the equations for moment and extensional force resultants, (2.14) through (2.17). Defining:

$$A_s \equiv (\frac{42}{11} - \frac{42}{11} x^2)$$

$$B_s \equiv (\tfrac{3}{2} - \tfrac{5}{2}x)\frac{w_o}{h}c_1' + (\tfrac{5}{2}x - \tfrac{7}{2}x^2)\frac{w_o}{h}c_2' + x^2(\frac{28}{11} - \frac{12}{11}x^2)^2\frac{w_o}{h}$$

$$D_s \equiv (\frac{42}{11} - \frac{30}{11} x^2)$$

$$E_s \equiv (\tfrac{3}{2} - 2x)c_1' \frac{w_o}{h} + (2x - \tfrac{5}{2}x^2)c_2' \frac{w_o}{h} + \frac{x^2}{2}(\frac{28}{11} - \frac{12}{11}x^2)^2\frac{w_o}{h}$$

we may write:

$$M_r\dot{\kappa}_r = \left(\frac{4}{3K}\right)^{1/n} \frac{n}{n+1} h^{2+1/n} \left(\frac{\dot{w}_o}{a^2}\right)^{1+1/n} \left[\frac{1}{2A_s} \left|B_s + \tfrac{1}{2}A_s\right|^{1+1/n}\right.$$

$$- \frac{n}{(2n+1)A_s^2} \left|B_s + \tfrac{1}{2}A_s\right|_s^{2+1/n} + \frac{1}{2A_s} \left|B_s - \tfrac{1}{2}A_s\right|^{1+1/n}$$

$$+ \left.\frac{n}{(2n+1)A_s^2} \left|B_s - \tfrac{1}{2}A_s\right|_s^{2+1/n}\right] \cdot \left[\frac{28}{11} - \frac{36}{11} x^2\right] \qquad (D.13)$$

$$N_r\dot{e}_r = \left(\frac{4}{3K}\right) \frac{n}{n+1} h^{2+1/n} \left(\frac{\dot{w}_o}{a^2}\right)^{1+1/n} \frac{1}{A_s} \left[\left|B_s + \tfrac{1}{2}A_s\right|^{1+1/n}\right.$$

$$\left. - \left|B_s - \tfrac{1}{2}A_s\right|^{1+1/n}\right] \cdot \left[(1 - 2x)c_1' \frac{w_o}{h} + (2x - 3x^2)c_2' \frac{w_o}{h}\right.$$

$$\left. + x^2\left(\frac{28}{11} - \frac{12}{11}x^2\right)^2 \frac{w_o}{h}\right] \qquad (D.14)$$

$$M_\theta\dot{\kappa}_\theta = \left(\frac{4}{3K}\right) \frac{n}{n+1} h^{2+1/n} \left(\frac{\dot{w}_o}{a^2}\right)^{1+1/n} \left[\frac{1}{2D_s} \left|E_s + \tfrac{1}{2}D_s\right|^{1+1/n}\right.$$

$$- \frac{n}{(2n+1)D_s^2} \left|E_s + \tfrac{1}{2}D_s\right|_s^{2+1/n} + \frac{1}{2D_s} \left|E_s - \tfrac{1}{2}D_s\right|^{1+1/n}$$

$$+ \left.\frac{n}{(2n+1)D_s^2} \left|E_s - \tfrac{1}{2}D_s\right|_s^{2+1/n}\right] \cdot \left[\frac{28}{11} - \frac{12}{11} x^2\right] \qquad (D.15)$$

$$N_\theta\dot{e}_\theta = \left(\frac{4}{3K}\right)^{1/n} \frac{n}{n+1} h^{2+1/n} \left(\frac{\dot{w}_o}{a^2}\right)^{1+1/n} \frac{1}{D_s} \left[\left|E_s + \tfrac{1}{2}D_s\right|^{1+1/n}\right.$$

$$\left. - \left|E_s - \tfrac{1}{2}D_s\right|^{1+1/n}\right] \cdot \left[(1-x)c_1' \frac{w_o}{h} + (x-x^2)c_2' \frac{w_o}{h}\right].$$

$$(D.16)$$

The internal energy dissipation rate is:

$$\dot{V} = 2\pi a^2 \int_0^1 (M_r \dot{\kappa}_r + M_\theta \dot{\kappa}_\theta + N_r \dot{e}_r + N_\theta \dot{e}_\theta)\, x dx \qquad (D.17)$$

giving with (D.13) through (D.16):

$$\dot{V} = 2\pi a^2 \left(\frac{4}{3K}\right)^{1/n} \frac{n}{n+1} h^{2+1/n} \left(\frac{\dot{w}_o}{a^2}\right)^{1+1/n} I_s \qquad (D.18)$$

where I_s is the integral of the bracketed geometric terms in the above expression. From the principle of virtual velocities:

$$\frac{d\dot{V}}{d\dot{w}_o} \delta\dot{w}_o = 2\pi \int_0^a q\, \delta\dot{w}\, r dr \qquad (D.19)$$

which gives:

$$\dot{w}_o^{1/n} \left(\frac{1}{a^2}\right)^{1+1/n} 2\pi a^2 \left(\frac{4}{3K}\right)^{1/n} h^{2+1/n} I_s\, \delta\dot{w}_o =$$

$$2\pi q\, \delta\dot{w}_o \int_0^a \left(1-\frac{r^2}{a^2}\right)\left(1-\frac{3}{11}\frac{r^2}{a^2}\right) r dr = 2\pi q \delta\dot{w}_o \frac{5}{22} a^2. \qquad (D.20)$$

So:

$$\dot{w}_o = \left[\frac{q a^{2+2/n}}{\left(\frac{4}{3K}\right)^{1/n} h^{2+1/n} \frac{22}{5} I_s}\right]^n \qquad (D.21)$$

or $$\dot{w}_o = \left[\left(\frac{a}{h}\right)^{2+1/n} \left(\frac{3Ka}{4}\right)^{1/n} q \frac{1}{\frac{22}{5} I_s}\right]^n \qquad (D.22)$$

or $$\frac{\dot{w}_o}{Kaq^n} = \left(\frac{a}{h}\right)^{2n+1} \frac{3}{4} \left[\frac{1}{\frac{22}{5} I_s}\right]^n. \qquad (D.23)$$

APPENDIX E

Illustration of Technique for Finding the Minimum Energy Integral

As explained in Chapter II, the quantities c_1' and c_2' are determined by requiring that the internal energy dissipation rate (2.37) be minimized. Since the integration required to evaluate (2.37) must be done numerically, this minimization must be accomplished through a systematic search. The minimization must be done for each case ($\frac{w_o}{h}$, n) of interest; but, by considering a systematically varied series of cases, a set of curves such as those in Figures 2.2 and 2.4 can be obtained.

The procedure used for minimization can be illustrated by considering a typical case, n = 5.0 and $\frac{w_o}{h}$ = 1.0 for clamped edges. The computer program listed in Appendix H, when provided an initial value for c_1' and a value for c_2', will compute the integral, I_c, for the given c_1' and c_2' values at regular intervals of 0.3. In the accompanying plots, the quantity Φ rather than the integral I_c is plotted so that Φ may be transferred directly to Figure 2.2. As $\Phi = f(\frac{1}{I_c})$, the maximum value of Φ corresponds to the minimum value of I_c. As seen in the plots, c_1' is varied until a peak is found for a particular value of c_2'. Peaks are then found for other values of c_2' until a maximum is found with respect to c_2'. The resulting envelope of curves gives a maximum value of Φ which gives a point on the plot of Figure 2.2. The procedure is then repeated for the other values of $\frac{w_o}{h}$ and n.

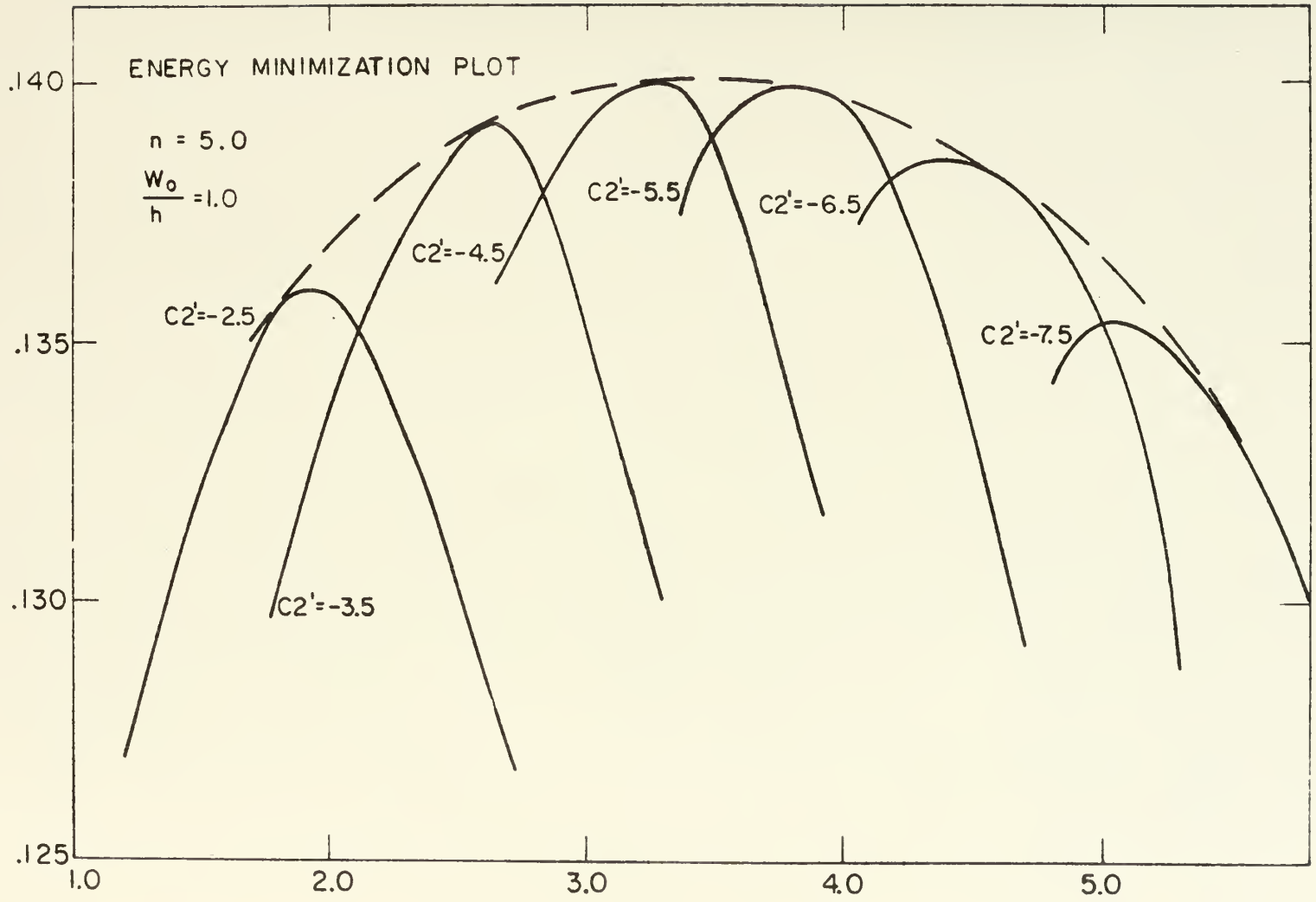
ENERGY MINIMIZATION PLOT
n = 5.0
$\frac{W_o}{h}$ = 1.0
C2'=-2.5
C2'=-3.5
C2'=-4.5
C2'=-5.5
C2'=-6.5
C2'=-7.5
.140
.135
.130
.125
Φ
1.0
2.0
3.0
4.0
5.0
C 1'

FIG. E.1

There is no mathematical assurance that the value of Φ found as above represents a unique and absolute maximum value. The initial area of search was that suggested for the analytical solution of the n = 1.0 case; and a very broad parameter search with respect to c_1' and c_2' gave no evidence of any higher maxima. The agreement between the experimental results and the theoretical results suggests that the values of Φ obtained are, in fact, the proper ones.

APPENDIX F

Tabulation of Data from Plate Experiments

The following tables list the data taken during the plate experiments discussed in Chapter I.A. All tests were taken at room temperature which generally was 75°F ±3°F with some points outside these limits. It is, of course, a well known fact that creep behavior in metals is affected by temperature. Within the relatively narrow temperature band here considered, however, such effects may be expected to be rather small and definitely secondary to the influence of pressure and geometry effects which were to be investigated in the plate tests. Examination of the data reveals no appreciable systematic influence of temperature in these tests. All times are in hours and minutes, all deflections are in inches, all pressures in pounds per square inch, and all temperatures in °F.

TEST 1

8 LB. PLATE 3.0 psi

Time Hrs-Mins	r=0	r=½"	r=1"	r=1½"	r=2"	r=2¼"	Temp. °F
00	.0052						72
01	53	.0049	.0033	.0021	.0005	.0001	
03	54	49	33½	21	05	01½	
15	57	53	36	22	06	01½	
32	58½	55	37	24	06¼	01½	72
50	60	57	38½	24	07	02	
1-00	61	57	39	24	07	02	72
1-30	63	59	40	25	07½	02	
2-00	64	61	41½	26	09	02	72
2-42	66	63	43	27	09	02	
3-00	67	64	43	27½	09	02	72
4-45	71	67	61	29	10	02	
5-20	72½	68	47	29¾	10	02½	72
6-00	73	68½	48	30	10	02½	
6-30	74	70	48½	31	10	02½	72
25-00	92	88	62	39	14	07	74
47-00	.0110	.0105	75	47	17	08	76
52-00	14	08	78	48	18	08½	76
73-00	23	20	86	53	20	10	76
100-30	30	26½	90	55¼	21	10	76
125-40	34	30	93	57	21½	11	76

TEST 2

8 LB. PLATE 3.0 psi

Time	r=0	r=½"	r=1"	r=1½"	r=2"	r=2¼"	Temp. °F
00	.0052						
01	53	.0045	.0036	.0020	.0007	.0002	77
03	54	45	37	21	07	02	
15	56	51	38½	23	08½	02	
32	58	53	40	23½	09	02	76
50	59	53	41	24	09	02	
1-00	59½	53½	41	24	09	02	76
3-50	65	62	45	28	11	02	76
4-30	67	64	46	28	11½	02¾	76
5-00	68	64¾	47	29	12	03	76
5-32	69	65	48	29	12	03	76

TEST 3

8 LB. PLATE 4.1 psi

Time Hrs-Mins	r=0	r=½"	r=1"	r=1½"	r=2"	r=2¼"	Temp. °F
00	.0352						
01	.0388	.0353	.0280	.0181	.0060	.0023	69
03	.0405	70	93	89	63	25	
07	26	85	.0304	97	65	26	
11	33	94	11	.0201	67	26	
18	44	.0404	19	05	69	28	
30	56	15	28	10	71	29	68½
47	68	26	36	16	73	29	
1-00	75	33	41	19	74	30	68½
1-26	84	41	47	23	75	31	
1-49	93	48	54	27	77	31	69
2-30	.0510	64	66	34	80	36	
3-00	17	70	72	37	81	36	69
4-10	32	84	81	44	83	37	
5-00	40	91	88	48	85	37	69
5-30	46	98	92	51	86	38	
5-50	49	.0500	94	52	87	38	69½

TEST 4

8 LB. PLATE 4.1 psi

Time	r=0	r=½"	r=1"	r=1½"	r=2"	r=2¼"	Temp. °F
00	.0310						70
01	.0355	.0311	.0251	.0145	.0055	.0017	
03	63	25	62	51	58	18	
06	78	38	77	57	60	19	
11	91	50	83	61	62	21	
15	98	56	88	64	63	21	70
22	.0407	64	94	67	64	21	
30	18	73	.0300	72	65	22	
45	30	85	09	77	68	22	
1-00	37	91	15	80	69	23	70
1-41	56	.0410	28	88	72	24	
2-00	62	15	32	91	74	25	70
2-30	71	24	39	95	76	25	
3-00	79	31	45	97	77	25	70½
3-33	87	39	50	.0201	78	25	
4-06	94	45	56	04	80	26	71
4-30	.0500	50	60	07	80	27	
5-00	05	55	64	09	82	27	71

TEST 5

8 LB. PLATE 6.1 psi

Time Hrs-Mins	r=0	r=½"	r=1"	r=1½"	r=2"	r=2¼"	Temp. °F
00	.0824						79
01	.0869	.0805	.0614	.0376	.0150	.0055	
03	96	28	32	87	55	57	
06	.0916	47	46	95	59	59	
15	44	75	66	.0408	64	62	
25	61	94	81	17	68	64	
31	68	.0902	86	21	70	64	79
45	87	15	98	27	74	66	
1-00	99	28	.0708	34	77	66	80
1-30	.1020	48	23	44	80	68	
2-00	35	64	34	52	84	70	80
3-00	59	89	53	64	90	72	
3-36	72	.1000	62	69	93	73	81
4-45	93	20	76	79	98	75	
5-15	.1107	27	86	83	.0200	82	81
6-00	19	40	93	88	03	82	

TEST 6

8 LB. PLATE 6.1 psi

Time	r=0	r=½"	r=1"	r=1½"	r=2"	r=2¼"	Temp. °F
00	.0840						
01	.0883	.0842	.0631	.0379	.0156	.0073	76½
03	.0908	65	49	90	61	75	
07	33	86	66	.0400	65	78	
15	55	.0910	83	11	70	80	
34	85	36	.0707	24	76	85	76½
48	98	49	17	30	79	86	
1-00	.1006	57	22	34	80	87	76½
1-25	21	70	35	41	83	89	
1-50	33	81	44	47	87	92	77
2-00	38	87	48	49	88	93	
3-15	61	.1009	68	59	92	95	78
4-20	78	23	81	66	96	97	
5-50	98	43	98	76	.0201	.0100	78

TEST 7

8 LB. PLATE 8.01 psi

Time Hrs-Mins	r=0	r=½"	r=1"	r=1½"	r=2"	r=2¼"	Temp. °F
00	.1270						73
01	.1313	.1251	.0943	.0613	.0244	.0120	
03	39	76	65	28	50	24	
06	65	98	82	39	55	29	
12	88	.1321	.1002	52	60	32	73
34	.1429	57	36	73	70	38	
1-00	54	84	57	88	76	42	
1-27	75	.1403	74	98	81	46	73
2-00	91	22	88	.0708	86	48	
3-23	.1524	49	.1114	26	93	54	73
4-00	34	58	22	32	96	55	
5-15	52	76	36	42	.0301	58	74

TEST 8

8 LB. PLATE 8.01 psi

Time	r=0	r=½"	r=1"	r=1½"	r=2"	r=2¼"	Temp. °F
00	.1252						76
01	.1301	.1247	.0921	.0586	.0237	.0095	
03	28	74	42	99	43	98	
05	43	88	55	.0607	47	99	
18	89	.1333	91	33	57	.0104	
30	.1413	54	.1012	45	62	10	76
45	31	70	28	55	66	12	
1-00	45	83	39	63	69	14	76
1-15	56	93	48	69	72	15	
1-30	65	.1403	56	75	75	16	
2-20	89	23	76	87	80	19	76
3-06	.1504	40	90	97	85	21	
3-35	17	51	98	.0703	88	24	75
4-00	24	57	.1104	07	89	24	76
4-45	36	68	14	15	93	27	76
5-45	50	83	26	23	96	30	
6-00	53	86	29	25	97	30	76

TEST 9

6 LB. PLATE 2.39 psi

Time Hrs-Mins	r=0	r=½"	r=1"	r=1½"	r=2"	r=2¼"	Temp. °F
00	.0099						74
01	.0100	.0091	.0067	.0025	.0012	.0001	
09	12¾	.0102½	74½	31	13¾	01¾	
15	15½	05	77	32	14	01¾	
21	18	07½	78½	33	14¾	02	
30	20	11	80	34¾	15	02	
45	23	13⅓	82¾	36	16	03	74
1-00	25¾	14	84	37¼	16⅔	03	
1-15	27⅓	17	86	38	16¾	03	
1-30	29¼	19¾	87¼	38¾	17	03⅓	
2-00	32¾	23¾	90	40¾	18	05	74
3-17	37	30	93⅓	43	19	05	
4-00	38¾	31¾	95	44¼	19	05¼	74
4-30	39½	32	96¼	44¾	19	05¼	
4-45	39¾	32	96½	44¾	19	05½	
5-00	41¼	33¼	97	45¼	19¼	05½	74
5-15	41¼	33⅔	97½	45½	19¼	05½	
5-30	41⅓	33¾	97¾	45½	19½	05½	
6-15	41¾	36¾	99	47	20	05½	74

TEST 10

6 LB. PLATE 2.39 psi

Time	r=0	r=½"	r=1"	r=1½"	r=2"	r=2¼"	Temp. °F
00	.0097						74
01	.0100	.0089	.0068	.0026	.0010	.0000	
09	09	.0100	75	31	12	00	74
15	12	03	77½	32	12	00½	
21	14	05	79	33	13	01	
30	16½	07	80½	34	13	01	
46	19½	11	82½	36	13½	01	74
1-00	21½	13	84	37	14	01	
1-15	23	13½	85	38	14½	01	
1-30	24¼	14¾	86	38	14¾	01	
2-00	27½	18	88¾	39¾	15	02	74
3-15	33	23	92¼	42	16	02¼	
4-00	34½	25¼	94	43⅓	17	02½	
4-30	35	27	94¼	44	17	02¾	
5-00	35¼	28	95½	44¾	17	02¾	
5-15	35¼	28	95¾	44⅞	17	02¾	
5-30	35⅓	28¼	96	45	17	03	
6-15	35⅔	29⅔	97	45¼	17	03	

TEST 11

6 LB. PLATE 4.1 psi

Time Hrs-Mins	r=0	r=½"	r=1⅛"	r=1⅝"	r=2"	Temp °F
00	.0510					76
01	57	.0498	.0350	.0265	.0081	
06	79	27	71	80	86	
12	94	42	81	87	89	
15	.0600	47	85	90	90	76
21	09	54	91	94	92	
30	19	63	98	99	94	76
45	31	74	07	05	96	
1-00	40	82	13	09	97½	76
1-15	47½	88	18	13	00	
1-30	52	93	22	15	00½	
2-00	62	03	29	20	02½	76
2-30	71	11	35	24	04	
3-00	79	20	41	28	06	76
4-02	90½	32	49	34	08½	
4-30	97¾	36	53	37	09	76
4-45	99	39	55	38	10	
5-00	.0701	41	57	40	12	
5-15	03½	43	59	41½	12	76

TEST 12

6 LB. PLATE 4.1 psi

Time Hrs-Mins	r=0	r=½"	r=1"	r=1½"	r=2"	Temp °F
00	.0530					76
01	.0574	.0519	.0399	.0247	.0092	
06	12	52	24	63	98	
12	26	67	34	71	01	76
15	33	71	37	73	02	
24	43	81	44	79	05	
30	52	89	50	82	06	
53	72	.0607	65	92	10	76
2-22	.0708	41	94	.0310	17	76
2-45	15	47	99	13	18	
3-00	21	51	.0502	15	19	76
3-31	29	59	09	20	21	
4-30	40½	70	18	26	23	
5-00	44	75½	23	28	24	76
5-30	51	79½	27	31	25	
6-00	54	83	30	34	26	76
6-12	57	85	31	34	26½	

TEST 13

6 LB. PLATE 6.1 psi

Time Hrs-Mins	r=0	r=½"	r=1"	r=1½"	r=2"	r=2¼"	Temp °F
00	.0880						76
01	.0927	.0852	.0650	.0441	.0175	.0071	
03	51	74	68	53	80	73	
06	68	90	80	62	84	75	
11	85	.0905	94	71	88	78	
15	94	15	.0701	76	90	79	
30	.1017	38	20	90	96	81	76
40	29	49	28	96	98	83	
45	33	54	33	99	.0200	83	
1-00	45	64	42	.0505	03	85	76
1-17	57	78	53	11	05	87	
1-31	66	84	59	15	06	89	77
2-00	83	.0100	71	24	11	91	
2-30	94	11	80	31	13	92	77
3-00	.1104	22	89	37	15	93	77½
4-15	26	43	.0807	50	21	95	
4-45	33	51	14	54	23	96	77½
5-30	45	60	23	60	26	.0100	

TEST 14

6 LB. PLATE 6.1 psi

Time	r=0	r=½"	r=1"	r=1½"	r=2"	r=2¼"	Temp °F
00	.0878						
02	.0936	.0865	.0643	.0438	.0152	.0078	80
06	62	88	65	51	57	82	
15	87	.0915	85	65	62	86	
31	.1016	42	.0706	79	68	97	80
45	32	56	18	88	71	98	
1-00	44	68	28	94	74	.0100	80
1-23	60	83	40	.0503	78	03	
1-30	66	88	45	06	79	04	
2-00	79	98	55	13	81	05	80
2-30	91	.1013	66	21	84	07	
2-45	97	17	70	24	84	07	
3-16	.1106	26	77	30	86	08	80
4-00	18	37	87	36	89	09	
5-00	30	48	98	44	92	11	
5-30	36	56	.0802	48	94	12	80

TEST 15

6 LB. PLATE 8.0 psi

Time Hrs-Mins	r=0	r=½"	r=1"	r=1½"	r=2"	r=2¼"	Temp °F
00	.1308						75
01	.1354	.1265	.1009	.0679	.0255	.0114	
03	78	88	28	93	61	16	
06	98	.1308	44	.0705	66	19	
15	.1427	36	72	25	74	23	75
24	57	54	84	36	80	27	
30	63	61	92	42	83	29	75
45	73	78	.1108	54	88	31	
1-00	87	91	19	63	92	33	75
1-15	97	.1403	29	70	96	35	
1-36	.1510	14	40	79	.0300	36	75½
2-00	24	27	51	88	05	38	
2-45	44	51	69	.0803	11	44	76
3-00	50	59	74	07	12	44	
4-20	74	81	97	25	20	47	76
5-04	87	95	.1206	33	24	48	
5-30	93	.1500	12	38	26	49	76½
6-00	.1600	06	18	43	28	50	

TEST 16

6 LB. PLATE 8.0 psi

Time	r=0	r=½"	r=1"	r=1½"	r=2"	r=2¼"	Temp °F
00	.1295						76
01	.1342	.1248	.1009	.0636	.0265	.0087	
03	68	78	30	53	72	89	
06	88	97	47	65	77	92	
15	.1417	.1322	73	83	86	96	76
24	34	44	88	97	91	98	
45	65	68	.1113	.0716	.0300	.0103	
1-00	78	85	25	27	05	04	76
1-16	90	98	37	35	09	06	
1-30	99	.1406	44	42	12	07	
2-00	.1517	19	60	53	18	09	76
2-30	31	36	71	63	23	10	
3-04	44	47	83	73	27	12	
3-30	53	59	92	80	30	13	76

TEST 17

4 LB. PLATE 0.82 psi

Time Hrs-Mins	r=0	r=½"	r=1"	r=1½"	r=2"	r=2¼"	Temp °F
00	.0110						75
01	.0112	.0106	.0080	.0050	.0018	.0003	
03	15	08	82	50	18	03	
06	18	13	84	52	20	04	
15	23	16	88	53	20	04	74½
30	27	21	91	56	21	04	
1-00	33	26	94	58	22	04	75
1-34	39	32	98	59	23	05	
3-00	45	38	.0103	63	25	05	74½
4-15	53	46	08	66	26	06	
5-04	56	48	10	67	27	06	74½
6-00	57	50	11	68	27	06	

TEST 18

4 LB. PLATE 0.82 psi

Time	r=0	r=½"	r=1"	r=1½"	r=2"	r=2¼"	Temp °F
00	.0127						73
01	.0131	.0122	.0080	.0055	.0020	.0018	
03	33	25	81	56	21	19	
06	35	27	83	57	23	20	
15	39	31	86	59	22	20	73
30	42	33	87	60	23	21	
1-00	45	37	89	61	24	22	73
1-30	47	39	89	62	24	22	
2-00	49	42	91	63	25	22	
2-18	49	42	91	63	25	22	73

TEST 19

4 LB. PLATE 1.840 psi

Time Hrs-Mins	r=0	r=½"	r=1"	r=1½"	r=2"	r=2¼"	Temp °F
00	.0845						76½
01	.0871	.0820	.0653	.0452	.0170	.0045	
03	83	32	64	55	73	46	
06	92	41	72	61	75	47	
15	.0906	55	83	68	79	48	
21	11	60	88	71	81	48	
31	18	68	93	76	83	49	76½
45	24	74	98	80	84	49	
1-00	29	80	.0702	83	86	50	76½
1-31	34	86	08	88	87	50	
2-00	42	92	13	92	89	51	76½
2-30	47	98	18	95	91	51	
3-00	51	.0901	22	98	92	52	77

TEST 20

4 LB. PLATE 1.840 psi

Time	r=0	r=½"	r=1"	r=1½"	r=2"	r=2¼"	Temp °F
00	.0820						79
01	.0848	.0783	.0638	.0438	.0162	.0053	
03	61	98	49	46	65	55	
06	70	.0804	56	50	68	56	
12	79	14	63	56	70	57	79
18	85	24	68	61	72	58	
26	91	31	72	65	74	58	79½
30	94	33	75	67	75	58	
1-00	.0907	46	85	74	79	61	79½
1-15	12	49	89	76	80	63	
1-30	16	56	92	79	81	63	79
2-00	20	58	98	84	83	64	
2-30	28	67	.0702	86	85	65	
3-30	35	76	09	92	88	66	79
4-19	44	84	14	96	91	68	
4-30	44	86	15	97	92	68	79
5-30	50	92	19	.0500	94	68	
6-00	52	94	21	02	95	68	79
6-33	55	96	22	03	95	68	

TEST 21

4 LB. PLATE 4.1 psi

Time Hrs-Mins	r=0	r=½"	r=1"	r=1½"	r=2"	r=2¼"	Temp °F
00	.1610						79½
01	.1651	.1572	.1333	.0998	.0377	.0159	
03	68	87	47	.1010	83	61	
06	81	98	57	19	88	64	
12	95	14	72	31	95	67	
15	.1700	19	77	34	97	69	79½
25	11	33	87	44	.0402	70	
30	14	37	90	47	04	71	80
51	27	48	.1403	57	10	74	
1-00	31	54	06	61	11	75	80
1-30	41	63	16	68	16	79	
2-00	49	70	23	75	19	80	80
2-45	58	78	30	81	24	82	
3-00	61	81	32	83	25	83	80
3-30	64	86	37	88	28	87	79½
4-03	69	88	41	91	31	89	
4-30	72	92	45	94	32	90	79-

TEST 22

4 LB. PLATE 4.1 psi

Time	r=0	r=½"	r=1"	r=1½"	r=2"	r=2¼"	Temp °F
00	.1580						81
01	.1610	.1538	.1313	.0973	.0435	.0136	
03	30	53	29	85	42	40	
06	44	68	40	95	48	42	
15	63	91	56	.1011	56	46	
24	75	.1602	65	19	63	48	
30	80	06	69	23	65	49	
48	91	18	79	32	71	51	
1-00	96	21	83	35	73	52	81
1-30	.1706	33	92	43	78	54	
2-00	13	43	99	50	82	55	81
3-05	25	54	.1411	59	86	59	
4-00	33	63	17	66	90	60	81
4-30	37	68	20	69	95	62	
5-05	40	70	23	71	96	62	80½
6-00	46	76	28	75	98	63	80

TEST 23

4 LB. PLATE 6.1 psi

TIME Hrs-Mins	r=0	r=½"	r=1"	r=1½"	r=2"	r=2¼"	Temp °F
00	.1875						76
01	.1918	.1820	.1554	.1138	.0488	.0243	
03	39	35	70	53	96	46	
06	51	47	83	63	.0503	51	
15	66	66	95	77	12	54	
25	75	78	.1601	85	18	55	76
37	82	85	07	91	21	57	
45	85	89	09	93	23	58	
1-00	89	94	13	94	26	60	76
1-15	93	94	17	99	27	61	
1-33	95	.1901	18	.1202	29	61	
2-00	99	02	23	05	30	62	76
3-00	.2009	07	27	09	34	63	76½
4-00	14	08	30	12	35	64	77
5-00	17	18	39	17	38	71	
5-33	20	19	39	18	39	71	77½

TEST 24

4 LB. PLATE 6.1 psi

Time	r=0	r=½"	r=1"	r=1½"	r=2"	r=2¼"	Temp °F
00	.1925						84
01	.1970	.1873	.1583	.1187	.0451	.0212	
03	.2000	97	.1605	.1203	62	18	
06	16	.1908	20	14	71	22	
08	24	14	27	20	76	24	
15	45	37	43	33	84	28	84
26	64	60	58	47	95	32	
30	68	62	62	49	96	33	84
45	81	72	73	58	.0502	36	
1-00	90	81	81	73	07	38	84
1-30	.2103	93	93	73	15	41	
2-00	14	.2004	.1702	80	20	44	84
2-34	24	10	10	85	25	48	
3-00	29	19	15	89	27	49	84
3-30	35	20	20	94	30	50	
4-02	40	29	26	.1300	31	51	84
4-30	45	33	29	03	34	52	
5-00	49	39	34	06	36	54	
5-30	54	44	37	09	38	55	84

APPENDIX G

Spectrochemical Analysis Report

The reported analysis was made by Mr. Walter W. Correia of the STRNAD Spectrographic Laboratory at M.I.T. The sample labels, "4", "6", and "8" are for the 4 lb. plate, 6 lb. plate, and 8 lb. plate respectively. The analysis samples were taken from tensile test specimens randomly selected from those actually used in the tensile experiments. From this data one may infer:

4 lb. plate	Pb > 99.67%
6 lb. plate	Pb > 99.96%
8 lb. plate	Pb > 99.29%

MASSACHUSETTS INSTITUTE OF TECHNOLOGY
STRNAD SPECTROGRAPHIC LABORATORY
Rm. 13-4151

Report of Spectrochemical Analysis

To. Peter T. Tarpgaard

Charged To:

Date Received:

Date Reported: March 3, 1970

Sample Description: Pb

SAMPLE	4	6	8		SAMPLE	4	6	8		SAMPLE	4	6	8	
Ag	VVFT	VFT	VFT		Mg	VFT	VFT	VFT		Ti				
Al					Mn					Tl				
As					Mo					U				
Au					Na					V				
B					Nb					W				
Ba					Ni					Y				
Be					Os					Zn				
Bi	T	FT-T	T		P	H	H	H		Zr				
C					Pb					Ce				
Ca	VVFT	VFT	VVFT		Pd					Dy				
Cd	T		VFT		Pt					Er				
Co					Rb					Eu				
Cr					Re					Gd				
Cs					Rh					Ho				
Cu	VVFT	FT	VFT		Ru					La				
Fe					Sb	FT-T	FT-T	T		Lu				
Ga					Sc					Nd				
Ge					Se					Pr				
Hf					Si	VFT	VFT	VVFT		Sm				
Hg					Sn	FT		L		Tb				
In	T				Sr					Tm				
Ir					Ta					Yb				
K					Te									
Li					Th									

Remarks: Sn in sample 8 approx. 0.5%-0.3%

Work by: Book No. Spec 8 Page No. 28

Reported by:

Key: VVFT < 0.0001 %
VFT 0.0001 % - 0.001 %
FT 0.001 % - 0.01 %
T 0.01 % - 0.1 %
L 0.1 % - 1.0 %
M 1.0 % - 10.0 %
H > 10.0 %

APPENDIX H

Computer Programs

I. Program for Clamped Edge Case

The following listing is for the program used in the numerical evaluation of the energy dissipation rate integral for the clamped edge circular plate. The program consists of a main part and two subroutines. Subroutine SAMS evaluates the moment terms, $M_r\dot{\kappa}_r + M_\theta\dot{\kappa}_\theta$, at a radial position x, where x = r/a. Simlarly Subroutine JOES evaluates the extensional force terms, $N_r\dot{e}_r + N_\theta\dot{e}_\theta$, at a position x. The main program uses five point Gauss quadrature to evaluate the total integral over x. The program is written in FORTRAN IV.

The inputs to the program are n, c_1', c_2', w_o/h, and α_1. The input format is F10.5 which means each input quantity is alloted 10 spaces and if no decimal is inserted by the programmer the decimal is assumed to be to the left of the last five spaces in the field. The format for the input card is as follows:

Field	Quantity
1-10	n
11-20	c_1'
21-30	c_2'
31-40	w_o/h
41-50	α_1

The last data card must have a negative number in the field 1-10. This causes the program to exit. For each data card

the program computes and prints seven sets of output data where:

$$(c_1')_{n+1} = (c_1')_n + .3 \qquad \text{(H.1)}$$

starting with the input value of c_1' plus .1. All other parameters remain constant through all seven iterations. The output is in ten columns as follows:

Column	Quantity
1	n
2	c_1'
3	c_2'
4	w_o/h
5	α_1
6	A_m, the integral of $M_r\dot{\kappa}_r + M_\theta\dot{\kappa}_\theta$
7	A_n, the integral of $N_r\dot{e}_r + N_\theta\dot{e}_\theta$
8	$A_m+A_n = I_c$
9	Φ
10	Φ^n

where $\Phi = \dfrac{3-\alpha_1}{12\ I_c}$.

CLAMPED EDGE CASE

```
    5 READ (2,60)EN,C1A,C2A,WH,A1
   60 FORMAT (5F10.5)
      IF (EN) 10,20,20
   20 C2 = C2A
      DO 120 J = 1,21,3
      EJ = J
      C1 = C1A +(EJ*.10)
      U = 0.0
      CALL SAMS (U,C1,C2,WH,EN,A1,VMX)
      DI0 = VMX
      U = .9061798459
      CALL SAMS (U,C1,C2,WH,EN,A1,VMX)
      DI1 = VMX
      U = U*(-1.0)
      CALL SAMS (U,C1,C2,WH,EN,A1,VMX)
      DI2 = VMX
      U = .5384693101
      CALL SAMS (U,C1,C2,WH,EN,A1,VMX)
      DI3 = VMX
      U = U*(-1.0)
      CALL SAMS (U,C1,C2,WH,EN,A1,VMX)
      DI4 = VMX
C  COMPUTE INTEGRAL WITH 5 PT GAUSS QUADRATURE
      VM = .50*(.5688888889*DI0+.2369268851*DI1+.2369268851*DI2
     1   +.4786286705*DI3+.4786286705*DI4)
      U = 0.0
      CALL JOES (U,C1,C2,WH,EN,A1,VNX)
      DI0 = VNX
      U = .9061798459
      CALL JOES (U,C1,C2,WH,EN,A1,VNX)
      DI1 = VNX
      U = U*(-1.0)
      CALL JOES (U,C1,C2,WH,EN,A1,VNX)
      DI2 =VNX
      U = .5384693101
      CALL JOES (U,C1,C2,WH,EN,A1,VNX)
```

120

```
      DI3 = VNX
      U = U*(-1.0)
      CALL JOES (U,C1,C2,WH,EN,A1,VNX)
      DI4 =VNX
      VN = .50*(.5688888889*DIO+.2369268851*DI1+.2369268851*DI2
     1   +.4786286705*DI3+.4786286705*DI4)
      VT = VM + VN
      VTA = (3.0-A1)/(12.0*VT)
      VTAN = VTA**EN
      WRITE (3,700)EN,C1,C2,WH,A1,VM,VN,VT,VTA,VTAN
  700 FORMAT (5F10.5,5E13.5)
  120 CONTINUE
      GO TO 5
   10 CALL EXIT
      END
```

```
      SUBROUTINE SAMS (U,C1,C2,WH,EN,A1,VMX)
      X = .5*U+.5
      A2 = 1.0 -A1
      FA = (2.0*A1*(3.0-7.0*(X**2.0)))+(3.0*A2)
      FAA = ABS (FA)
      FB =EN/((2.0*EN+1.0)*FA*FAA)
      FC = ((1.5-2.5*X)*C1*WH)+((2.5*X-3.5*(X**2.0))*C2*WH)
     1  +(16.0*(X**2.0)*(A1**2.0)*((1.0-X**2.0)**2.0)*WH)
     2  +(16.0*(X**2.0)*A1*A2*(1.0-X**2.0)*WH)
     3  +(4.0*(X**2.0)*(A2**2.0)*WH)
      FD = .5*FAA
      FE = FC+FD
      S1 = 1.0
      S2 = 1.0
      IF (FE) 11,12,12
   11 S1 = -1.0
   12 FEA = ABS(FE)
      FEA1 = FEA**(1.0+1.0/EN)
      FEA2 = (FEA**(2.0+1.0/EN))*S1
      FF = FC-FD
      IF (FF) 13,14,14
   13 S2 = -1.0
   14 FFA = ABS(FF)
      FFA1 = FFA**(1.0+1.0/EN)
      FFA2 = (FFA**(2.0+1.0/EN))*S2
      RM = ((1.0/(2.0*FA))*(FEA1+FFA1))-(FB*(FEA2-FFA2))
      RMK = RM*((4.0*A1*(1.0-3.0*(X**2.0)))+2.0*A2)
      EA = (2.0*A1*(3.0-5.0*(X**2.0)))+(3.0*A2)
      EAA = ABS(EA)
      EB = EN/((2.0*EN+1.0)*EA*EAA)
      EC = ((1.5-2.0*X)*C1*WH)+((2.0*X-2.5*X**2.0)
     1  *C2*WH)+(8.0*WH*(X**2.0)*(A1**2.0)*((1.0-X**2.0)**2.0))
     2  +(8.0*WH*(X**2.0)*A1*A2*(1.0-X**2.0))+(2.0*(X**2.0)*(A2**2.0)*
     3  WH)
      ED = .5*EAA
      EE = EC+ED
```

```
      S1 =1.0
      S2 =1.0
      IF (EE) 15,16,16
   15 S1 = -1.0
   16 EEA = ABS(EE)
      EEA1 = EEA**(1.0+1.0/EN)
      EEA2 = (EEA**(2.0+1.0/EN))*S1
      EF = EC-ED
      IF (EF)17,18,18
   17 S2 = -1.0
   18 EFA = ABS (EF)
      EFA1 = EFA**(1.0+1.0/EN)
      EFA2 = (EFA**(2.0+1.0/EN))*S2
      TM = ((1.0/(2.0*EA))*(EEA1+EFA1))-(EB*(EEA2-EFA2))
      TMK = TM*((4.0*A1*(1.0-X**2.0))+2.0*A2)
      VMX = ((ABS(RMK))+(ABS(TMK)))*X
      RETURN
      END
```

```
      SUBROUTINE JOES (U,C1,C2,WH,EN,A1,VNX)
      X = .5*U+.5
      A2 = 1.0 - A1
      BA = (2.0*A1*(3.0-7.0*(X**2.0)))+(3.0*A2)
      BB = ((1.5-2.5*X)*C1*WH)+(((2.5*X)-(3.5*X**2.0))*C2*WH)
     1  +(16.0*WH*(X**2.0)*(A1**2.0)*((1.0-X**2.0)**2.0))
     2  +(16.0*(X**2.0)*A1*A2*(1.0-X**2.0)*WH)+(4.0*(X**2.0)
     3  *(A2**2.0)*WH)
      BC = .5*BA
      BD = BB+BC
      BDA = ABS (BD)
      BDAN = BDA**(1.0+1.0/EN)
      BE = BB-BC
      BEA = ABS(BE)
      BEAN = BEA**(1.0+1.0/EN)
      BF = ((1.0-2.0*X)*C1*WH)+((2.0*X-3.0*X**2.0)*C2*WH)
     1  +(16.0*WH*(X**2.0)*(A1**2.0)*((1.0-X**2.0)**2.0))
     2  +(16.0*A1*A2*WH*(X**2.0)*(1.0-X**2.0))
     3  +(4.0*(X**2.0)*(A2**2.0)*WH)
      RNE = (1.0/BA)*(BDAN-BEAN)*BF
C     THIS IS NR*ER TERM
      CA = (2.0*A1*(3.0-5.0*(X**2.0)))+(3.0*A2)
      CB = ((1.5-2.0*X)*C1*WH)+((2.0*X-2.5*(X**2.0))*C2*WH)
     1  +(8.0*(X**2.0)*(A1**2.0)*WH*((1.0-(X**2.0))**2.0))
     2  +(8.0*(X**2.0)*A1*A2*(1.0-(X**2.0))*WH)
     3  +(2.0*(X**2.0)*(A2**2.0)*WH)
      CC = .5*CA
      CD = CB+CC
      CDA = ABS(CD)
      CDAN = CDA**(1.0+1.0/EN)
      CE = CB-CC
      CEA = ABS(CE)
      CEAN = CEA**(1.0+1.0/EN)
      CF = ((1.0-X)*C1*WH)+((X-(X**2.0))*C2*WH)
      TNE = (1.0/CA)*(CDAN-CEAN)*CF
      VNX = ((ABS(RNE))+(ABS(TNE)))*X
      RETURN
      END
```

II. Program for Simply Supported Case

The following program for the simply supported case is exactly like that for the clamped case except that a different assumed velocity profile is used.

The input data, in format F10.5, is as follows:

Field	Quantity
1-10	n
11-20	c_1'
21-30	c_2'
31-40	w_o/h

Here again the last data card must have a negative number in field 1-10 to cause the program to exit. The output data is exactly as in the clamped edge program discussed in Part A except that the column for α_1 is omitted and here

$$\Phi = \frac{1}{\frac{22}{5} I_s}.$$

SIMPLE SUPPORT CASE

```
    5 READ (2,50) EN,C1A,C2A,WH
   50 FORMAT(4F10.5)
      IF (EN) 10,20,20
   20 C2 = C2A
      DO 120 J = 1,2,3
      EJ = J
      C1 = C1A +(EJ*.10)
      U = 0.0
      CALL SAMSS (U,C1,C2,WH,EN,VMX)
      DI0 = VMX
      U = .9061798459
      CALL SAMSS (U,C1,C2,WH,EN,VMX)
      DI1 = VMX
        = U*(-1.0)
      CALL SAMSS (U,C1,C2,WH,EN,VMX)
      DI2 = VMX
      U = .5384693101
      CALL SAMSS (U,C1,C2,WH,EN,VMX)
      DI3 = VMX
      U = U*(-1.0)
      CALL SAMSS (U,C1,C2,WH,EN,VMX)
      DI4 = VMX
C     COMPUTE INTEGRAL WITH 5 PT GAUSS QUADRATURE
      VM = .50*(.2688888889*DI0+.2369268851*DI1+.2369268851*DI2
     1    +.4786286705*DI3+.4786286705*DI4)
      U = 0.0
      CALL JOESS (U,C1,C2,WH,EN,VNX)
      DI0 = VNX
      U = .9061798459
      CALL JOESS (U,C1,C2,WH,EN,VNX)
      DI1 = VNX
      U = U*(-1.0)
      CALL JOESS (U,C1,C2,WH,EN,VNX)
      DI2 =VNX
      U = .5384693101
      CALL JOESS (U,C1,C2,WH,EN,VNX)
```

```
      DI3 = VNX
      U = U*(-1.0)
      CALL JOESS (U,C1,C2,WH,EN,VNX)
      DI4 =VNX
      VN = .50*(.5688888889*DI0+.2369268851*DI1+.2369268851*DI2
     1   +.4786286705*DI3+.4786286705*DI4)
      VT = VM + VN
      VTA = 1.0/((132.0/30.0)*VT)
      VTAN = VTA**EN
      WRITE (3,700)EN,C1,C2,WH,VM,VN,VT,VTA,VTAN
  700 FORMAT (4F10.5,5E13.5)
  120 CONTINUE
      GO TO 5
   10 CALL EXIT
      END
```

```
      SUBROUTINE SAMSS (U,C1,C2,WH,EN,VMX)
      X = .5*U+.5
      FA = (42.0/11.0)-((42.0/11.0)*(X**2.0))
      FAA = ABS (FA)
      FB =EN/((2.0*EN+1.0)*FA*FAA)
      FC = ((1.5-2.5*X)*C1*WH)+((2.5*X-3.5*(X**2.0))*C2*WH)
     1  +((X**2.0)*(((28.0/11.0)-(12.0/11.0)*X**2.0)**2.0)*WH)
      FD = .5*FAA
      FE = FC+FD
      S1 = 1.0
      S2 = 1.0
      IF (FE) 11,12,12
   11 S1 = -1.0
   12 FEA = ABS(FE)
      FEA1 = FEA**(1.0+1.0/EN)
      FEA2 = (FEA**(2.0+1.0/EN))*S1
      FF = FC-FD
      IF (FF) 13,14,14
   13 S2 = -1.0
   14 FFA = ABS(FF)
      FFA1 = FFA**(1.0+1.0/EN)
      FFA2 = (FFA**(2.0+1.0/EN))*S2
      RM = ((1.0/(2.0*FA))*(FEA1+FFA1))-(FB*(FEA2-FFA2))
      RMK = RM*((28.0/11.0)-((36.0/11.0)*(X**2.0)))
      EA = (42.0/11.0)-((30.0/11.0)*(X**2.0))
      EAA = ABS(EA)
      EB = EN/((2.0*EN+1.0)*EA*EAA)
      EC = ((1.5-2.0*X)*C1*WH)+((2.0*X-2.5*X**2.0)
     1 *C2*WH)+(((.5*(X**2.0))*(((28.0/11.0)-(12.0/11.0)*X**2.0)
     2  **2.0)) *WH)
      ED = .5*EAA
      EE = EC+ED
      S1 =1.0
      S2 =1.0
      IF (EE) 15,16,16
   15 S1 = -1.0
```

```
   16 EEA = ABS(EE)
      EEA1 = EEA**(1.0+1.0/EN)
      EEA2 = (EEA**(2.0+1.0/EN))*S1
      EF = EC-ED
      IF (EF)17,18,18
   17 S2 = -1.0
   18 EFA = ABS (EF)
      EFA1 = EFA**(1.0+1.0/EN)
      EFA2 = (EFA**(2.0+1.0/EN))*S2
      TM = ((1.0/(2.0*EA))*(EEA1+EFA1))-(EB*(EEA2-EFA2))
      TMK = TM*((28.0/11.0)-((12.0/11.0)*(X**2.0)))
      YMX = ((ABS(RMK))+(ABS(TMK)))*X
      RETURN
      END
```

```
      SUBROUTINE JOESS (U,C1,C2,WH,EN,VNX)
      X = .5*U+.5
      BA = (42.0/11.0)-((42.0/11.0)*(X**2.0))
      BB = ((1.5-2.5*X)*C1*WH)+(((2.5*X)-(3.5*X**2.0))*C2*WH)
     1  +((X**2.0)*(((28.0/11.0)-(12.0/11.0)*X**2.0)**2.0)*WH)
      BC = .5*BA
      BD = BB+BC
      BDA = ABS (BD)
      BDAN = BDA**(1.0+1.0/EN)
      BE = BB-BC
      BEA = ABS(BE)
      BEAN = BEA**(1.0+1.0/EN)
      BF = ((1.0-2.0*X)*C1*WH)+((2.0*X-3.0*X**2.0)*C2*WH)
     1  +((X**2.0)*(((28.0/11.0)-(12.0/11.0)*(X**2.0))**2.0)*WH)
      RNE = (1.0/BA)*(BDAN-BEAN)*BF
C     THIS IS NR*ER TERM
      CA = (42.0/11.0)-((30.0/11.0)*(X**2.0))
      CB = ((1.5-2.0*X)*C1*WH)+((2.0*X-2.5*(X**2.0))*C2*WH)
     1  +((.5*(X**2.0))*(((28.0/11.0)-(12.0/11.0)*(X**2.0))**2.0)*WH)
      CC = .5*CA
      CD = CB+CC
      CDA = ABS(CD)
      CDAN = CDA**(1.0+1.0/EN)
      CE = CB-CC
      CEA = ABS(CE)
      CEAN = CEA**(1.0+1.0/EN)
      CF = ((1.0-X)*C1*WH)+((X-(X**2.0))*C2*WH)
      TNE = (1.0/CA)*(CDAN-CEAN)*CF
      VNX = ((ABS(RNE))+(ABS(TNE)))*X
      RETURN
      END
```

APPENDIX I

Computation of Total Deflection

The discussion in Chapter II was centered about determining the deformation rate, $\dot{w}_o$. In practical problems it is frequently the total deflection, w_o, at some time, t*, which is of interest. It has been shown that $\dot{w}_o$ is a function of $\frac{w_o}{h}$, and also that the material creep constants, K and n, may change with time. To compute w_o, therefore, a piecewise linearization technique can be employed in which the deformation process is broken into a sufficient number of linearized time segments to provide the accuracy desired. One such technique is discussed in this Appendix.

In dividing the deformation process into time segments some guidance can be obtained from the shape of the tensile test curves and from the shape of the Φ versus $\frac{w_o}{h}$ curves, Figures 2.2 and 2.4. The time segments should be relatively short during primary creep and may be longer when deformation is proceeding more slowly. As the deformation process proceeds, $\frac{w_o}{h}$ increases; and when $\frac{w_o}{h}$ has changed enough to make a significant change in Φ a new linear segment should be introduced.

Having divided the total time of interest, from t=0 to t=t*, into n segments one can proceed as follows:

Let $t=t_s$ be the time at the beginning of the segment under consideration and $t=t_f$ the time at the end. From tensile test data determine the appropriate values for

the creep constants, K and n, at the time t_c, in the center of the given time segment, where:

$$t_c = \frac{t_f - t_s}{2}. \tag{I.1}$$

Using these values of K and n; and using the value of $\frac{w_o}{h}$ at the beginning of the time segment, compute $\dot{w}_o$ with the appropriate equation from Chapter II, (2.53) for clamped edge or membrane or (2.57) for simple support. Multiply this value of $\dot{w}_o$ by the total time length of the segment, $t_f - t_s$, and add the result to the value of w_o at t_s. This gives w_o at t_f. The procedure is then repeated for the next segment, and the next, and so forth until t* is reached.

In illustration, consider the case of Test 13, a 6 lb. plate under 6.1 psi pressure. Assume that it is desired to compute w_o at t=8 hours. The total time is broken into two segments, a relatively short initial segment from t=0 to t=2 hours, and a longer segment, where the deformation is more gradual, from t=2 hours to t=t*=8 hours. Values of K and n are determined at the median times of the segments, which in this case are t=1 hours and t=5 hours. From the tensile test results in Chapter II the appropriate values are seen to be:

$$\text{t=1 hour} \qquad \text{n=5.0} \qquad K=4.1 \times 10^{-18} \tag{I.2}$$

$$\text{t=5 hours} \qquad \text{n=5.0} \qquad K=1.7 \times 10^{-18} \tag{I.3}$$

In test 13 the initial deflection was .0880" giving:

$$\frac{w_o}{h} = .840. \tag{I.4}$$

If test data is not available the initial deformation can be computed using elastic or plastic analysis. Using (I.2) and (I.4) and the appropriate value of Φ from Figure 2.2 in equation (2.48) the value of $\dot{w}_o$ for the first segment is found to be .0090"/hr. Deflection at t=2 hours may now be determined:

$$(w_o)_{t=2} = .0880 + 2(.0090) = .1060 \qquad (I.5)$$

which gives:

$$(\frac{w_o}{h})_{t=2} = 1.01 \qquad (I.6)$$

Using (I.3) and (I.6) with Figure 2.2 and equation (2.48) we find for the second segment that $\dot{w}_o$ = .0020"/hr. Deflection at t=8 hours is:

$$(w_o)_{t=8} = .1060 + 6(.0020) = .1180" \qquad (I.7)$$

A plot of this two step linearization and of the measured experimental curve is shown in Figure I.1. Also shown is a three step linear approximation made with the technique described above with periods $0 \leq t \leq 1$ hour, $1 \leq t \leq 3$ hours, and $3 \leq t \leq 8$ hours. Still closer approximations to the actual curve could be made by dividing the time period into more segments.

In the practical application of these results it is important that initial deflection of the plate be known. Computing this initial deflection, however, may be no simple matter. Finite deflection analysis techniques for plastic and elasto-plastic deformation of plates are usually quite complex. For materials in which creep is important there is often a high degree of sensitivity to the speed of application of load

[28] which makes even the selection of appropriate elastic and plastic material constants a rather difficult task. In fact, such elasticity concepts as yield stress and Young's modulus may become rather meaningless for some materials under conditions where creep is important.

In cases where the initial deflection is expected to be quite small and elastic, one could calculate initial deflection using the bending solution of Timoshenko and Woinowsky-Krieger [29]. For larger elastic deformation the large deflection solution of Timoshenko and Woinowsky-Krieger [30] is available. The large deflection elasto-plastic deformation of circular plates is treated by Ohashi and Murakami [31][32], and the large deflection of elastic-perfectly plastic circular plates has been analyzed by Crose and Ang [33].

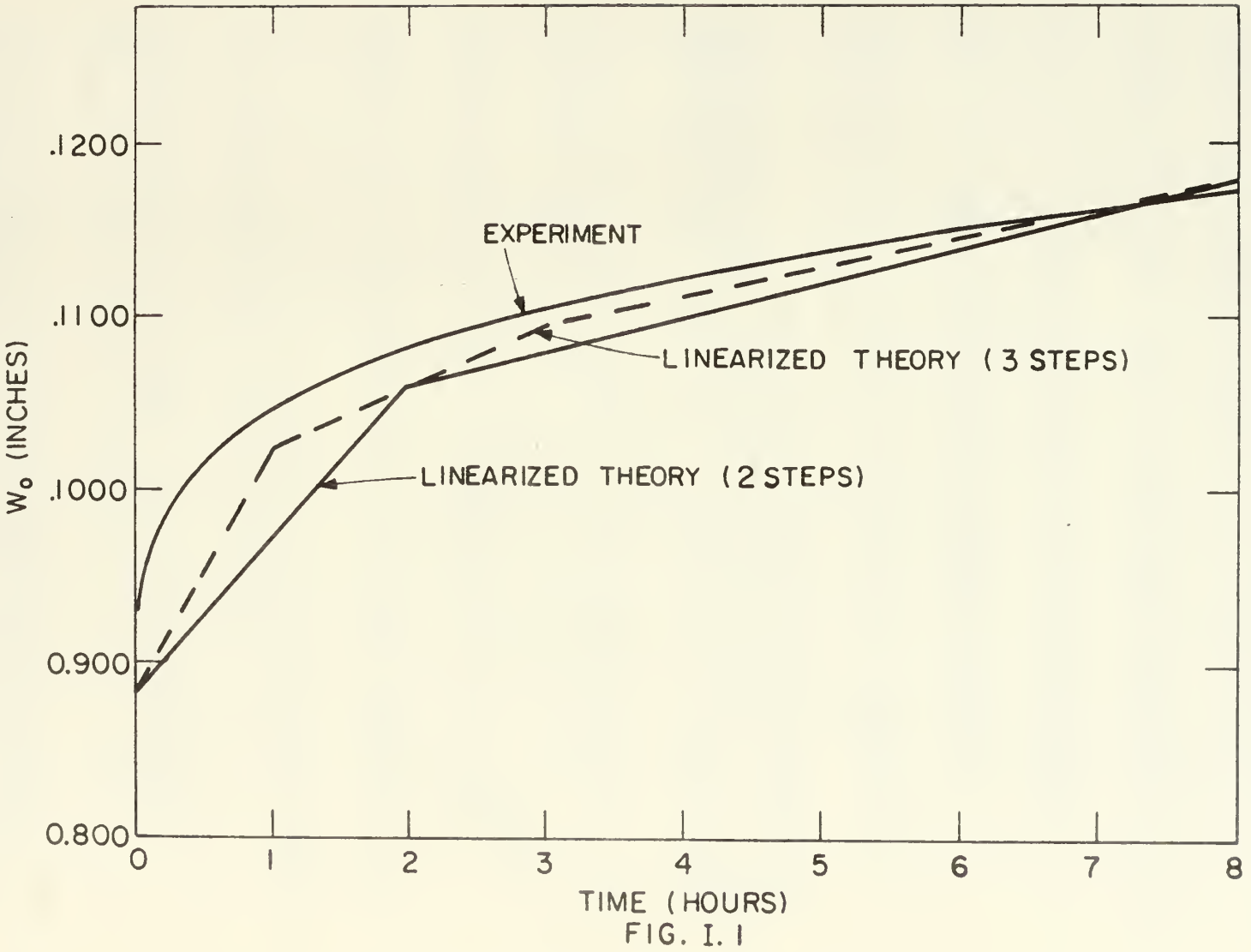

FIG. I. 1

Comparison of stepwise solution for w_o with experiment

References

1. Trouton, F.T. and Rankine, A.O., "On the Stretching and Torsion of a Lead Wire beyond the Elastic Limit" 'Phil. Mag.' October 1904.

2. Andrade, E.N.da C., "On the Viscous Flow in Metals, and Allied Phenomena", Proc. of the Royal Society, A, Vol.84, No. 1, 1910.

3. Norton, F.H., Creep of Steel at High Temperatures, McGraw-Hill, New York, 1929.

4. Nadai, A., Theory of Flow and Fracture of Solids, Vol. II, p.521, McGraw-Hill, New York, 1963.

5. Soderberg, C.R., "The Interpretation of Creep Tests for Machine Design", Trans. of the American Society of Mechanical Engineers, Vol. 58, p. 733, 1936.

6. Odqvist, F.K.G., Proc. Fourth International Congress of Applied Mechanics, Cambridge, 1934, p. 228; Plasticitetsteori, Royal Swedish Institute for Engineering Research, Spec. Publ., p. 77, 1934; Proc. Royal Swedish Inst. Engn. Res., No. 141, 1936.

7. Bailey, R.W., "The Utilization of Creep Test Data in Engineering Design", Proc. of the Institution of Mechanical Engrs., Vol. 131, p. 131-349, 1935.

8. Drucker, D.C., "A More Fundamental Approach to Plastic Stress-Strain Relations", Proceedings of the First U.S. Congress App. Mech., A.S.M.E., p. 487, 1951.

9. Hopkins, H.G. and Prager, W., "The Load Carrying Capacities of Circular Plates", J. Mech. Phys. Solids, Vol. 2, p. 1, 1953.

10. Wahl, A.M., "Analysis of Creep in Rotating Disks Based on the Tresca Criterion and Associated Flow Rule", J. Appl. Mech., Vol. 23, p. 231, 1956.

11. Venkatraman, B. and Hodge, P.G., "Creep Behavior of Circular Plates", J. Mech. and Physics of Solids, Vol. 6, p. 163, 1958. (see also J. Mech. Physics of Solids, Vol. 12, p. 191, 1964.)

12. Odqvist, F.K.G., "Applicability of the Elastic Analogue to Creep Problems of Plates, Membranes and Beams", Creep in Structures, Proc. IUTAM Colloquium, Stanford University, 1960, Hoff, N.J. (ed.), Springer, Berlin, 1962, p. 139-159.

13. Patel, S.A. and Venkatraman, B., "On the Creep Analysis of Some Structures", Creep in Structures, op. cit., p. 43-64.

14. Venkatraman, B. and Patel, S.A., "Creep Analysis of Annular Plates", J. of the Franklin Institute, Vol. 275, No. 1, 1963, p. 13.

15. Sankaranarayanan, R., "Creep Behavior of Orthotropic Circular Plates", J. of the Aeronautical Society of India, Vol. 19, No. 3, 1967, p. 81.

16. Odqvist, F.K.G., Mathematical Theory of Creep and Creep Rupture, Oxford Mathematical Monographs, London, 1966, p. 80.

17. Onat, E.T. and Yüksel, H., "On the Steady Creep of Shells", Proc. Third U.S. National Congress App. Mech., ASME, 1958, p. 625.

18. Jones, N., "Combined Distributed Loads on Rigid-Plastic Circular Plates with Large Deflections", Int. J. Solids Structures, Vol. 5, 1969, p. 51-64.

19. Jones, N., "Impulsive Loading of a Simply Supported Circular Rigid Plastic Plate", J. App. Mech., March, 1968, p. 59-65.

20. Timoshenko, S. and Woinowsky-Krieger, S., Theory of Plates and Shells, 2nd Edition, McGraw-Hill, New York, 1959, Art. 97.

21. Ibid., Art. 16.

22. Gifkins, R.C., "The Influence of Thallium on the Creep of Lead", J. Inst. of Metals, Vol. 81 (8), Apr. 1953, p. 417-425.

23. Timoshenko and Woinowsky-Krieger, op. cit., Art. 16.

24. Ibid., Art. 97.

25. Jones, N., "Consistent Equations for the Large Deflections of Structures", Bulletin Mech. Eng. Education, Vol. 9, 1970.

26. Timoshenko and Woinowsky-Kreiger, op. cit., Art. 16.

27. Mendelson, Alexander, Plasticity: Theory and Application, Macmillian, New York, 1968. Chapter 14.

28. Soden, P.D.W. and Sowerby, R., "Large Deformation of Time-Dependent Materials in Uniaxial Tension", Journal of Strain Analysis, Vol. 4, No. 3, 1969, pp. 199-207.

29. Timoshenko and Woinowsky-Krieger, op. cit., Art. 16.

30. Ibid., Art. 97.

31. Ohashi, Y. and Murakami, S., "The Elasto-Plastic Bending of a Clamped Thin Circular Plate", Proceedings of the Eleventh International Congress of Applied Mechanics, Munich, 1964, pp. 212-223.

32. Ohashi, Y, and Murakami, S., "Large Deflection in Elastoplastic Bending of a Simply Supported Circular Plate Under a Uniform Load", Journal of Applied Mechanics, Vol. 33, Series E, No. 4, Dec. 1966, pp. 866-870.

33. Crose, J.G., and Ang, A.H.-S., "A Large Deflection Analysis Method for Elastic-Perfectly Plastic Circular Plates", Civil Engineering Studies, Structural Research Series No. 323, University of Illinois, Urbana, Ill., June 1967.

Acknowledgement

The author gratefully acknowledges the assistance of Professor Norman Jones whose active and continuing interest, guidance, and encouragement have been so much a part of this work. He also wishes to thank Professors J. Harvey Evans and Alaa Mansour for their suggestions and assistance through the course of the investigation.

This work was supported by a grant from the Applied Research Division of the Naval Ship Systems Command.

Biographical Note

The author was born in Tennessee and reared in West Virginia where he attended public schools. He entered the U. S. Naval Academy at Annapolis, Maryland in 1955 and graduated with the degree of Bachelor of Science in 1959. Following graduation he served in the U. S. Navy in destroyers and submarines until entering graduate school at M.I.T. in the summer of 1965. From 1965 to 1968 he was enrolled in Course XIII-A, Naval Construction and Engineering, and received the degree of Master of Science in Mechanical Engineering and the degree of Naval Engineer in June of 1968. In 1967 he was awarded the Graduate Paper Honor Prize of The Society of Naval Architects and Marine Engineers as co-author of a paper entitled "Utilization of Propeller Shrouds as Steering Devices". He was enrolled in the Department of Naval Architecture and Marine Engineering at M.I.T. from 1968 to 1970 as a candidate for the degree of Doctor of Philosophy.

Thesis 118600
T152 Tarpgaard
The influence of finite deformation upon the creep behavior of circular plates.